'Butamben, a specific local anesthetic and aspecific ion channel modulator'

Beekwilder, J.P.

'BUTAMBEN, A SPECIFIC LOCAL ANESTHETIC AND ASPECIFIC ION CHANNEL MODULATOR'

PROEFSCHRIFT

ter verkrijging van

de graad van Doctor aan de Universiteit Leiden,

op gezag van Rector Magnificus prof. mr. P.F. van der Heijden,

volgens besluit van het College voor Promoties

te verdedigen op donderdag 22 mei 2008

klokke 13.45 uur

door

Jeroen Petrus Beekwilder

geboren te Helmond

in 1973

Promotiecommissie

Promotor:	Prof. Dr. D.L. Ypey
Copromotor:	Dr. R.J. van den Berg
Referent:	Dr. M.W. Veldkamp (Academisch Medisch Centrum, Amsterdam)

Overige leden:

Prof. Dr. A. Dahan
Prof Dr. W.J. Wadman (Universiteit van Amsterdam)

The publication of the thesis has been supported financially by
Cyberonics Europe, Vagus Nerve Stimulation (VNS),
which is gratefully acknowledged.

INDEX/INHOUDSOPGAVE

CHAPTER 1

GENERAL INTRODUCTION

Pain is a functional property of the human body. It is a warning for danger and damage. Yet, if pain is accompanied by the inability to take away its cause, it loses its usefulness and can become a chronic nuisance. It directly affects the 'quality of life'. Besides the personal tragedy for the people involved, there are also economic effects due to the fact that the pain prevents people from functioning normally in our society. Therefore, pain is of a growing concern in the medical field nowadays.

The methods that are currently being used in the treatment of intractable pain all have limited success or severe side effects. This is most obvious in the case of nerve lesioning (Candido and Stevens, 2003) and the use of systemic morphine (Donnelly et al., 2002). So, alternatives are more than welcome and many of them are being studied at this moment. The ideal alternative would have a reversible action, which would last as long as necessary and would only block the malicious pain without affecting any other system of the body. The present thesis describes a study of the mechanism of pain suppression by a local anesthetic, butamben, applied as a suspension on the hard membrane (dura mater) enveloping the spinal cord (Shulman, 1987). This method has an ultra-long duration (a few months), has a reversible action and selectively suppresses pain without affecting motor function (Korsten et al., 1991). Furthermore, it does not involve expensive or difficult to handle chemicals. These ideal features make the method really interesting, however, the exact mechanism of action remains unclear to date. Therefore, the role of this drug is investigated in this thesis by studying its effects on ion channels in pain signal producing neurons, which is a group of sensory neurons dedicated to the detection of possible tissue damage.

Pain physiology

Pain receptors, or nociceptors, are merely free nerve endings appearing in many tissues of the body. They are sensitive to various stimuli, causing a local depolarization of the membrane. The cell bodies (somata) of these primary afferent pain neurons are located in the dorsal root ganglia, like for all somatic sensation. The dorsal root ganglion (DRG) neuron extends a single process, which then bifurcates into a branch to the periphery at one side and a branch that turns to the central nervous system at the other side (Figure 1).

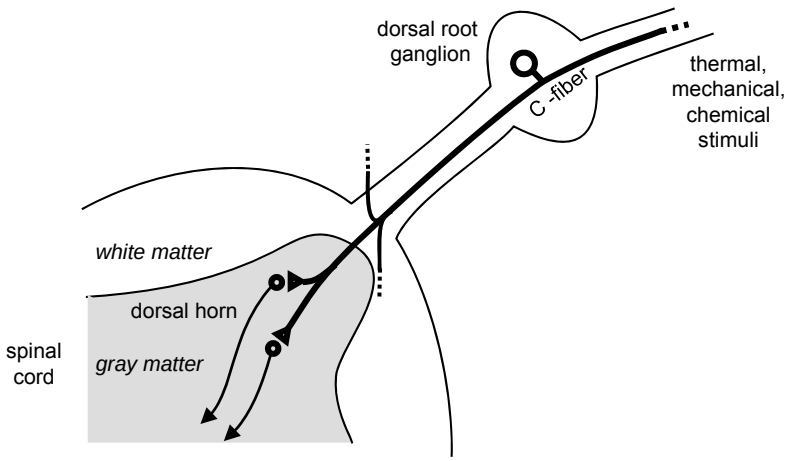

Figure 1: Schematic diagram of the location of the dorsal root ganglion (DRG) with its sensory neurons, including pain sensitive neurons. A pain fiber transmits its pain signaling action potentials from the periphery to the external layers of the dorsal horn of the spinal cord.

Pain is transmitted through two different kinds of nerve fibers (Ganong, 2003). Fast myelinated fibers, Aδ- and to a smaller extent Aβ-fibers, conducting the pain signals in the form of action potentials with a conduction velocity, largely depending on species, of 5-60m/s (Djouhri and Lawson, 2004). These nerves are aroused by either heat (>45˚C) or mechanical stimuli. These events are accompanied by a sharp or pricking pain sensation. Secondly, there are the slow unmyelinated C-fibers, characterized by their slower conduction velocity of 0.5-2 m/s. These fibers are useless for stimuli that require fast action in order to prevent tissue damage. The nerve endings of C-fibers can be found in the skin as well as deep tissues and are not only activated by thermal and mechanical but also by chemical stimuli. The latter are often associated with cell damage, such as tissue acidity (protons), which stimulates the vanilloid pain receptor VR-1 (Ganong, 2003). The pain sensation resulting from aroused C-fibers can be described as long lasting and burning. The C-fibers are at the origin of chronic pain.

The DRG neurons project their sensory information on the dorsal horn of the spinal cord (Ganong, 2003). Just before entering the dorsal horn the nerves

bifurcate and ascend as well as descend in order to enter nerve tracts that lead to the dorsal horns of neighbouring spinal cord segments. Most nerves end in the outer or marginal layers I-III of the dorsal horn on relay- or interneurons. Substance P has been identified as one of the neurotransmitters released by the dorsal root ganglion neurons. From the dorsal horn the pain information is sent to the thalamus and subsequently to other higher brain areas. Finally, the perception of pain is generated in the cortex.

The signal transmission for the whole tract from the pain receptors to the cortex is mediated by dynamic ion fluxes across the membranes of the neurons involved. These ionic fluxes are mediated and regulated by the ion channels in these neuronal membranes and are the subject of this thesis.

ION CHANNELS

Ion pumps and channels in the lipid membranes of cells are used by the cell to regulate the ionic composition of the intracellular (and extracellular) fluid. This regulation is a dynamic process and is essential for a wide variety of processes that can be divided into cell maintenance or development at one side and signal transduction and information processing at the other side. To this end, ion channels are tunnel-shaped macromolecular proteins that vary in their selective permeability for ions and their gating properties (Hille, 2001). The permeability of the ion channels can be highly specific for one type of ion, like for instance calcium, or it can be permeable to merely every ion, like gap junctional channels. An open channel passively conducts the ions along the electrochemical gradient, as opposed to ion pumps, which bring ions across the membrane against the electrochemical gradient at the cost of energy in the form of ATP. Gating of the channel can be regulated by numerous stimuli, some of which are membrane potential, temperature, ion concentrations and the presence of ligands. The actual opening of the channel occurs by a gate and is called activation, whereas closing of that so-called activation gate is called *de*activation. It is also possible however, that within a channel a different gate is closing causing a block of the

ionic flow. This is called *in*activation. Re-opening of that inactivation gate is called recovery from inactivation or de-inactivation. The two or more gates of

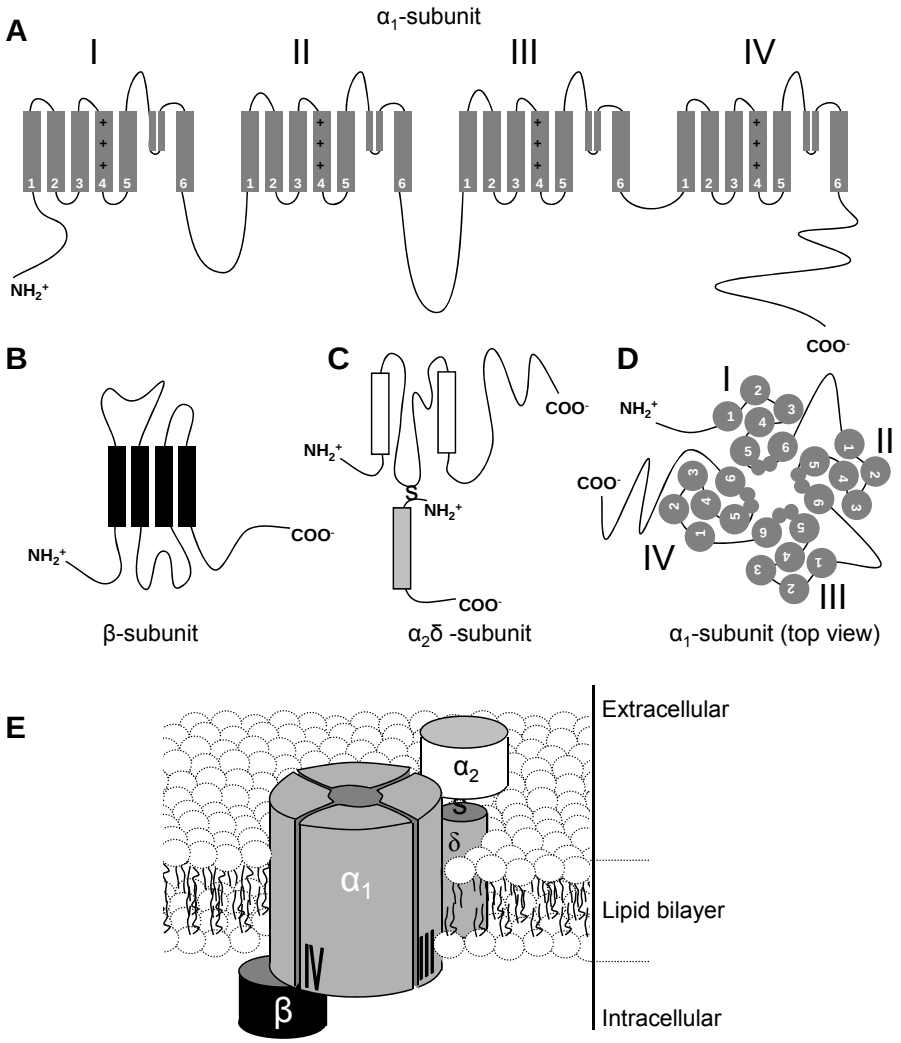

Figure 2: The structure of voltage gated calcium channels. (A) Transmembrane looping of the α1-subunit. The repeated domains are labeled with I, II, III and IV. (B) Looping of the cytoplasmic β-subunit. (C) Structure of the α2δ-subunit. The extracellular α2 and membrane spanning δ part are linked with a sulfide bridge. (D) Top view of the presumed configuration of the α1-subunit. (E) Cartoon of an assembled voltage gated calcium channel 'floating' in the lipid bilayer.

the channels can be, but are not necessarily, coupled.

In this study we looked mainly at the effect of the local anesthetic butamben on voltage-gated calcium and potassium channels, which will be discussed in the following sections.

Calcium channels

Under normal conditions intracellular calcium concentrations are kept very low, typically ~100-200 nM in neurons (Ganong, 2003). This is roughly 10^4 times lower than the extracellular calcium concentration. This steep gradient allows the cell to raise the intracellular calcium concentration quickly by an order of magnitude. The increased intracellular calcium concentration is used in the cell as a signal to trigger various kinds of actions. For instance, upon an increase in the calcium concentration close to a docked transmitter-containing vesicle in a presynaptic terminal, the vesicle will release its transmitter content in the extracellular space facing the postsynaptic membrane with its receptors for the transmitter. The resting calcium concentration is tightly regulated by calcium pumps and exchangers, removing the redundant calcium, while calcium channels serve to generate intracellular calcium signals by allowing a calcium inflow in order to (transiently) raise the calcium concentration. A prolonged increased intracellular calcium concentration is damaging and can even lead to cell death. Calcium channels are present in almost every excitable cell where they serve a variety of functions (Hille, 2001). Prominent among these are neurotransmitter release, gene transcription and, especially in the heart, action potential shaping and excitation contraction coupling.

Functional (voltage-gated) calcium channels consist of several subunits (Fig. 2). The α_1-subunit is the pore forming subunit that consists of four homologous domains, each with 6 transmembrane segments. The α_1-subunit can interact with several other noncovalently associated subunits, among which are the cytoplasmic β- and the transmembrane $\alpha_2\delta$-subunit. The β-subunit increases the current density and modulates both activation and inactivation kinetics (Varadi et al., 1991; Shistik et al., 1995). Furthermore, it is involved in second-messenger regulation and influences the pharmacological properties of the α_1-subunit (Moreno et al., 1997; Roche and Treistman, 1998). At this moment, four types of β-subunits have been identified. The $\alpha_2\delta$-subunit consists of two parts from a

single gene that are linked via disulfide bonds. It too has modulatory effects on the calcium current kinetics as well as pharmacological properties (Klugbauer et al., 1999).

Voltage-gated calcium currents have been divided into subtypes (Hille, 2001). These subtypes vary in their properties of activation, deactivation, inactivation and recovery from inactivation. The current that can be evoked at slightly depolarized potentials (~-40 mV) is called low-voltage-activated (LVA) or T-type. The high-voltage activated (HVA) calcium current is activated at strongly depolarized potentials (~ 0 mV). These currents can be pharmacologically separated into subtypes with the use of drugs and specific toxins. Examples of toxins inhibiting HVA calcium currents are ω-conotoxin-GVIA (N-type currents) and dihydropyridines (L-type). Recently, the different subtypes have been matched with several genes that encode for the α-subunit of the different subtypes. At this moment, three main families have been identified: Ca_V1-Ca_V3, each consisting of 3 or 4 members. Table 1 shows the different subtypes.

α_1 name	former name	Specific blocker	Current type
$Ca_V1.1$	α_{1S}	dihydropyridines	L-type
$Ca_V1.2$	α_{1C}	dihydropyridines	L-type
$Ca_V1.3$	α_{1D}	dihydropyridines	L-type
$Ca_V1.4$	α_{1F}	dihydropyridines	L-type
$Ca_V2.1$	α_{1A}	ω-Agatoxin-IVA	P/Q-type
$Ca_V2.2$	α_{1B}	ω-conotoxin-GVIA	N-type
$Ca_V2.3$	α_{1E}	-	R-type
$Ca_V3.1$	α_{1G}	Kurtoxin, mibefradil	T-type
$Ca_V3.2$	α_{1H}	Kurtoxin, mibefradil	T-type
$Ca_V3.3$	α_{1I}	Kurtoxin, mibefradil	T-type

Table 1: Voltage gated calcium channel genes and the associated current subtype.

Action potentials in fast myelinated nerve fibers are carried by sodium channels. The nodes of Ranvier contain, besides the sodium channels, also potassium channels, but calcium channels are absent (Waxman and Ritchie, 1993). However, the slow unmyelinated C-fibers do contain calcium channels (Quasthoff et al., 1996; Mayer et al., 1999). Several lines of research indicate a role for calcium channels in pain transmission, in particular the N- and T-type. Modifying the T-type currents in vivo has shown that they are involved in pain transmission. Agents that selectively enhance T-type currents result in exaggerated thermal and mechanical nociception, whereas T-type current reducing agents do the opposite (Todorovic et al., 2001). Apparent contradictory results were found in mice lacking one of the T-type channels (Kim et al., 2003). There T-type currents were shown to have an anti-nociceptive role, albeit in the central nervous system rather than peripheral. The N-type, which is the main subtype of calcium current present in dorsal root ganglia, plays a role too. Mice lacking the N-type calcium channel gene $Ca_V2.2$ show suppressed responses to painful stimuli (Saegusa et al., 2001). Furthermore, intrathecally applied ziconotide (synthetic form of ω-conotoxin-MVIIA), an N-type calcium current blocker, has been shown to have analgesic effects in humans (Cox, 2000). Although the exact roles remain to be determined, it is clear that calcium channels are involved in pain transmission.

Potassium channels

Potassium channels are the most diverse group of ion channels (Gutman et al., 2003). Their functions in excitable cells range from setting the membrane potential to shaping the action potential and modulating firing patterns (Hille, 2001).

The voltage gated potassium channels (K_V) are structurally similar to the voltage gated calcium channels. However, the α-subunit of the K_V channels is homologous to a single domain in the Ca_V-α1-subunit. With both the NH_2- and the COOH-terminal in the cytoplasm, it has six transmembrane segments with a pore loop between the fifth and the sixth segment. Four of these subunits together form a tetramere, which acts as a functional channel.

Kv1		Shaker-related	
	Kv1.1	Delayed rectifier	drg
	Kv1.2	Delayed rectifier	drg
	Kv1.3	Delayed rectifier	drg
	Kv1.4	A-type current	drg
	Kv1.5	Delayed rectifier	drg
	Kv1.6	Delayed rectifier	drg
	Kv1.7	Delayed rectifier	
	Kv1.8	Delayed rectifier	
Kv2		Shab-related	
	Kv2.1	Delayed rectifier	drg
	Kv2.2	Delayed rectifier	drg
Kv3		Shaw-related	
	Kv3.1	Delayed rectifier	drg
	Kv3.2	Delayed rectifier	drg
	Kv3.3	A-type current	
	Kv3.4	A-type current	drg
Kv4		Shal-related	
	Kv4.1	A-type current	drg
	Kv4.2	A-type current	drg
	Kv4.3	A-type current	drg
Kv5			
	Kv5.1	Modifier of Kv2 channels	
Kv6			
	Kv6.1	Modifier of Kv2 channels	
	Kv6.2	Modifier	
	Kv6.3	Modifier	
Kv7			
	Kv7.1	Delayed rectifier	
	Kv7.2	Delayed rectifier, M-current	drg
	Kv7.3	Delayed rectifier, M-current	drg
	Kv7.4	Delayed rectifier	drg
	Kv7.5	Delayed rectifier, M-current	drg
Kv8			
	Kv8.1	Modifier	
Kv9			
	Kv9.1	Modifier	drg
	Kv9.2	Modifier	drg
	Kv9.3	Modifier	

K_V10		Ether-a-go-go (EAG)	
	$K_V10.1$	Delayed rectifier, also conducts Ca^{2+}	
	$K_V10.2$	Outward rectifying	
K_V11		Ether-a-go-go-related (ERG)	
	$K_V11.1$	ERG, inward rectifier	drg
	$K_V11.2$	ERG	drg
	$K_V11.3$	ERG	drg
K_V12		Ether-a-go-go-like	
	$K_V12.1$	ELK, slow activation/deactivation	
	$K_V12.2$	ELK	
	$K_V12.3$	ELK, slow activation	

Table 2: Family of voltage activated potassium channels (K_V) with a short description and demonstrated presence in dorsal root ganglia (drg).

The K_V channels can be divided into several families (Coetzee et al., 1999). Table 2 shows the known K_V channels and their possible prevalence in dorsal root ganglions. The most common K_V channels are homologous to the channel families found in the insect genus *Drosophila*, which were identified first: Shaker ($K_V1.x$), Shab ($K_V2.x$), Shaw ($K_V3.x$) and Shal ($K_V4.x$). In addition, in mammals several other families have been found (K_V5-K_V12).

The Shaker potassium currents display two kinds of inactivation, N- and C-type inactivation, referring to the N- and C-terminus, respectively. N-type inactivation involves a ball-and-chain mechanism, where the N-terminus of each of the four subunits forms an inactivation particle that can reversibly occlude the channel pore (Hoshi et al., 1990). Independent of this N-type inactivation is C-type inactivation. The latter type of inactivation is a result of conformational changes in the selectivity filter and the outer pore mouth (Liu et al., 1996).

Different types of these K_V-channels can form heteromultimeric channels with properties distinct from homomultimeric channels (Isacoff et al., 1990; Ruppersberg et al., 1990). Although not all combinations seem to be found in vivo, this results in an enormous number of possible channel variants that allow cells to 'mold' their own potassium currents according to the required functions.

Like for calcium channels, auxiliary subunits can be added to modify the current. The most well defined group of these subunits is the Kvβ-subunits. This β-

subunit has been found to bind to the α-subunit of the Shaker-related Kv1 family (Sewing et al., 1996). It lacks transmembrane segments and binds noncovalently to the cytoplasmic N-terminus of the α-subunit in a 1:1 stochiometry. So, functional channels contain four α- and four β-subunits. At this moment, three Kvβ-genes have been identified, each with several splice variants. Although the effects that the β-subunits have on the ion currents seem to depend on the α-subunit composition of the channels, in general they accelerate N-type inactivation (Pongs et al., 1999). Another modulatory protein associated with a subgroup of the K_V channels is the KchAP. Its role has not been clarified, but there are indications that it acts as a chaperone protein (Kuryshev et al., 2000).

The combination with the different auxiliary subunits gives rise to an extra increase in diversity of the already highly diverse group of voltage gated potassium channels.

Kv1.1 is one of the major K_V-subunits and it plays an important role in different functional areas. Kv1.1 is present in developing neurons where it has been suggested to be involved in migration of neurons (Hallows and Tempel, 1998). Furthermore, several human disorders, like epilepsy and episodic ataxia, have been linked to Kv1.1 channels (Browne et al., 1994; Smart et al., 1998). And most relevant to this thesis, it plays an important role in pain transmission. Mice treated with antisense oligonucleotide of the Kv1.1 gene lack central analgesia induced by morphine and baclofen (Galeotti et al., 1997). Studies with mice lacking the Kv1.1 gene showed that the mice had hyperalgesia compared to the wildtype mice (Clark and Tempel, 1998). Also, a decreased efficacy of morphine was found in these null mutant mice. These studies show that Kv1.1 plays and important role in nociceptive and antinociceptive signaling pathways.

A special form of voltage gated potassium channels are the *erg* or Kv11 channels. *Erg* channels are homologous to the Drosophila *ether-a-go-go* channels. This name was derived from the mutant behavior, which displayed 'go-go-dancing' upon exposure to ether. In humans, the *erg* channels were originally thought to mainly play a role in the heart. There they are responsible for the action potential repolarizing current (Curran et al., 1995). Certain mutations in these channels are responsible for long QT syndrome, causing cardiac arrhythmias. However, more recent studies have revealed three different genes encoding for

erg in mammals (Shi et al., 1997), two of which (*erg2* and *erg3*) are specific to the nervous system. In mice it has been shown that all three variations are expressed in the dorsal root ganglia (Polvani et al., 2003). In neurons, the *erg* channels are linked to neuro-excitablility (Sacco et al., 2003).

Currents conducted by *erg* channels are characterized by a slow activation gate. A relatively fast C-type inactivation gate prevents a large current upon depolarization. However, subsequent repolarizing results in a fast relieve of inactivation, leading to an increase in current, despite a smaller driving force. This is due to a drastic increase in conductance by a fast recovery from inactivation, whereas the deactivation process takes much more time. It is this last feature that makes the *erg* channels excellent models for studying deactivation.

LOCAL ANESTHETICS

Local anesthetics have important functional properties, since regional application to nerve tissue results in a local block of nerve impulse conduction, which is reversible leaving no damage. These properties make the local anesthetics invaluable for surgical or dental procedures, which do not require or even cannot stand general anesthesia. After discovery of the first local anesthetic cocaine, from the leaves of the coca shrub, many would follow; all with slightly different properties (cf. Fig. 3). The molecular structure they share consists of hydrophilic and hydrophobic domains separated by an intermediate ester (e.g. butamben, Fig. 3) or amide linkage (e.g. lidocaine). It is generally accepted that the major mechanism of action of local anesthetics involves their interaction with one or more specific binding sites on or inside the voltage gated sodium channel (Ragsdale et al., 1994; Wang et al., 2000), the predominant ion channel type causing excitability in nerve and muscle cells. The resulting inhibition of the sodium current prevents the generation and conduction of the action potential. At least, this seems to be the case for peripheral nerve block. In epidural and spinal anesthesia, however, the mechanism may be more complex.

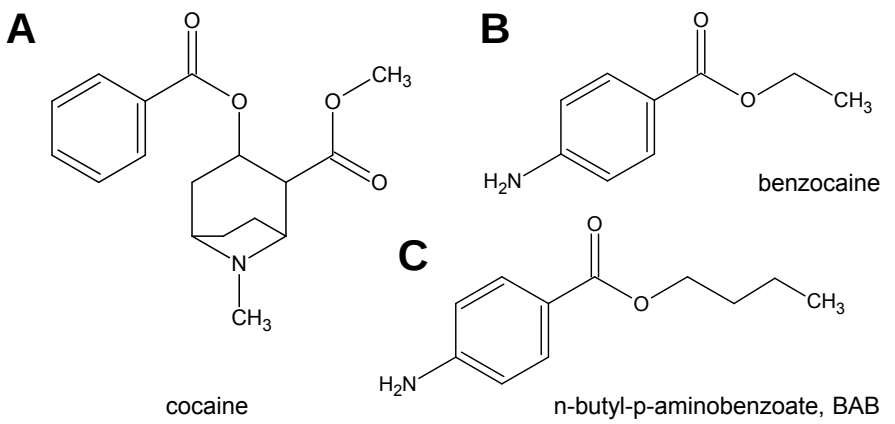

Figure 3: Comparison of the molecular structures of the local anesthetic esters cocaine, benzocaine and butamben (n-butyl-p-aminobenzoate, BAB).

It is likely to involve, besides sodium channels, other targets, such as calcium channels (Butterworth and Strichartz, 1990).

The local anesthetic n-butyl-p-aminobenzoate (abbreviated as BAB), the object of study of the present thesis, consists of a butyl ester-linked to an aminobenzoate (Fig. 3). This makes it very similar to the widely used local anesthetic benzocaine, which is an ethyl ester-linked to an aminobenzoate. The ester linkage ensures that the local anesthetic can be broken down by cholinesterase. BAB, also known as butamben, was considered of low usability, since its use was limited to topical anesthesia, due to very low water solubility (~140 mg/l at room temperature). So, soon after its development in the early twentieth century it was almost forgotten. More recently however, a renewed interest in this drug came when Shulman described ultra-long lasting selective analgesia in his patients with a 10 % aqueous suspension of BAB (Shulman, 1987). A suspension is a condition of a substance whose particles are dispersed through a fluid but not dissolved in it. Epidural injections of the BAB suspension lead to reduction of the pain for up to several months without impairing motor function. These observations have been confirmed by Korsten et al. (1991) in the

early 90s and they could even improve conditions for preparing the suspension (Grouls et al., 1991).

The long lasting effect of BAB on patients can be explained by the slow release of BAB from the suspension particles to their surroundings. The suspension serves as a depot. The question remains why BAB shows better results in selectively suppressing pain than other local anesthetics. The low octanol/water partition coefficient and the low permeability of the dura-arachnoid barrier are the unique parameters that are likely to be involved (Grouls et al., 1997; Grouls et al., 2000). However, the actual mechanism by which BAB displays its action is still unknown, but ion channels are likely targets, because ion channel block would directly affect signal transduction and transmission in pain transmitting neurons.

METHODS AND TECHNIQUES

The patch–clamp technique

The main technique used in this thesis is the patch-clamp technique in its whole-cell configuration (Hamill et al., 1981). The principle on which it is based is very simple and is known as Ohm's law: V=I*R, where V is the voltage (in Volt, V), I is the current (in Ampere, A) and R the resistance (in Ohm, Ω), the inverse of conductance G (in Siemens, S; thus, R=1/G). The idea is to get one electrode at the intracellular side of the cell membrane and another on the extracellular side and measure the resistance (or conductance) of the membrane (Fig. 4). In that configuration the bilayered membrane is the largest resistor between the two electrodes, thus any leak of current through transmembrane ion channels can easily be measured upon applying voltage across the membrane. The ions in the intra- and extracellular solution act as charge carriers. The charge and the direction of flow of the ions determine the sign of the current. For example, positive ions moving from the intracellular recording electrode through the membrane to the outside of the cell constitute positive (outward) current. The variable membrane resistance (R_V) or conductance (G_V) can be measured with

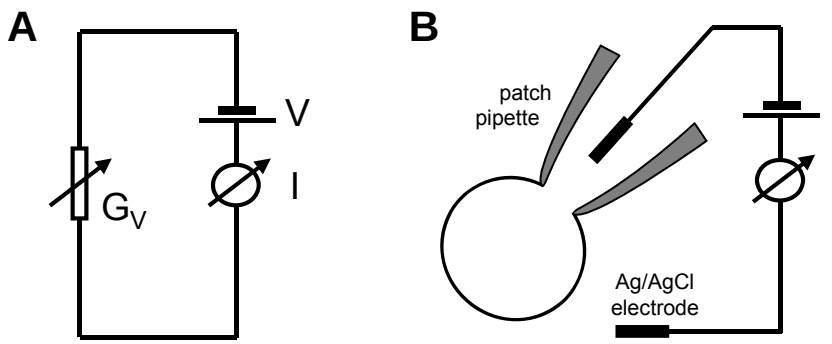

Figure 4: Schematic presentation of the voltage clamp set-up. (A) With a constant voltage source (V) and a current meter (I) the variable membrane conductance Gv can be measured. (B) Voltage-clamp conductance measurement as in (A), but with the variable conductance Gv exchanged by the membrane in the whole-cell configuration. Both the electrodes in the bath and pipette are Ag/AgCl-electrodes.

either a voltage source and a current meter in series or a current source and a voltage meter in parallel. The first method is called voltage clamp (Fig. 4A) and the latter current clamp (not shown).

To get the two electrodes at both sides of the membrane a glass pipette filled with a conducting ion solution and an inserted electrode is brought to the cell. The tip of this pipette seals with its opening to the cell membrane. With the second reference electrode in the extracellular bath solution, the configuration obtained is called the cell-attached mode. This mode allows the recording of single channel currents (in voltage-clamp) in a membrane patch of an undisrupted cell. By applying a suction pulse one can open the cell from the cell-attached mode. The membrane in the pipette mouth then breaks locally and the pipette solution will flow freely into the intracellular space, now to replace the intracellular solution. The electrode in the pipette is then in direct electrical contact with the inside of the cell membrane. This is the whole-cell configuration used in this thesis (Fig. 4B). Other possible patch-clamp measurement configurations (See Hamill et al., 1981) are not described here. The currents obtained in the whole-cell are a sum of all the currents through individual channels. When measuring from a patch containing only a small number of channels, it is possible to see the channel opening and closing of individual

channels. These so-called single channel measurements allow you to measure the actions of single protein molecules. Few techniques allow you to look at the functional behavior of single molecules on such a fast time scale. Therefore, patch clamping is a very useful technique that is implemented in a wide variety of research areas.

Other than using regular voltage or current clamp it is possible to make a combination of these techniques, the so-called 'action potential clamp' (Doerr et al., 1989). By recording an action potential in current clamp mode and applying the measured action potential shape in the voltage clamp mode to the cell, one can see the ion current flow during an action potential. During a normal action potential the individual ion channels can be considered as 'voltage-clamped' by the majority of the other channels. The 'applied' voltage in that case also has the shape of the action potential. By applying the same action potential to an isolated current type, like calcium currents, to be obtained by blocking all other channels, it is possible to see the calcium current in a more natural way.

Drug application and perfusion

Several problems or possible artifacts accompany drug application. When investigating the effect of a certain drug on ionic currents it is important to make sure that the effects measured are caused by the drug and not by other events. For instance, the ionic currents should be measured with a constant flow of extracellular solution. Changes in the velocity or direction of the flow may have direct effects on the current amplitude and kinetics (Bouskila and Bostock, 1998).

Another problem can be that the actual concentration reaching the cell is not the same as the dissolved concentration. This is important for substances that can be degraded, or be absorbed by materials present in the experimental setup. Notorious is the tubing that often is used for perfusion. 'Loading' the tubes with the used concentration before the actual experiment can prevent a lot of trouble. In all cases it is important to check the actually applied concentration with other methods where possible. The hydrophobic BAB has at room temperature a maximum solubility of ~700 µM. Making solutions with concentrations close to this maximum should be done very carefully. Ethanol, in which BAB dissolves very easily, can be used as an intermediate solvent, but

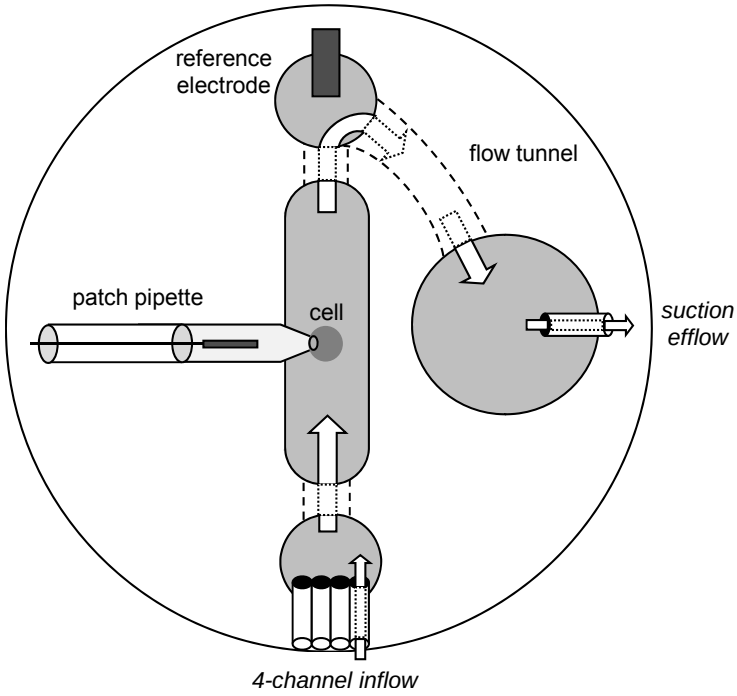

Figure 5: Schematic presentation of the micro-superfusion system used in this thesis, showing a stainless steel multi-chambered disk (19 mm diameter, 1 mm height), which could be placed inside a culture dish. Four micro-baths had been excavated in the disk and were connected through submerged tunnels, as shown in the figure (not on scale). The recording bath (~3x11 mm), drawn with cell with connected patch pipette, has a volume of ~32 µl. The shape results in a constant laminar flow feeded by one of the four superfusion inlets. The separation of the inflow and outflow from the recording bath limits the disturbing effects of vibration of the liquid. The flow is driven by gravity and was set in our experiments at ~300 µl/min. As a result the medium is fully replaced within approximately 30 s.

implies that control experiments have to be done in order to check whether the solvent or vehicle is responsible for any of the measured effects. Preheating the solutions (not too high, keeping in mind that BAB has its melting point at 58˚C) and constant stirring are necessary to prevent the formation of BAB crystals, which can take a long time to dissolve again. Furthermore, BAB binds very easily to polyethylene tubing as well as filters. BAB concentration can be checked using a spectrophotometer at a wavelength of 292 nm (Grouls et al., 1991). Absorption should be directly correlated with BAB concentration.

A schematic presentation of the perfusion system is shown in Figure 5. It consists of a coin-like piece of metal with an excavated elongated micro-bath (~32 µl), which can be inserted into the cell chamber in the set-up. Access holes for the perfusion tubes and the reference electrode and connecting micro-perfusion tunnels are also illustrated. Further explanations are provided in the legend.

In the present thesis all these precautions have been taken to study the effects of BAB.

Ion current isolation by subtraction

Highly specific blockers of ion channels can be used to identify currents from a single type of ion channel. Examples in this thesis are dendrotoxin-K and ω-conotoxin-GVIA. Dendrotoxin-K is a component of the fast and dangerous black mamba (*Dendroaspis polylepis*) venom (Harvey, 2001). Untreated envenomation by a black mamba causes death by paralysis of the respiration muscles. The 7-kDa dendrotoxin-K peptide has a high specificity for Kv1.1 subunits. Only homomultimeric channels with Kv1.1 subunits and heteromultimeric channels with two adjacent Kv1.1 subunits are blocked by dendrotoxin-K in the nanomolar range (Wang et al., 1999). The marine cone snail *Conus geographus* produces among other toxins ω-conotoxin-GVIA in its venom. With a harpoon-like tooth it injects its venom, which causes fish to become paralyzed (Olivera et al., 1991). Although the snails hunt mainly fish, the stinging can be fatal to humans as well. The ω-conotoxin-GVIA is specific for the $Ca_v2.2/\alpha_{1B}$- subunit or N-type calcium channels (Regan et al., 1991).

In our experiments the specificity of these peptides is used to discriminate between different types of current. For ω-conotoxin-GVIA that would be the N-type calcium current and for dendrotoxin-K, this is the Kv1.1 potassium current. If a certain toxin blocks only channels of interest, then the remaining current represents all channels insensitive to the drug. By subtracting the remaining current from the control or total current, the drug-sensitive current can be obtained.

It is difficult to look at effects of other drugs, e.g. BAB, on the subtracted currents, though not impossible as shown in the present thesis. Since the toxins block the channels irreversibly, the toxin-sensitive current can only be obtained

once in every cell. So, one cannot obtain paired data from the same cell (control and drug-affected currents) on the effects of BAB on the subtracted current. However, the subtraction can be done in the presence of different concentrations of BAB. If the whole toxin application and subtraction is done in the presence of concentration x, the subtracted current will represent the toxin-sensitive component in the presence of x µM BAB. This results in unpaired toxin-sensitive currents, which can be analyzed as a function of BAB concentration x.

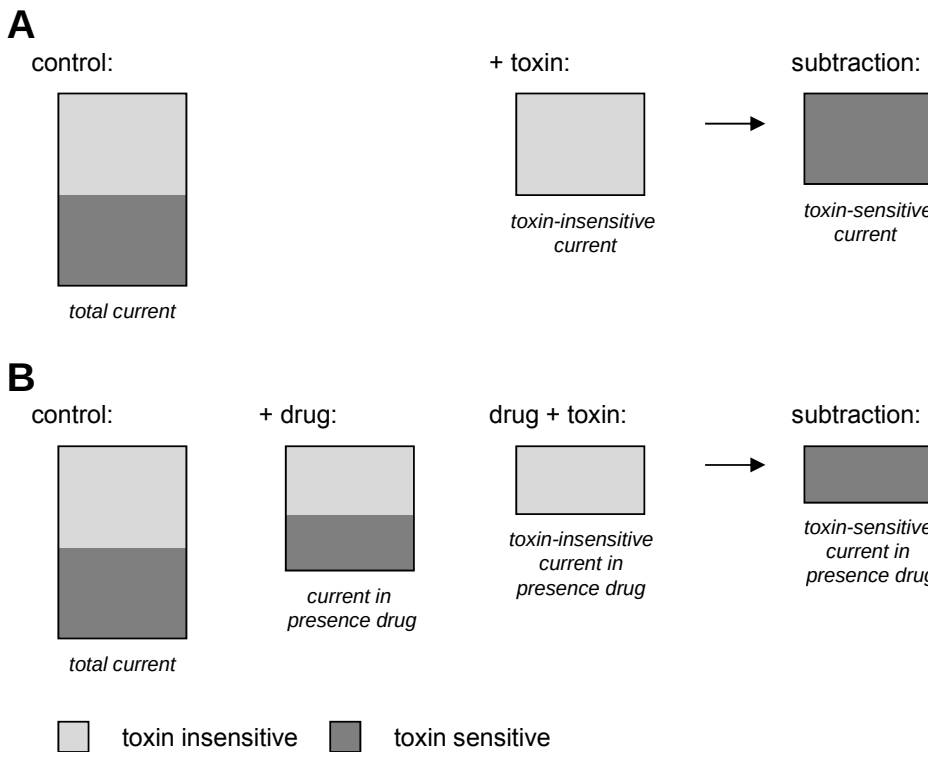

Figure 6: Schematic presentation of combined subtraction method. (A) Control subtraction procedure where the remaining current after toxin application is subtracted from the control current. The resulting current represents the toxin-sensitive current. (B) Before toxin application a drug (e.g. BAB) is applied resulting in a reduction of the total current. In the presence of this drug the toxin is applied. By subtracting the remaining current after drug- and toxin application from the current after drug-, but before toxin application one obtains the toxin-sensitive current in the presence of the drug. The drug concentration can be varied in a population of cells. So, the resulting subtracted currents can be used as unpaired data for constructing a concentration response relation.

This subtraction method is illustrated in Figure 6. Since the specific blockers bind irreversibly to the channels, as opposed to BAB, the BAB application is unlikely to interfere with the steady-state toxin binding and vice versa. Effects of variations between individual cells are diminished by an increasing number of experiments. With the same idea, the kinetics of the obtained subtracted currents can also be analyzed.

The method of subtraction demands stable conditions. Whole-cell parameters, like membrane capacity and series resistance, should stay constant during the application of the toxin. Therefore, the subtracted current traces should not show capacitive transients or membrane leak, since these would reflect changes in at least one of the parameters.

The method of subtraction is a valuable tool, but has an increased number of possible artifacts and misinterpretations, so the researcher should be extra alert.

Cloned versus native ion channels

Since the introduction of the patch clamp technique, ion currents have been measured in cells in primary culture, i.e. cells directly isolated from a tissue from the living animal. The channels conducting the ionic currents have been expressed by the cells under physiological conditions in a functional organism. With the identification of the genes encoding the ion channel proteins it became possible to bring the appropriate coding DNA or RNA into other cell systems where the channels can be expressed by the 'host' cell. Using expression systems with relatively small own 'native' conductances, it is possible to create uniform currents encoded by a known single gene. The two methods working with either cloned or native ion channels have both their advantages and supplement each other.

In the present study we used primary cultures of dorsal root ganglion (DRG) neurons (Figs 1, 7A) obtained from neonatal mice. We also used cultered undifferentiated PC12 cells (Fig. 7B). This cancer cell line has been established in the 70s of the 20^{th} century from a transplantable rat adrenal pheochromocytoma. PC12 cells grow slowly, have features resembling chromaffin cells and have functional voltage gated calcium channels (Avidor et al., 1994). Finally, we used the HEK-tsA201 cell line as an artificial ion channel

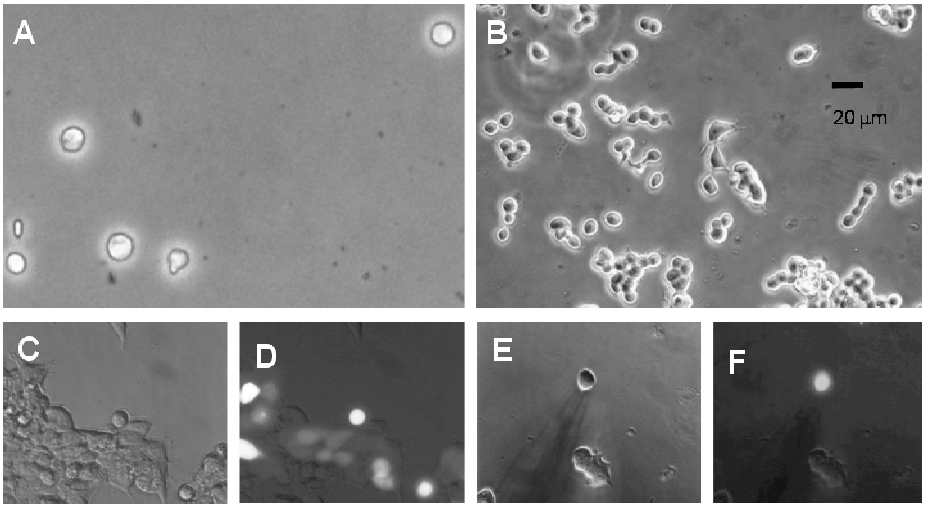

Figure 7: (A) Primary culture of acutely dissociated neonatal mouse DRG neurons within a few hours after dissociation, as seen with phase contrast microscopy. The phase-bright round sensory neuron somata are ~20 µm in diameter. The neurons have not yet grown neuronal processes at this stage, which is a requirement for good voltage-clamp recording of membrane currents. (B) phase-contrast photo of low density culture of undifferentiated PC12 cells, as used in the experiments of Chapter 5. Note the rounded morphology of the small dividing cells and the flattened polygonal cells, spreading on the dish. (C) Transfected ~50% confluent tsA-201 cell cultures (one to a few days old), as used in this study, photographed with phase contrast microscopy. The cDNA encoding for cytoplasmic Green Fluorescent Protein (GFP) is coexpressed with the cDNA of the chosen ion channel, but the transfected cells cannot be recognized with phase contrast illumination. (D) The culture in 'B' is shown with fluorescent illumination in order to identify the transfected cells. The emission at a wavelength of 508 nm during excitation with 395 nm is shown. A high correlation exists between cells expressing cytoplasmic GFP (green fluorescing at various intensities) and expressing the cotransfected ion channel. (E,F) An isolated single cell in a culture just prior to the cell-attached configuration is shown with phase contrast (E) and with fluorescence (F) illumination. The shadows in panels 'E' and 'F' in the bottom left of the pictures are the patch pipette. Isolated single cells were chosen, because coupling to neighbour cells spoils the quality of the voltage-clamp recording of whole-cell membrane currents. Cell diameter of the rounded cells in panels 'C' to 'F' is ~20 µm.

expression system (Fig. 7C-F). The advantage of using native cells is that it reveals the currents to be studied in the presence of its naturally associated processes. The membrane- or cytoplasm composition can be different between cells. This difference can have effects on the functioning of the expressed ion

channels. Furthermore, ion channels can be part of a bigger (yet unidentified) complex affecting the functioning of the channels. Finally, modulatory factors are present in these native dissociated neurons. The advantages of using cell line cultures like PC12 is that they are easily available and do not require sacrificing laboratory animals. Although their properties may have changed during long term culturing, they are often useful for specific questions. In conclusion, in native cells ion channels can be studied in their physiological environment.

The tsA201 cell line (Margolskee et al., 1993) is a subclone of HEK293 cells (Human Embryonic Kidney). tsA201 cells have a limited number of native ion channels, but have the possibility to incorporate cDNA and express the encoded protein in vast amounts. If the cells express a protein they normally lack, it is called heterologous expression (Fig. 7C,E). In order to get the DNA in the cell cytoplasm, several techniques have been developed. A well known method to transfer DNA into the cells uses a calcium-phosphate/plasmid precipitate, which enters the cell via endocytosis (Graham and van der Eb, 1973). In Chapter 2 of this thesis we used DOTAP, a cationic liposome, which associates in a complex manner with the DNA, in order to transfer it into the cell. The complex has been characterized as a "spaghetti-and-meatball" structure (Lasic, 1997; Zuidam and Barenholz, 1998). In Chapter 6 of this thesis we used a similar alternative, the commercially available Lipofectamine 2000, which is also a cationic lipid-based transfection reagent.

The advantage of studying expressed cloned ionic currents versus native ion currents is that the gene encoding the ion channel is known and that its product can be studied in isolation. When studying ion channels in cellular or multicellular processes it is beneficiary to combine the two methods, since the results will complement each other, making it easier to come to solid conclusions. Where the expressed ion channels give information about isolated interactions, the native channels allow you to study properties of ion channels in their physiological environment and therefore investigate the physiological roles of these properties.

AIM OF THIS STUDY

The mechanism of selective analgesia by BAB is still unknown. Effects of BAB on voltage-gated sodium channels in sensory neurons have been described before (Van den Berg et al., 1995; Van den Berg et al., 1996). However, the effects observed in the treated patients are unlikely to be caused by effects on sodium channels alone (Butterworth and Strichartz, 1990). So, in order to explain how BAB works, it is important to look at the effects of BAB on all ion channel types involved in pain signal transmission. The obtained results do not only give information about the mechanism of selective analgesia, but they also provide information about local anesthetic action in general and lead to more insight in the physiology of the studied ion channels.

In the present thesis study we have investigated the effects of BAB on non-sodium voltage-activated channels expected to be important in pain fiber excitability, e.g. potassium and calcium channels. In Chapter 2 we first report on the effect of BAB on native total K_V and Kv1.1 current in DRG neurons and on cloned Kv1.1 channels expressed in tsA cells. BAB turned out to reduce both native total K_V currents (including Kv1.1) and cloned Kv1.1 currents while at the same time accelerating activation, deactivation and inactivation. In Chapter 3 we explored the effect of BAB on calcium channels and on N-type channels in particular. These currents were also reduced with accelerated kinetics. In Chapter 4 we focus on BAB-effects on the low-voltage activated T-type calcium currents in dorsal root ganglion neurons and see similar effects. Chapter 5 reveals that L-type calcium currents in PC12 cells are sensitive to BAB as well and in Chapter 6 we take a look at effects of BAB on the hERG potassium current. Because the simultaneous current reduction and kinetics acceleration by BAB were key features of the effects of BAB on all channels investigated in this thesis, they were put into several mathematical models in order to shed light on the mechanism behind the BAB effects at the ion channel level.

All investigated channels are present in the dorsal root ganglia in considerable numbers (Carbone and Lux, 1984; Doerr et al., 1989; Beckh and Pongs, 1990; Polvani et al., 2003) and may be involved in pain physiology or have already been shown to do so (Galeotti et al., 1997; Clark and Tempel, 1998; Hatakeyama et al.,

2001; Kim et al., 2001; Saegusa et al., 2001; Todorovic et al., 2001). Finally, we integrate in a general discussion (Chapter 7) all the results in a general picture of the mechanism of action of BAB on voltage activated cation channels and of possible mechanisms of the specific analgesic action of epidural BAB suspensions in the treatment of intractable pain.

References

Avidor B, Avidor T, Schwartz L, De Jongh KS, Atlas D (1994) Cardiac L-type Ca2+ channel triggers transmitter release in PC12 cells. FEBS Lett 342:209-213.

Beckh S, Pongs O (1990) Members of the RCK potassium channel family are differentially expressed in the rat nervous system. EMBO J 9:777-782.

Bouskila Y, Bostock H (1998) Modulation of voltage-activated calcium currents by mechanical stimulation in rat sensory neurons. Journal Of Neurophysiology 80:1647-1652.

Browne DL, Gancher ST, Nutt JG, Brunt ER, Smith EA, Kramer P, Litt M (1994) Episodic ataxia/myokymia syndrome is associated with point mutations in the human potassium channel gene, KCNA1. Nat Genet 8:136-140.

Butterworth JFt, Strichartz GR (1990) Molecular mechanisms of local anesthesia: a review. Anesthesiology 72:711-734.

Candido K, Stevens RA (2003) Intrathecal neurolytic blocks for the relief of cancer pain. Best Pract Res Clin Anaesthesiol 17:407-428.

Carbone E, Lux HD (1984) A low voltage-activated, fully inactivating Ca channel in vertebrate sensory neurones. Nature 310:501-502.

Clark JD, Tempel BL (1998) Hyperalgesia in mice lacking the Kv1.1 potassium channel gene. Neurosci Lett 251:121-124.

Coetzee WA, Amarillo Y, Chiu J, Chow A, Lau D, McCormack T, Moreno H, Nadal MS, Ozaita A, Pountney D, Saganich M, Vega-Saenz dM, Rudy B (1999) Molecular diversity of K+ channels. Ann NY AcadSci 868:233-285.

Cox B (2000) Calcium channel blockers and pain therapy. Curr Rev Pain 4:488-498.

Curran ME, Splawski I, Timothy KW, Vincent GM, Green ED, Keating MT (1995) A molecular basis for cardiac arrhythmia: HERG mutations cause long QT syndrome. Cell 80:795-803.

Djouhri L, Lawson SN (2004) Abeta-fiber nociceptive primary afferent neurons: a review of incidence and properties in relation to other afferent A-fiber neurons in mammals. Brain Res Brain Res Rev 46:131-145.

Doerr T, Denger R, Trautwein W (1989) Calcium currents in single SA nodal cells of the rabbit heart studied with action potential clamp. Pflugers Arch 413:599-603.

Donnelly S, Davis MP, Walsh D, Naughton M (2002) Morphine in cancer pain management: a practical guide. Support Care Cancer 10:13-35.

Galeotti N, Ghelardini C, Papucci L, Capaccioli S, Quattrone A, Bartolini A (1997) An antisense oligonucleotide on the mouse Shaker-like potassium channel Kv1.1 gene prevents antinociception induced by morphine and baclofen. J Pharmacol Exp Ther 281:941-949.

Ganong WF (2003) Review of Medical Physiology. , 21st Edition. New York: McGraw-Hill.

Graham FL, van der Eb AJ (1973) Transformation of rat cells by DNA of human adenovirus 5. Virology 54:536-539.

Grouls R, Korsten E, Ackerman E, Hellebrekers L, van Zundert A, Breimer D (2000) Diffusion of n-butyl-p-aminobenzoate (BAB), lidocaine and bupivacaine through the human dura-arachnoid mater in vitro. Eur J Pharm Sci 12:125-131.

Grouls RJ, Ackerman EW, Machielsen EJ, Korsten HH (1991) Butyl-p-aminobenzoate. Preparation, characterization and quality control of a suspension injection for epidural analgesia. Pharm Weekbl Sci 13:13-17.

Grouls RJ, Ackerman EW, Korsten HH, Hellebrekers LJ, Breimer DD (1997) Partition coefficients (n-octanol/water) of N-butyl-p-aminobenzoate and other local anesthetics measured by reversed-phase high-performance liquid chromatography. J Chromatogr B Biomed Sci Appl 694:421-425.

Gutman GA, Chandy KG, Adelman JP, Aiyar J, Bayliss DA, Clapham DE, Covarriubias M, Desir GV, Furuichi K, Ganetzky B, Garcia ML, Grissmer S, Jan LY, Karschin A, Kim D, Kuperschmidt S, Kurachi Y, Lazdunski M, Lesage F, Lester HA, McKinnon D, Nichols CG, O'Kelly I, Robbins J, Robertson GA, Rudy B, Sanguinetti M, Seino S, Stuehmer W, Tamkun MM, Vandenberg CA, Wei A, Wulff H, Wymore RS (2003) International Union of Pharmacology. XLI. Compendium of voltage-gated ion channels: potassium channels. Pharmacol Rev 55:583-586.

Hallows JL, Tempel BL (1998) Expression of Kv1.1, a Shaker-like potassium channel, is temporally regulated in embryonic neurons and glia. J Neurosci 18:5682-5691.

Hamill OP, Marty A, Neher E, Sakmann B, Sigworth FJ (1981) Improved patch-clamp techniques for high-resolution current recording from cells and cell-free membrane patches. Pflugers Arch 391:85-100.

Harvey AL (2001) Twenty years of dendrotoxins. Toxicon 39:15-26.

Hatakeyama S, Wakamori M, Ino M, Miyamoto N, Takahashi E, Yoshinaga T, Sawada K, Imoto K, Tanaka I, Yoshizawa T, Nishizawa Y, Mori Y, Niidome T, Shoji S (2001) Differential nociceptive responses in mice lacking the alpha(1B) subunit of N-type Ca(2+) channels. Neuroreport 12:2423-2427.

Hille B (2001) Ionic Channels of Excitable Membranes. Sunderland MA: Sinauer Associates.

Hoshi T, Zagotta WN, Aldrich RW (1990) Biophysical and molecular mechanisms of Shaker potassium channel inactivation. Science 250:533-538.

Isacoff EY, Jan YN, Jan LY (1990) Evidence for the formation of heteromultimeric potassium channels in Xenopus oocytes. Nature 345:530-534.

Kim C, Jun K, Lee T, Kim SS, McEnery MW, Chin H, Kim HL, Park JM, Kim DK, Jung SJ, Kim J, Shin HS (2001) Altered nociceptive response in mice deficient in the alpha(1B) subunit of the voltage-dependent calcium channel. Mol Cell Neurosci 18:235-245.

Kim D, Park D, Choi S, Lee S, Sun M, Kim C, Shin HS (2003) Thalamic control of visceral nociception mediated by T-type Ca2+ channels. Science 302:117-119.

Klugbauer N, Lacinová L, Marais E, Hobom M, Hofmann F (1999) Molecular diversity of the calcium channel alpha2delta subunit. J Neurosci 19:684-691.

Korsten HH, Ackerman EW, Grouls RJ, van Zundert AA, Boon WF, Bal F, Crommelin MA, Ribot JG, Hoefsloot F, Slooff JL (1991) Long-lasting epidural sensory blockade by n-butyl-p-aminobenzoate in the terminally ill intractable cancer pain patient. Anesthesiology 75:950-960.

Kuryshev YA, Gudz TI, Brown AM, Wible BA (2000) KChAP as a chaperone for specific K(+) channels. Am J Physiol Cell Physiol 278:C931-C941.

Lasic DD (1997) Liposomes in Gene Delivery: CRC Press.

Liu Y, Jurman ME, Yellen G (1996) Dynamic rearrangement of the outer mouth of a K+ channel during gating. Neuron 16:859-867.

Margolskee RF, McHendry-Rinde B, Horn R (1993) Panning transfected cells for electrophysiological studies. Biotechniques:906-911.

Mayer C, Quasthoff S, Grafe P (1999) Confocal imaging reveals activity-dependent intracellular Ca2+ transients in nociceptive human C fibres. Pain 81:317-322.

Moreno H, Rudy B, Llinas R (1997) beta subunits influence the biophysical and pharmacological differences between P- and Q-type calcium currents expressed in a mammalian cell line. PNAS 94 (25):14042-14047.

Olivera BM, Rivier J, Scott JK, Hillyard DR, Cruz LJ (1991) Conotoxins. J Biol Chem 266:22067-22070.

Polvani S, Masi A, Pillozzi S, Gragnani L, Crociani O, Olivotto M, Becchetti A, Wanke E, Arcangeli A (2003) Developmentally regulated expression of the mouse homologues of the potassium channel encoding genes m-erg1, m-erg2 and m-erg3. Gene Expr Patterns 3:767-776.

Pongs O, Leicher T, Berger M, Roeper J, Bahring R, Wray D, Giese KP, Silva AJ, Storm JF (1999) Functional and molecular aspects of voltage-gated K+ channel beta subunits. Ann NY Acad Sci 868:344-355.

Quasthoff S, Adelsberger H, Grosskreutz J, Arzberger T, Schroder JM (1996) Immunohistochemical and electrophysiological evidence for omega- conotoxin-sensitive calcium channels in unmyelinated C-fibres of biopsied human sural nerve. Brain Res 723:29-36.

Ragsdale DS, McPhee JC, Scheuer T, Catterall WA (1994) Molecular determinants of state-dependent block of Na+ channels by local anesthetics. Science 265:1724-1728.

Regan LJ, Sah DW, Bean BP (1991) Ca2+ channels in rat central and peripheral neurons: high-threshold current resistant to dihydropyridine blockers and omega-conotoxin. Neuron 6:269-280.

Roche JP, Treistman SN (1998) The Ca2+ channel beta(3) subunit differentially modulates G-protein sensitivity of alpha(1A) and alpha(1B) Ca2+ channels. J Neurosci 18 (3):878-886.

Ruppersberg JP, Schroter KH, Sakmann B, Stocker M, Sewing S, Pongs O (1990) Heteromultimeric channels formed by rat brain potassium-channel proteins. Nature 345:535-537.

Sacco T, Bruno A, Wanke E, Tempia F (2003) Functional roles of an ERG current isolated in cerebellar Purkinje neurons. J Neurophysiol 90:1817-1828.

Saegusa H, Kurihara T, Zong S, Kazuno A, Matsuda Y, Nonaka T, Han W, Toriyama H, Tanabe T (2001) Suppression of inflammatory and neuropathic pain symptoms in mice lacking the N-type Ca2+ channel. EMBO J 20:2349-2356.

Sewing S, Roeper J, Pongs O (1996) Kv beta 1 subunit binding specific for shaker-related potassium channel alpha subunits. Neuron 16:455-463.

Shi W, Wymore RS, Wang HS, Pan Z, Cohen IS, McKinnon D, Dixon JE (1997) Identification of two nervous system-specific members of the erg potassium channel gene family. J Neurosci 17:9423-9432.

Shistik E, Ivanina T, Puri T, Hosey M, Dascal N (1995) Ca2+ current enhancement by alpha 2/delta and beta subunits in Xenopus oocytes: contribution of changes in channel gating and alpha 1 protein level. J Physiol 489 (Pt 1):55-62.

Shulman M (1987) Treatment of cancer pain with epidural butyl-amino-benzoate suspension. Regional Anesth 12:1-4.

Smart SL, Lopantsev V, Zhang CL, Robbins CA, Wang H, Chiu SY, Schwartzkroin PA, Messing A, Tempel BL (1998) Deletion of the K(V)1.1 potassium channel causes epilepsy in mice. Neuron 20:809-819.

Todorovic SM, Jevtovic-Todorovic V, Meyenburg A, Mennerick S, Perez-Reyes E, Romano C, Olney JW, Zorumski CF (2001) Redox modulation of T-type calcium channels in rat peripheral nociceptors. Neuron 31:75-85.

Van den Berg RJ, Wang Z, Grouls RJ, Korsten HH (1996) The local anesthetic, n-butyl-p-aminobenzoate, reduces rat sensory neuron excitability by differential actions on fast and slow Na+ current components. Eur J Pharmacol 316:87-95.

Van den Berg RJ, Van Soest PF, Wang Z, Grouls RJ, Korsten HH (1995) The local anesthetic n-butyl-p-aminobenzoate selectively affects inactivation of fast sodium currents in cultured rat sensory neurons. Anesthesiology 82:1463-1473.

Varadi G, Lory P, Schultz D, Varadi M, Schwartz A (1991) Acceleration of activation and inactivation by the beta subunit of the skeletal muscle calcium channel. Nature 352:159-162.

Wang FC, Bell N, Reid P, Smith LA, McIntosh P, Robertson B, Dolly JO (1999) Identification of residues in dendrotoxin K responsible for its discrimination between neuronal K+ channels containing Kv1.1 and 1.2 alpha subunits. Eur J Biochem 263:222-229.

Wang SY, Nau C, Wang GK (2000) Residues in Na(+) channel D3-S6 segment modulate both batrachotoxin and local anesthetic affinities. Biophys J 79:1379-1387.

Waxman SG, Ritchie JM (1993) Molecular dissection of the myelinated axon. Ann Neurol 33:121-136.

Zuidam NJ, Barenholz Y (1998) Electrostatic and structural properties of complexes involving plasmid DNA and cationic lipids commonly used for gene delivery. Biochim Biophys Acta 1368:115-128.

CHAPTER 2

KV1.1 CHANNELS OF DORSAL ROOT GANGLION NEURONS ARE INHIBITED BY N-BUTYL-P-AMINOBENZOATE, A PROMISING ANESTHETIC FOR THE TREATMENT OF CHRONIC PAIN

J.P. Beekwilder, M.E. O'Leary, L.P. van den Broek, G.Th.H. Van Kempen, D.L. Ypey and R.J. Van den Berg.

J Pharmacol Exp Ther (2003) 304:531-8

ABSTRACT

In this study, we investigated the effects of the local anesthetic n-butyl-p-aminobenzoate (BAB) on the delayed rectifier potassium current of cultured dorsal root ganglion (DRG) neurons using the patch clamp technique. The majority of the K current of small DRG neurons rapidly activates and slowly inactivates at depolarized voltages. BAB inhibited the whole-cell K current of these neurons with an IC_{50} of 228 μM. Dendrotoxin K (DTX_K), a specific inhibitor of Kv1.1, reduced the DRG K current at +20 mV by 34%, consistent with an important contribution of channels incorporating the Kv1.1 subunit to the delayed rectifier current. To further investigate the mechanism of BAB inhibition, we examined its effect on Kv1.1 channels heterologously expressed in mammalian tsA201 cells. BAB inhibits the Kv1.1 channels with an IC_{50} of 238 μM, similar to what was observed for the native DRG current. BAB accelerates the opening and closing of Kv1.1, but does not alter the midpoint of steady state activation. BAB appears to inhibit Kv1.1 by stabilizing closed conformations of the channel. Co-expression with the Kvβ1 subunit induces rapid inactivation and reduces the BAB sensitivity of Kv1.1. Comparison of the heterologously expressed Kv1.1 and native DRG currents indicates that the Kv β1 subunit does not modulate the gating of the DTX_K-sensitive Kv1.1 channels of DRG neurons. Inhibition of the delayed rectifier current of these neurons may contribute to the long duration anesthesia attained during the epidural administration of BAB.

Epidural administration of local anesthetics is a widely used technique for achieving short-term regional anesthesia. A promising new approach for the management of chronic pain is the epidural administration of sustained release formulations of local anesthetics. For example, epidural injections of the local anesthetic n-butyl-p-aminobenzoate (BAB) has proved to be effective in treating the intractable pain associated with advanced stages of cancer (Korsten et al., 1991; Shulman et al., 1998). A single epidural treatment with BAB can effectively relieve chronic pain for prolonged intervals (>30 days). Surprisingly, the pain relief produced by BAB is not associated with any demonstrable loss of motor function suggesting that BAB selectively targets the nociceptive nerve fibers of the dorsal root (Korsten et al., 1991; Shulman et al., 1998; McCarthy et al., 2002). Because BAB is hydrophobic and uncharged at physiological pH, it partitions into lipid bilayers but does not effectively distribute into the systemic circulation (Kuroda et al., 2000; Shulman et al., 1998). The analgesia produced by BAB is highly localized with no detectable anesthesia in adjacent spinal segments (Korsten et al., 1991; Grouls et al., 2000). The absence of significant side effects coupled with the long duration anesthesia provides considerable support for the use of BAB formulations in the treatment of chronic pain.

The mechanism of BAB anesthesia and the origin of its highly selective block of nociception is not known. Studies of the mechanisms of BAB anesthesia have focused on small dorsal root ganglion (DRG) neurons as the most likely site of BAB action. In patch-clamp studies, BAB was found to inhibit the voltage-gated sodium currents of these neurons (Van den Berg et al., 1995; Van den Berg et al., 1996) which are believed to include the cell bodies of pain fibers (cf. Harper and Lawson, 1985). Small DRG neurons express several distinct components of Na current that differ in gating kinetics and sensitivity to tetrodotoxin (TTX) (Kostyuk et al., 1981; Roy and Narahashi, 1992). The TTX-sensitive and TTX-resistant Na currents of cultured DRG neurons display considerable differences in sensitivity to BAB (Van den Berg et al., 1995; Van den Berg et al., 1996). The inhibition of DRG Na currents is likely to contribute to the BAB anesthesia.

By comparison, the role of K channels in peripheral nerve anesthesia has not been extensively investigated. In large part, this reflects our rather sparse understanding of the K channels that are expressed in peripheral nerves and their role in the electrical excitability of these neurons. A variable combination of rapidly inactivating A-type (I_A) and slowly or non-inactivating (I_K) K currents are observed in most DRG neurons (Kostyuk et al., 1981; Gold et al., 1996; Akins and McCleskey, 1993). Pharmacological studies suggest that the I_A and I_K components of DRG K current can be further subdivided into several distinct components (Safronov et al., 1996). Current estimates suggest that as many as six different channels may contribute to the outward K current in these neurons (Gold et al., 1996). Dendrotoxin, a selective inhibitor of Kv1 channels (Harvey, 2001), induces repetitive action potential firing of sensory neurons by selectively inhibiting the delayed rectifier current (Hall et al., 1994; Penner et al., 1986; Stansfeld et al., 1986; Stansfeld et al., 1987; McAlexander and Undem, 2000; Glazebrook et al., 2002). The message encoding for Kv1.1 is present in the DRG (Beckh and Pongs, 1990; Glazebrook et al., 2002) and immunocytochemistry indicates that Kv1.1 channels are expressed in small DRG neurons (Hallows and Tempel, 1998; Ishikawa et al., 1999; Glazebrook et al., 2002). In addition, Kv1.1 knockout mice display hyperalgesia, consistent with an important role for these channels in nociception (Clark and Tempel, 1998).

In this study, we found that BAB produces a concentration-dependent inhibition of the whole-cell K current of cultured DRG neurons. Dendrotoxin K (DTX_K), a specific inhibitor of channels incorporating the Kv1.1 subunit (Robertson et al., 1996), inhibited the slowly inactivating K current of small DRG neurons indicating that Kv1.1 channels contribute to the delayed rectifier current in these cells. The mechanism of BAB inhibition was further investigated by examining its effect on Kv1.1 channels expressed in mammalian cells. BAB produces a concentration-dependent inhibition of the heterologously expressed Kv1.1 that is comparable to that observed for the native DRG K current. The data suggest that BAB inhibition of DRG Kv1.1 channels may contribute to the long-duration anesthesia produced by the epidural administration by this drug.

METHODS

Neonatal mice were sacrificed by decapitation in accordance with the standards of the Animal Ethical Committee of Leiden University Medical Center. The dorsal root ganglia (DRG) from all accessible levels of the spinal cord were collected and mechanically dissociated on a glass coverslip coated with poly-L-lysine (Mol. Wt. 70,000-150,000; Sigma) in 0.5 ml of F-12 Ham Kaighn's modified media supplemented with $CaCl_2$ (0.15 g/l), glutamine (0.29 g/l), $NaHCO_3$ (2.5 g/l), glucose (7.0 g/l) and 10% horse serum (GibcoBRL). The ganglia cells were allowed to attach to the coated glass coverslips for 2.5 h in a humidified 5% CO_2 atmosphere at 37°C after which an additional 2 ml of F-12 medium was added. The cells were cultured for 3-8 hours before selecting small (~20 μm) spherical neurons devoid of neurite outgrowth for patch clamp experiments.

The cDNAs of the rat[1] Kv1.1 potassium channel and the Kvβ1 subunit (Rettig et al., 1994), were subcloned into pcDNA3.1(-) (Invitrogen, San Diego, CA). The cDNA for eGFP (Clontech, Palo Alto, CA) was subcloned into pcDNA3.1(+) vectors (Invitrogen, San Diego, CA). tsA201 cells were cotransfected with cDNA encoding Kv1.1 and cDNA encoding for GFP, a green fluorescent marker that facilitates the identification of transfected cells, in a 1:1 ratio. The Kv1.1/GFP cDNA mixture was added to 0.5 ml of DMEM (Sigma) enriched with 10% fetal bovine serum (GibcoBRL) and 1% penicillin-streptomycin (Sigma). 25μl of 1,2-dioleoyl-sn-glycero-3-trimethylammonium-propane (DOTAP) (Roche Diagnistics GmbH, Mannheim, Germany) was slowly added and incubated for 15 min at room temperature. The cDNA/DOTAP mix was transferred to a 100-mm culture dish of 50% confluent tsA201 cells bathed in 10 ml of enriched DMEM. After 3 hours, the transfection solution was removed and replaced with 20 ml of enriched DMEM. After 24 hours, the cells were replated on glass coverslips. The cells were incubated an additional 12-24 hours before selecting GFP-positive cells (excitation: 488 nm, emission 507 nm) for use in patch-clamp studies. For experiments with the Kvβ1 subunit tsA201 cells were cotransfected with Kv1.1, GFP and Kvβ1 in a 1:1:2 ratio.

[1] In J Pharmacol Exp Ther (2003) 304:531-8 wrongly referred to as human

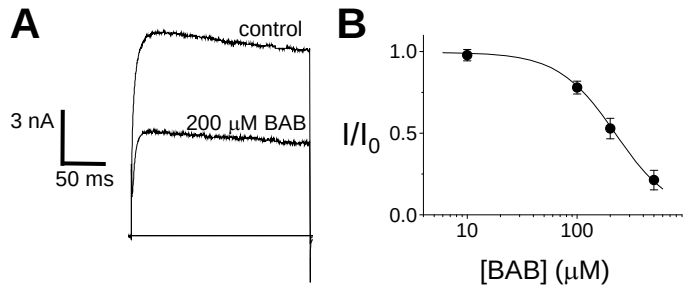

Figure 1. BAB inhibition of the native K current of small DRG neurons. A. Whole-cell patch clamp recording of K current from an acutely dissociated DRG neuron. Currents were elicited by depolarizing to +20 mV from a holding potential of –80 mV. Current recorded from the same cell is shown before and after the bath application of 200 μM BAB. B. Currents measured in the presence of BAB were normalized to drug-free controls and plotted versus the concentration. The smooth curve is a fit to the Hill equation $I/I_O = (1+([BAB]/IC_{50})^n)^{-1}$ with an IC_{50} of 223 ± 10 μM and Hill coefficient of 1.7 ± 0.1 (n = 32).

For the patch clamp experiments, a cover slip was mounted in a small perfusion chamber (75 μl) and continuously perfused (~300 μl/min) with extracellular solution. Patch pipettes were fabricated from borosilicate glass (Clark GC-150 TF-15) on a custom two-stage horizontal puller and had resistances between 1 and 2 MΩ. For DRG neurons the external solution consisted of (in mM): NaCl 35, KCl 5, $MgCl_2$ 3, HEPES 10, Sucrose 180, pH 7.35 (NaOH) with 300 nM tetrodotoxin (Sigma). The pipette solution was (in mM): NaCl 20, KCl 118, EGTA 5, HEPES 10, MgATP 2, pH 7.35 (NaOH). In experiments with tsA201 cells the extracellular solution consisted of (in mM): NaCl 136, KCl 2, $CaCl_2$ 1.5, $MgCl_2$ 1, HEPES 10, pH 7.4 (NaOH) . The pipette solution was (in mM): KCl 115, $MgCl_2$ 1, EGTA 10 HEPES 10, pH 7.4 (KOH). BAB was added to the extracellular solution from a stock of BAB in ethanol (1-500 μM). The final ethanol concentration in the extracellular solution was in all cases, including control experiments, 0.1 %. Dendrotoxin-K (Alomone, Jerusalem, Israel) was dissolved in distilled water before dilution in extracellular solution to a final concentration of 10 nM. Voltage pulses were generated by pClamp 8 (Axon Instruments, Foster City, CA) and recorded using a List EPC 7 patch-clamp amplifier (List Medical, Darmstadt, Germany). The series resistance of the patch pipettes was 75% compensated and current recordings were filtered at 3 kHz. All currents were leak subtracted using P/4 subtraction.

Membrane capacitance of the cells was estimated from the decay of the transient elicited by a 10 mV depolarizing voltage pulse from a –80 mV holding potential.

The concentration-inhibition data were fitted to the Hill equation: $I/I_o = (1 + ([BAB]/IC_{50})^n)^{-1}$, where the IC_{50} is the concentration at which the current is reduced by 50% and n is the Hill coefficient. The activation data obtained from tail current measurements (Figure 4) were fitted to the Boltzmann equation: $I/I_o = (1+\exp-((V-V_{0.5})/k))^{-1}$ where V is the prepulse potential, $V_{0.5}$ the voltage at which the current is half maximally activated, and k is the slope factor. Unless otherwise stated the data are the Means $\pm$ SD for a given number (n) of cells.

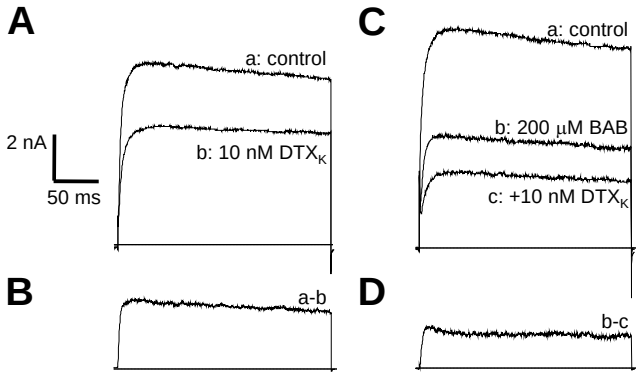

Figure 2. Inhibition of K current in a DRG neuron by dendrotoxin-K (DTX_K). A. K current elicited by depolarizing to +20 mV from a holding potential of –80 mV. Currents are shown before and after the bath application of 10 nM DTX_K. Currents were reduced 34 $\pm$ 7% by comparison to controls (n=7). B. The DTX_K-sensitive component of the DRG current (a-b) was isolated by subtracting the residual current remaining after application of DTX_K from the total DRG current in A. C. K current elicited by depolarizing to +20 mV from a holding potential of –80 mV. Currents are shown in control conditions, and after the sequential application of 200 μM BAB and 10 nM DTX_K + 200 μM BAB. D. The DTX_K-sensitive component as obtained by subtracting the current measured in the presence of BAB + DTX_K from the current measured in the presence of 200 μM BAB alone (b-c). Calibration bars in A apply to all panels.

RESULTS

BAB inhibition of the endogenous K current of dorsal root ganglion (DRG) neurons

To investigate the role of K channels in the BAB anesthesia, we used the patch-clamp technique to measure the whole-cell K current of small cultured DRG neurons (≈20 μm, 14 ± 3 pF, n=49), which are believed to represent the cell bodies of nociceptive pain fibers. The outward K currents were isolated by blocking sodium currents with tetrodotoxin (300 nM) and by applying test pulses close to the sodium reversal potential to minimize the contribution of the remaining TTX-resistant current. Calcium currents and calcium-activated currents were eliminated by removing external calcium and by including EGTA in the patch pipette. Cells were held at –80 mV and currents were elicited by depolarizing steps to +20 mV (Figure 1A). The majority of the K current in these cells appears to be best classified as the slowly inactivating or non-inactivating variety. Only a relatively minor contribution of the rapidly inactivating I_A component was observed in our study. Bath application of BAB (200 μM) reduced the amplitude of the current (Figure 1A). BAB inhibited the whole-cell K current of the small DRG neurons in a concentration-dependent fashion with an IC_{50} of 223 ± 10 μM (Figure 1B).

Kv1.1 channels contribute to the delayed rectifier current of DRG neurons

At least four distinct components have been shown to contribute to the slowly inactivating and sustained K current of DRG neurons but the molecular identities of the underlying channels have not been established (Safronov et al., 1996). Previous studies have shown that small DRG neurons express a slowly inactivating dendrotoxin-sensitive K current, suggesting that members of the Kv1 family may contribute to the delayed rectifier current in these cells (Hall et al., 1994; Penner et al., 1986; Stansfeld et al., 1986; Stansfeld et al., 1987; McAlexander and Undem, 2000; Glazebrook et al., 2002). To further investigate the channels underlying the slowly inactivating K current, we applied dendrotoxin-K (DTX_K), a specific inhibitor of Kv1.1 channels (Robertson et al., 1996). DTX_K (10 nM) decreased the whole-cell K current of DRG neurons by 34 ± 7 % (n=7) (Figure 2A). The DTX_K-sensitive component of the DRG current was

isolated by subtracting the current remaining after application of DTX_K from the total K current (Figure 2B). The DTX_K-sensitive component rapidly activated and displayed little inactivation during the 250 ms depolarization. The high sensitivity to DTX_K indicates that Kv1.1 channels, or heteromultimeric channels incorporating the Kv1.1 subunit, contribute to the slowly inactivating K current in these neurons.

We attempted to gain additional insight into the mechanism of BAB inhibition by investigating the overlap of the BAB- and DTX_K-sensitive components of the native DRG K current. In the absence of BAB, DTX_K (10 nM) inhibited 34% of the DRG current. This contrasts with what is observed in presence of 200 μM BAB (Figure 2C+2D) which significantly (p=0.001) reduced the relative amplitude of the DTX_K–sensitive current (20 $\pm$ 5 %, n=6). This suggests that the toxin and BAB inhibit a common component of the DRG K current. The relative amplitude of the DTX_K-sensitive current was further reduced by pre-applying 500 μM BAB (9 ± 4 %, n=6, $p=1\cdot10^{-5}$) providing additional support inhibition of DTX_K-sensitive current by BAB. The high selectivity of DTX_K indicates that the reduction in the amplitude of the native DRG K current, at least in part, results from the inhibition of Kv1.1 channels. In many cases, high concentrations of BAB (500 μM) completely inhibited the DRG K current suggesting that in addition to Kv1.1, other delayed rectifier currents were inhibited at these concentrations.

BAB inhibition of heterologously expressed Kv1.1 channels

To further investigate the mechanism of BAB inhibition, the cDNA encoding for Kv1.1 was heterologously expressed in tsA201 cells. At +20 mV, the Kv1.1 channels rapidly activated but only slowly inactivated similar to the DTX_K-sensitive component of DRG K current (Figure 3A). BAB inhibited the homomultimeric Kv1.1 channels in a concentration-dependent fashion with an IC_{50} of 238 $\pm$ 10 μM (Figure 3B), similar to what is observed for the native DRG current. In addition to reducing the amplitude, BAB caused the current to decay more rapidly. In the absence of drug, the current decay could be well fitted by a single exponential with a time constant of 373 $\pm$ 47 ms and a relative amplitude of 0.26 $\pm$ 0.02 (n = 4). This is likely to reflect the slow inactivation of Kv1.1 channels. After application of 200 μM BAB, the peak current was reduced by 53 $\pm$ 2% and the decay time course was found to be biexponential with time

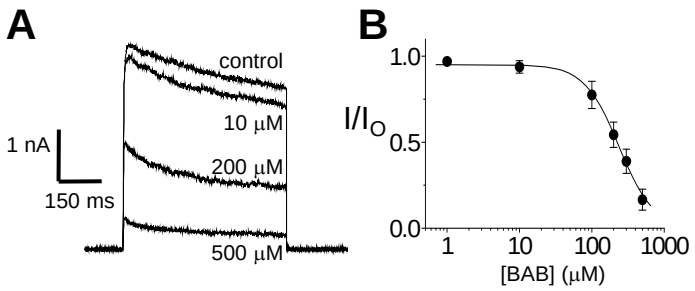

Figure 3. BAB inhibition of homotetrameric Kv1.1 channels. A. The Kv1.1 channel was heterologously expressed in tsA201 cells and currents were recorded by depolarizing to +20 mV from a holding potential of –80 mV. BAB (10 – 500 μM) progressively inhibits the whole-cell K current of the Kv1.1 channels. B. The current measured in the presence of BAB was normalized to drug-free control currents and plotted versus concentration. The smooth curve is a fit to the Hill equation with IC_{50} and Hill coefficient of 238 ± 10 μM and 1.8 ± 0.1 respectively. The data are means ± SD of 8-9 determinations at each concentration.

constants (relative amplitudes) of 36 ± 2 ms (0.11 ± 0.02) and 301 ± 56 ms (0.35 ± 0.01) respectively (n = 4). BAB induced a new rapid component of current decay and increased the relative amplitude of the slow component by comparison to drug-free controls. The data suggest that BAB may enhance the slow inactivation of Kv1.1. However, the onset of this component is too slow to account for the large reduction in the peak amplitude of the current. Other mechanisms, which have faster kinetics or that reduce the probability that a channel will open are likely to play a more prominent role in the BAB inhibition of these channels.

We also examined the effect of BAB on the reversal potential and activation gating of the Kv1.1 channels. For voltages between –80 and 0 mV the instantaneous current amplitudes were determined from the peak of the tail currents (Figure 4A) which were normalized and plotted versus the voltage (Figure 4B). Over this range of voltages, the current-voltage (I-V) relationship is linear with an extrapolated reversal potential of –89 ± 7 mV. Also plotted is the I-V relationship determined after the application of 200 μM BAB which has a reversal potential of -91 ± 11 mV. Although the peak current amplitudes are reduced, the reversal potentials are not significantly different indicating that BAB does not alter the selectivity of Kv1.1 channels (paired t-test, n=8).

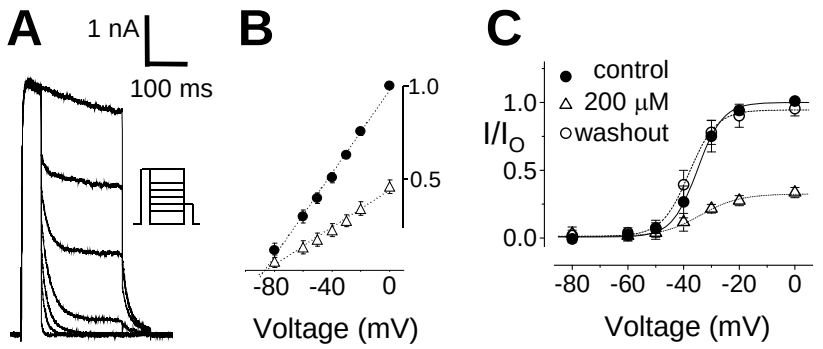

Figure 4. Effect of BAB on reversal potential and Kv1.1 activation. A. Currents were activated by stepping for 50 ms to 0 mV before applying a series of 200 ms test pulses to voltages between –80 and 0 mV followed by a step to –50 mV before returning to the holding potential. B. The current-voltage relationship was determined by measuring the peak amplitudes of the tails elicited by the variable voltage pulses. The currents were normalized to the current measured at 0 mV and plotted versus the voltage. The data are the means ± SD for 8 individual experiments. C. The activation was determined by plotting the normalized peak currents elicited by the –50 mV tail currents versus the prepulse voltage. The smooth curves are fits to a Boltzmann function with midpoints and slope factors of –35 ± 3 mV and 4.6 ± 1.0 mV for controls and –34 ± 3 mV and 7.0 ± 1.3 mV after application of 200 μM BAB (n = 8).

The effect of BAB on the activation of Kv1.1 was investigated by plotting the normalized peak amplitudes of the tail currents versus the prepulse potential (Figure 4C). In the absence of drug, the normalized current-voltage relationship was fitted to a Boltzmann function with a midpoint ($V_{0.5}$) and slope factor (k) of –35 ± 3 mV and 4.6 ± 1.0 mV respectively (n = 8). BAB (200 μM) reduced the tail current amplitudes but did not alter the midpoint of steady state activation ($V_{0.5}$ = -34 ± 3 mV). These effects were completely reversed upon removing BAB from the bath. The data indicate that in the presence of BAB, Kv1.1 channels display a reduced open probability or unitary conductance relative to the drug-free controls that cannot be attributed to a change in the voltage dependence of channel activation or selectivity. BAB may inhibit the Kv1.1 current through changes in the kinetics of gating or a reduction in the channel conductance.

BAB accelerates the activation and deactivation of Kv1.1 channels

Figure 5 shows Kv1.1 current measured at –30 mV before and immediately after the bath application of 200 μM BAB. The currents have been normalized to facilitate the comparison of the kinetics. BAB accelerates both the activation and deactivation time course of the current. To quantitatively compare the activation, we determined the time required for the current to reach its half-maximal amplitude. In eight paired experiments the half-maximal rise times were 10.7 $\pm$ 1.7 ms and 6.0 $\pm$ 1.0 ms before and after application of 200 μM BAB respectively. BAB significantly accelerates the rising phase of the current (paired t-test, $p<0.001$), an effect that cannot be attributed to a shift in the voltage dependence of activation (Figure 4B). We also examined the effect of BAB on the kinetics of activation at +20 mV, a voltage where the channels are maximally activated. At +20 mV the times to half of maximum amplitude were 2.6 $\pm$ 0.4 ms for controls and 2.4 $\pm$ 0.4 ms after application of BAB (n = 9). In the absence of drug, the half-maximal rise times at +20 mV were reduced by comparison to those measured at –30 mV and are consistent with the strong voltage dependence of Kv1.1 activation. Although the relative difference in the rise times of the control and drug-treated current at +20 mV is small, it was found to be significant in a paired t-test ($p<0.002$). This indicates that the more rapid rise

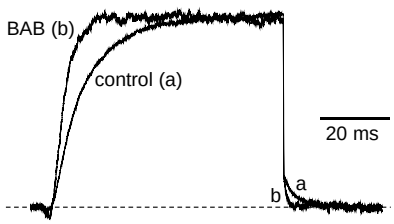

Figure 5. Superimposed Kv1.1 currents measured at –30 mV before and after application of 200 μM BAB. The amplitude of the current measured in the presence of BAB was normalized to the control in order to facilitate the comparison of the activation kinetics. The time course of activation was quantitatively evaluated by comparing the time required for the current to reach the half-maximal peak amplitude (see text).

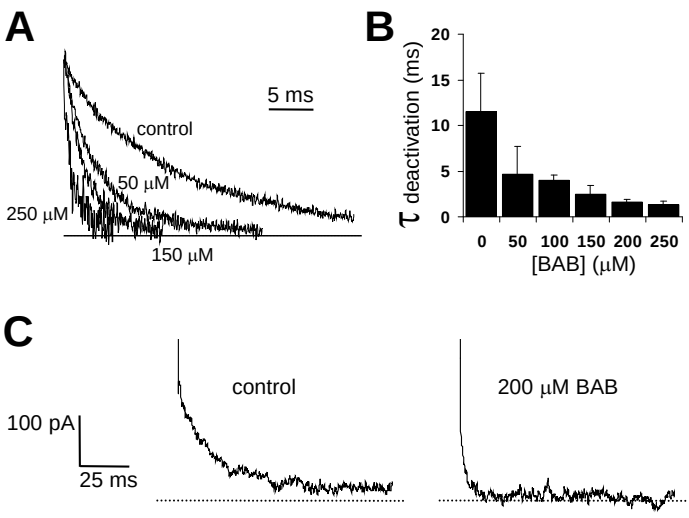

Figure 6. BAB accelerates the deactivation of Kv1.1 channels. A. Potassium currents evoked by a step to +20 mV for 50 ms and the tail currents measured upon return to –65 mV. The superimposed tail currents are shown before (control) and after the bath application of 50, 150 and 250 μM BAB. B. The decay of the tail current was fitted with a single exponential and the resulting time constants plotted versus the concentration (n = 7). C. Effect of BAB on the DTX_K-sensitive tail currents of cultured DRG neurons. The DTX_K-sensitive component was obtained by subtracting the current remaining after application of the toxin (10 nM) from the total K current (see Figure 2). The current of two cells are shown in the absence (left) and presence (right) of 200 μM BAB.

of the current observed after application of BAB results from a genuine increase in the activation kinetics and does not reflect contamination by deactivation, which is likely to contribute to the apparent activation kinetics at the less depolarized (-30 mV) test potential.

In addition to its effects on activation, BAB also enhances the deactivation of Kv1.1. Figure 6A shows a family of normalized Kv1.1 tail currents measured before and after application of BAB (50 – 250 μM). BAB accelerates the deactivation of the channels in a concentration-dependent fashion (Figure 6B). Also shown are two typical tail currents of DRG neurons in the absence and presence of 200 μM BAB (Figures 6C). The tail currents are well fitted by a single exponential with time constants (τ) of 17.0 ± 5.9 ms (n = 8) in the absence and

4.0 ± 1.4 ms (n = 9) in the presence of BAB. BAB produces a similar increase in the deactivation of both the heterologously expressed Kv1.1 and the native DRG K current. Overall, the data indicate that changes in both activation and deactivation kinetics may contribute to the BAB inhibition of Kv1.1 channels.

Effect of the Kvβ subunit on the gating and BAB sensitivity of Kv1.1

Previous studies have shown that co-expressing Kv1.1 and Kvβ subunits result in a rapidly inactivating A-type current. The N-terminus of the Kvβ1 subunit is proposed to act as an inactivation particle that occludes the internal vestibule of activated Kv1.1 channels (Rettig et al., 1994). We were therefore interested in determining the effects of the Kvβ1 subunit and rapid inactivation on the BAB sensitivity of Kv1.1 channels. Co-expressing the Kvβ1 and Kv1.1 subunits resulted in current that rapidly inactivated similar to what has been previously reported for this oligomeric channel (Figure 7A). Similar to the Kv1.1 channels, BAB inhibited the Kv1.1/Kvβ1 channel in a concentration-dependent inhibition fashion. The peak currents measured before and after application of BAB were normalized to drug-free controls and plotted versus the BAB concentration (Figure 7B). BAB inhibited the current with an IC_{50} and Hill coefficient of 343 ± 10 μM and 2.1 ± 0.2, respectively (n = 17). The BAB sensitivity of Kv1.1 (IC_{50} = 238 μM) was significantly reduced by co-expressing the channel with the Kvβ1 subunit. It is not clear if the reduced inhibition results from a conformational change in Kv1.1 induced by the Kvβ1 subunit or if rapid inactivation somehow weakens BAB binding.

To further investigate the role of inactivation in the BAB inhibition we examined its effects on the steady-state inactivation of the Kv1.1/Kvβ1 channel. Depolarizing prepulses were used to inactivate the channels before applying a standard test pulse to assay availability (Figure 7C, inset). The currents elicited by the test pulses were normalized to controls measured after prolonged hyperpolarization to –80 mV and plotted versus the prepulse voltage. The relative amplitudes of the test currents progressively decrease with prepulse voltage consistent with an increase in steady-state inactivation. The smooth curves are fits to the Boltzmann function with a midpoint ($V_{0.5}$) and slope factor (k) of –53 ± 3 mV and 3.4 ± 0.2 mV respectively (n = 4). BAB (200 μM) reduces the maximal current amplitude measured at hyperpolarized voltages by 12% but

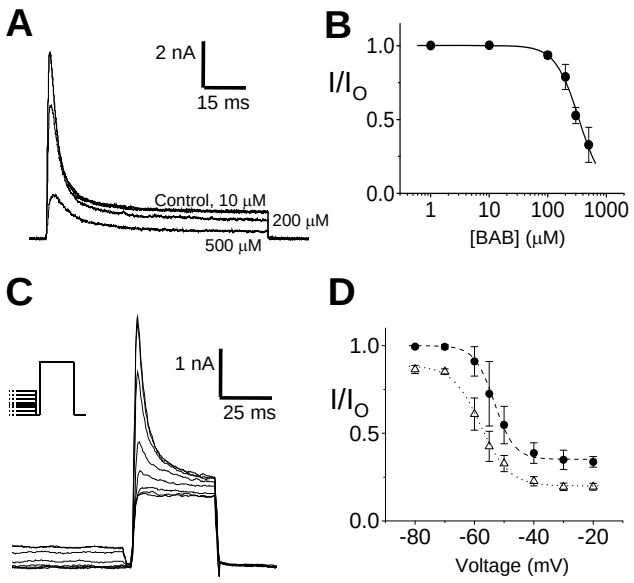

Figure 7. BAB effects on Kv1.1 channels co-expressed with the Kvβ1 subunit. A. Whole-cell current of cells expressing the Kv1.1 α and Kvβ1 subunits. Currents were elicited by depolarizing to +20 mV from a holding potential of –80 mV. Currents are shown before (control) and after bath application of 10, 200 and 500 μM BAB. B. The peak amplitude of the currents measured in the presence of BAB were normalized to the drug-free controls and plotted versus [BAB]. The smooth curve is a fit to the Hill equation with an IC_{50} of 343 ± 10 μM and coefficient of 2.1 ± 0.2. The data are means ± SD of 7 or 8 determinations at each concentration. C. The steady state inactivation was measured by applying 500 ms prepulses to voltages between –80 and –20 mV. Only the last 30 ms of the prepulses are shown for clarity. A short hyperpolarization to –80 mV for 4 ms was used to fully deactivate the channels before applying a standard test pulse to +50 mV. The peak amplitudes of the test currents were normalized to controls measured directly from the –80 mV holding voltage and plotted versus the prepulse potential. The smooth curves are fits to the Boltzmann function with midpoints and slope factors of –53 ± 3 mV and 3.4 ± 0.2 mV for controls (filled circles) and –56 ± 2 mV and 4.8 ± 0.7 mV after applying 200 μM BAB (open triangles) (n=4).

does not significantly alter the midpoint ($V_{0.5}$ = -56 ± 2 mV) or voltage sensitivity (k = 4.8 ± 0.7 mV) of inactivation. Hyperpolarizing shifts in steady-state inactivation are typical of drugs that preferentially affect channel inactivation. BAB does not inhibit the Kv1.1/Kvβ1 by preferentially interacting with the

inactivated state of the channel. Furthermore, the BAB inhibition persists at hyperpolarized voltages (-80 mV) where few of the Kv1.1/Kvβ1 channels are predicted to be inactivated. Overall, the data suggest that rapid inactivation does not play a prominent role in the BAB inhibition of Kv1.1. Conformational changes in the Kv1.1 channel induced by interaction with Kvβ1 may account for the reduced BAB sensitivity observed in these studies.

DISCUSSION

In this study, we investigated the anesthetic sensitivity of the slowly inactivating K current of small cultured DRG neurons of neonatal mice. The majority of the whole-cell K current of these neurons rapidly activates and slowly inactivates and has properties that are consistent with a delayed rectifier type current. We further investigated the role of Kv1 channels using DTX_K, a specific inhibitor of channels incorporating the Kv1.1 subunit (Wang et al., 1999). DTX_K inhibited 34% of the slowly inactivating DRG K current consistent with an important contribution of Kv1.1 to the delayed rectifier current in these neurons. This finding is in agreement with a recent study showing that DTX_K inhibits the delayed rectifier current of C-type neurons (Glazebrook et al., 2002). BAB inhibited the slowly inactivating K current of DRG neurons in a dose-dependent fashion with an IC_{50} of 223 μM. Our data indicate substantial overlap in the inhibition produced by BAB and DTX_K, supporting the conclusion that Kv1.1 channels contribute to the BAB-sensitive current in these small DRG neurons. The inhibition of Kv1.1 channels occurs within the range of BAB concentrations realized in the epidural space during the clinical administration of this drug (Grouls et al., 1997).

BAB inhibition of Kv1.1 channels

To better understand the mechanism we examined the effects of BAB on the current of heterologously expressed Kv1.1 channels. Kv1.1 rapidly activates and slowly inactivates similar to what is observed for the DTX_K-sensitive current of

DRG neurons. BAB inhibited Kv1.1 with an IC_{50} of 238 μM, which is nearly identical to what was observed for the inhibition of the native DRG K current (IC_{50} = 223 μM). In addition to reducing the current amplitude, BAB accelerated the activation and deactivation kinetics of Kv1.1 but did not produce any change in the midpoint of activation. A similar BAB-induced increase in the kinetics of deactivation was observed for the native DRG K current. Assuming a simple two state model for activation gating suggests that the opening and closing kinetics are equally enhanced by BAB. Such symmetrical changes in opening/closing rates are difficult to explain by the preferential binding of BAB to either the closed or open conformations of the channel. BAB does not appear to act by a state-dependent binding mechanism.

Several mechanisms could potentially explain the BAB inhibition of Kv1.1 channels. We initially considered that the inhibition produced by BAB could result from a channel blocking mechanism. However, simple blocking models generally predict slower deactivation because the channels often cannot close until the drug dissociates from its binding site (Armstrong, 1971). This is clearly inconsistent with the observed effects of BAB on either the heterologously expressed Kv1.1 or native DRG tail currents which were faster in the presence of the drug. BAB also induced a slow decay in the sustained current of heterologously expressed Kv1.1 that may be linked to the slow inactivation of these channels. However, the time course of this decay (τ = 36 ms) is too slow to account for the reduction in the amplitude of the peak current observed after the application of BAB. The observed kinetic changes also indicate that a reduction of single channel conductance cannot be the sole mechanism. Rather the data appears to favor an allosteric mechanism in which BAB biases the channels towards the closed state. Rapid deactivation may effectively stabilize the channels in closed (non-conducting) conformations and could account for the BAB-induced reduction in the amplitude of Kv1.1 and native K current in DRG neurons.

Co-expression of the Kvβ1 subunits confers rapid N-type inactivation on the slowly inactivating Kv1.1 channels (Rettig et al., 1994; Heinemann et al., 1996) and the message encoding for several of the Kvβ subunits is present in the sensory neurons of nodose ganglion (Glazebrook et al., 2002). Consistent with these previous findings we found that co-expressing the Kvβ1 subunit resulted in

rapid but incomplete inactivation of Kv1.1. This rapid inactivation contrasts with the native DTX_K-sensitive component of DRG K current, which slowly inactivates similar to what is observed when Kv1.1 channels are expressed alone. Our data therefore suggest that the endogenous Kv1.1 channels expressed in DRG neurons may not associate with the Kvβ1 subunit. Alternatively, Kv1.1 subunits may form heteromultimers with other Kv1 subunits (Isacoff et al., 1990; Ruppersberg et al., 1990) resulting in channels that retain sensitivity to DTX_K (Wang et al., 1999) but that are not strongly regulated by the Kvβ subunit. The rapidly inactivating Kv1.1/Kvβ1 oligomeric channel (IC_{50} = 343 μM) is considerable less sensitive to BAB than Kv1.1 (IC_{50} = 238 μM). BAB does not alter the kinetics of the current decay or steady state inactivation of the Kv1.1/Kvβ1 channels suggesting that N-type inactivation is not tightly linked to the BAB inhibition. Rather the data suggest that interaction with the Kvβ1 subunit may induce a conformational change in Kv1.1 that weakens BAB binding or that indirectly modulates the inhibitory mechanism.

Role of Kv1.1 channels in the long duration BAB anesthesia of DRG neurons

Voltage-gated K currents play an integral role in setting the resting membrane potential and in action potential repolarization, and are important determinates of spike frequency and burst adaptation (Rudy, 1988). Small DRG neurons, which are believed to reflect the cell bodies of unmyelinated C-fibers, display Kv1.1 immunoreactivity and the DRG contains RNA encoding for Kv1.1 channels (Beckh and Pongs, 1990; Hallows and Tempel, 1998;Ishikawa et al., 1999). The importance of Kv1 channels to the electrical excitability of DRG neurons is illustrated by studies showing that DTX_α, an inhibitor of several of the Kv1 channels, induces rapid repetitive firing of sensory neurons (McAlexander and Undem, 2000; Stansfeld et al., 1986; Glazebrook et al., 2002). This is further supported by studies of Kv1.1 null mice, which display hyperalgesia and reduced sensitivity to opiate therapy, symptoms frequently associated with neuropathic pain (Clark and Tempel, 1998). It suggests that the absence of Kv1.1 in the null mice causes sensory neurons to become hyperexcitable, similar to what is observed after application of DTX. This is consistent with data showing that the delayed rectifier current makes an important contribution to the resting membrane potential of small DRG neurons (Safronov et al., 1996). Overall, these

previous studies appear to be in good agreement of our data indicating that Kv1.1 channels contribute to the delayed rectifier current of DRG neurons.

A possibility is that like DTX, BAB inhibition of Kv1.1 may paradoxically increase rather than suppress the electrical excitability of DRG neurons. This might be expected to cause hyperalgesia similar to what was observed in the Kv1.1 null mice (Clark and Tempel, 1998). However, other effects of BAB should also be taken into account. Previous studies indicate that in addition to K channels, the endogenous Na currents of DRG neurons are also sensitive to BAB. At least two Na channels are known to contribute to the electrical excitability of small DRG neurons. $Na_V1.7$ is a rapidly gating TTX-sensitive Na channel and $Na_V1.8$ is a slowly gating TTX-resistant Na channel (Waxman et al., 1999). Although both channels are generally believed to contribute to the Na current of sensory neurons, Nav1.8 appears to be exclusively expressed in the cell bodies of C-fibers (Akopian et al., 1996; Sangameswaran et al., 1996). Recent work has demonstrated that low-frequency repetitive stimulation (1-2 Hz) significantly reduces the steady state availability of the $Na_V1.8$ channels, an effect that appears to be due to the unusually rapid onset of slow inactivation in these channels (Vijayaragavan et al., 2001). By comparison, $Na_V1.7$ channels are considerably less sensitive to repetitive stimulation and are more resistant to slow inactivation. Similar observations have been made for the native TTX-sensitive and TTX-resistant Na currents of DRG neurons (Rush et al., 1998;Scholz et al., 1998). BAB causes a hyperpolarizing shift of the steady-state inactivation of the TTX-sensitive Na currents (Van den Berg et al., 1995;Van den Berg et al., 1996). This is predicted to reduce the availability of these Na channels, an affect that would be exacerbated by the inhibition of Kv1.1 and depolarization of the resting membrane potential. Because of the substantial differences in the voltage dependence of the $Na_V1.7$ and $Na_V1.8$ channels, even a slight depolarization of the resting membrane potential would tend to selectively inactivate $Na_V1.7$ and therefore increase the relative amplitude of the slower gating TTX-resistant currents. This could have important implications for the firing behavior of DRG neurons (cf. Vijayaragavan et al., 2001). Inhibition of Kv1.1 may also delay and weaken the repolarization of DRG neurons following an action potential similar to what has been previously observed with DTX_K (Glazebrook et al., 2002). Delayed repolarization would tend to slow the

recovery of inactivated Na channels and further increase the refractory period for action potential firing.

Our current working hypothesis is that BAB influences the availability of ion channels responsible for maintaining the high electrical excitability of DRG neurons. BAB inhibition of Kv1.1 and peripheral nerve Na channels may contribute to the long duration anesthesia associated with the epidural administration of this drug.

ACKNOWLEDGMENTS

We thank Prof. Thomas Schmidt (Leiden University, The Netherlands) for providing us the GFP-cDNA and Dr. Manuel Covarrubias (Jefferson Medical College, Philadelphia, PA) for providing us the cDNAs for Kv1.1 and Kvβ1 and for commenting the manuscript.

References

Akins PT and McCleskey EW (1993) Characterization of potassium currents in adult rat sensory neurons and modulation by opioids and cyclic AMP. Neuroscience 56:759-769.

Akopian AN, Sivilotti L, and Wood JN (1996) A tetrodotoxin-resistant voltage-gated sodium channel expressed by sensory neurons. Nature 379:257-262.

Armstrong CM (1971) Interaction of tetraethylammonium ion derivatives with the potassium channel of giant axon. J Gen Physiol 58:413-437.

Beckh S and Pongs O (1990) Members of the RCK potassium channel family are differentially expressed in the rat nervous system. EMBO J. 9:777-782.

Clark JD and Tempel BL (1998) Hyperalgesia in mice lacking the Kv1.1 potassium channel gene. Neurosci.Lett. 251:121-124.

Glazebrook PA, Ramirez AN, Schild JH, Shieh CC, Doan T, Wible BA, Kunze DL (2002) Potassium channels Kv1.1, Kv1.2 and Kv1.6 influence excitability of rat visceral sensory neurons. J. Physiol (Lond) 541: 467-482.

Gold MS, Shuster MJ, and Levine JD (1996) Characterization of six voltage-gated K+ currents in adult rat sensory neurons. J.Neurophysiol. 75:2629-2646.

Grouls R, Korsten E, Ackerman E, Hellebrekers L, van Zundert, Breimer D. (2000) Diffusion of n-butyl-p-aminobenzoate (BAB) and bupivacaine through the human dura-arachnoid mater in vitro. Eur. J. Pharm. Sci. 12:125-131.

Grouls RJ, Meert TF, Korsten HH, Hellebrekers LJ, Breimer DD (1997) Epidural and intrathecal n-butyl-p-aminobenzoate solution in the rat. Comparison with bupivacaine. Anesthesiology 86:181-187.

Grupe A, Schroter KH, Ruppersberg JP, Stocker M, Drewes T, Beckh S, and Pongs O (1990) Cloning and expression of a human voltage-gated potassium channel. A novel member of the RCK potassium channel family. EMBO J. 9:1749-1756.

Hall A, Stow J, Sorensen R, Dolly JO, and Owen D (1994) Blockade by dendrotoxin homologues of voltage-dependent K+ currents in cultured sensory neurones from neonatal rats. Br.J.Pharmacol. 113:959-967.

Hallows JL and Tempel BL (1998) Expression of Kv1.1, a Shaker-like potassium channel, is temporally regulated in embryonic neurons and glia. J.Neurosci. 18:5682-5691.

Harper AA and Lawson SN (1985) Conduction velocity is related to morphological cell type in rat dorsal root ganglion neurones. J.Physiol (Lond) 359:31-46.

Harvey AL (2001) Twenty years of dendrotoxins. Toxicon 2001.Jan.;39.(1):15.-26. 39:15-26.

Heinemann SH, Rettig J, Graack HR, and Pongs O (1996) Functional characterization of Kv channel beta-subunits from rat brain. J.Physiol 493 (Pt 3):625-633.

Isacoff EY, Jan YN, and Jan LY (1990) Evidence for the formation of heteromultimeric potassium channels in Xenopus oocytes. Nature 345:530-534.

Ishikawa K, Tanaka M, Black JA, and Waxman SG (1999) Changes in expression of voltage-gated potassium channels in dorsal root ganglion neurons following axotomy. Muscle Nerve 22:502-507.

Korsten HH, Ackerman EW, Grouls RJ, van Zundert AA, Boon WF, Bal F, Crommelin MA, Ribot JG, Hoefsloot F, and Slooff JL (1991) Long-lasting epidural sensory blockade by n-butyl-p-aminobenzoate in the terminally ill intractable cancer pain patient. Anesthesiology 75:950-960.

Kostyuk PG, Veselovsky NS, Fedulova SA, and Tsyndrenko AY (1981) Ionic currents in the somatic membrane of rat dorsal root ganglion neurons-III. Potassium currents. Neuroscience 6:2439-2444.

Kuroda Y, Nasu H, Fujiwara Y, Nakagawa T (2000) Orientations and locations of local anesthetics benzocaine and butamben in phospholipid membranes as studied by 2H NMR spectroscopy. J. Membr. Biol. 177:117-28.

McAlexander MA and Undem BJ (2000) Potassium channel blockade induces action potential generation in guinea-pig airway vagal afferent neurones. J.Auton.Nerv.Syst. 78:158-164.

McCarthy RJ, Kerns JM, Nath HA, Shulman M, Ivankovich AD (2002) The antinociceptive and histologic effect of sciatic nerve blocks with 5% butamben suspension in rats. Anesth. Analg. 94:711-716.

Penner R, Petersen M, Pierau FK, and Dreyer F (1986) Dendrotoxin: a selective blocker of a non-inactivating potassium current in guinea-pig dorsal root ganglion neurones. Pflugers Arch. 407:365-369.

Rettig J, Heinemann SH, Wunder F, Lorra C, Parcej DN, Dolly JO, and Pongs O (1994) Inactivation properties of voltage-gated K+ channels altered by presence of beta-subunit. Nature 369:289-294.

Robertson B, Owen D, Stow J, Butler C, and Newland C (1996) Novel effects of dendrotoxin homologues on subtypes of mammalian Kv1 potassium channels expressed in Xenopus oocytes. FEBS Lett. 383:26-30.

Roy ML and Narahashi T (1992) Differential properties of tetrodotoxin-sensitive and tetrodotoxin-resistant sodium channels in rat dorsal root ganglion neurons. J.Neurosci. 12:2104-2111.

Rudy B, (1988) Diversity and ubiquity of K channels. Neuroscience 25:729-49.

Ruppersberg JP, Schroter KH, Sakmann B, Stocker M, Sewing S, and Pongs O (1990) Heteromultimeric channels formed by rat brain potassium-channel proteins. Nature 345:535-537.

Rush AM, Brau ME, Elliott AA, and Elliott JR (1998) Electrophysiological properties of sodium current subtypes in small cells from adult rat dorsal root ganglia. J.Physiol (Lond) 511:771-789.

Safronov BV, Bischoff U, and Vogel W (1996) Single voltage-gated K+ channels and their functions in small dorsal root ganglion neurones of rat. J.Physiol 493:393-408.

Sangameswaran L, Delgado SG, Fish LM, Koch BD, Jakeman LB, Stewart GR, Sze P, Hunter JC, Eglen RM, and Herman RC (1996) Structure and function of a novel voltage-gated, tetrodotoxin-resistant sodium channel specific to sensory neurons. J.Biol.Chem. 271:5953-5956.

Scholz A, Kuboyama N, Hempelmann G, and Vogel W (1998) Complex blockade of TTX-resistant Na+ currents by lidocaine and bupivacaine reduce firing frequency in DRG neurons. J.Neurophysiol. 79:1746-1754.

Shulman M, Lubenow TR, Nath HA, Blazek W, McCarthy RJ, and Ivankovich AD (1998) Nerve blocks with 5% butamben suspension for the treatment of chronic pain syndromes. Reg Anesth.Pain Med. 23:395-401.

Stansfeld CE, Marsh SJ, Halliwell JV, and Brown DA (1986) 4-Aminopyridine and dendrotoxin induce repetitive firing in rat visceral sensory neurones by blocking a slowly inactivating outward current. Neurosci.Lett. 64:299-304.

Stansfeld CE, Marsh SJ, Parcej DN, Dolly JO, and Brown DA (1987) Mast cell degranulating peptide and dendrotoxin selectively inhibit a fast-activating potassium current and bind to common neuronal proteins. Neuroscience 23:893-902.

Van den Berg RJ, Van Soest PF, Wang Z, Grouls RJ, and Korsten HH (1995) The local anesthetic n-butyl-p-aminobenzoate selectively affects inactivation of fast sodium currents in cultured rat sensory neurons. Anesthesiology 82:1463-1473.

Van den Berg RJ, Wang Z, Grouls RJ, and Korsten HH (1996) The local anesthetic, n-butyl-p-aminobenzoate, reduces rat sensory neuron excitability by differential actions on fast and slow Na+ current components. Eur.J.Pharmacol. 316:87-95.

Vijayaragavan K, O'Leary ME, and Chahine M (2001) Gating properties of Na(v)1.7 and Na(v)1.8 peripheral nerve sodium channels. J.Neurosci. 21:7909-7918.

Wang FC, Bell N, Reid P, Smith LA, McIntosh P, Robertson B, and Dolly JO (1999) Identification of residues in dendrotoxin K responsible for its discrimination between neuronal K+ channels containing Kv1.1 and 1.2 alpha subunits. Eur.J.Biochem. 263:222-229.

Waxman SG, Dib-Hajj S, Cummins TR, Black JA. (1999) Sodium channels and pain. Proc. Natl. Acad. Sci. 96:7635-9

CHAPTER 3

BLOCK OF TOTAL AND N-TYPE CALCIUM CONDUCTANCE IN MOUSE SENSORY NEURONS BY THE LOCAL ANESTHETIC N-BUTYL-P-AMINOBENZOATE (BUTAMBEN)

Jeroen P. Beekwilder, Daniel L.B. Winkelman, Gertrudis Th.H. van Kempen, Rutgeris J. van den Berg, Dirk L. Ypey.

Anesth Analg (2005) 100:1674-9

ABSTRACT

In order to contribute to the understanding of the mechanism underlying selective analgesia by epidural application of suspensions of the local anesthetic butamben (n-butyl-p-aminobenzoate, BAB), the effect of dissolved BAB on calcium channels in sensory neurons was investigated. Small-diameter dorsal root ganglion neurones from newborn mice were used to measure whole-cell barium or calcium currents through calcium channels upon voltage-clamp stimulation. BAB suppressed the voltage-step evoked barium current of these cells in a concentration dependent way with an IC_{50} of 207 ± 14 µM (n = 40). A similar concentration dependency was found for the pharmacologically isolated N-type component of the whole-cell barium current. The time constants of inactivation and deactivation of the N-type current became smaller in the presence of BAB suggesting that kinetic changes are involved in the inhibition of this current. BAB caused a similar inhibition of the total calcium current as well as its N-type component, when these currents were evoked by command potentials with the shape of an action potential. This inhibition of calcium currents by BAB should be considered in the search for the mechanism of selective analgesia by epidural suspensions of the local anesthetic.

INTRODUCTION

Treatments of chronic pain may cause severe side effects, among which motor dysfunction is most prominent. A relatively new and promising approach to chronic pain treatment is the epidural administration of an aqueous suspension of the local anesthetic n-butyl-p-aminobenzoate (BAB), also known as butamben (Shulman, 1987; Korsten et al., 1991; Shulman et al., 1998). Application of the BAB suspension to the spinal dura results in a long lasting (median 29 days) relief from pain, without impairing motor function. This indicates that the BAB suspension selectively inhibits pain signaling sensory neurons, but the mechanism of its specific analgesic action is still unknown.

The BAB molecule is an aminobenzoate, ester-linked to a butyl group. The structure is similar to that of other ester-linked local anesthetics, such as benzocaine and procaine, which profoundly affect sodium channels involved in impulse generation and transmission in neurons. Effects of BAB on sodium currents have previously been studied in small dorsal root ganglion (DRG) neurons (Van den Berg et al., 1995; Van den Berg et al., 1996). However, the widespread opinion that the action mechanism of local anesthetics is mediated by sodium channels alone is, particularly for epidural anesthesia, an 'unproven assumption' (Butterworth and Strichartz, 1990).

Recently, we have shown in DRG neurons an effect of BAB on potassium channels and Kv1.1 channels in particular, which could contribute to the analgesia caused by the BAB suspension (Beekwilder et al., 2003). Calcium channels also play an important role in action potential firing of sensory neurons. A variety of calcium channel subtypes is expressed in sensory neurons of rodents (Mintz et al., 1992; Diochot et al., 1995). In the rat, N-type calcium current comprises ~50% of the total calcium current and is involved in calcium entry during action potentials in small diameter DRG neurons (Scroggs and Fox, 1992a; Blair and Bean, 2002; Bell et al., 2004), which include the pain sensing neurons (Scroggs and Fox, 1992b).

In the present study, we addressed the question whether voltage activated calcium channels are affected by BAB. To this end, the patch-clamp technique in

whole-cell voltage-clamp configuration was applied to acutely isolated small-size DRG neurons from neonatal mice. We did find inhibitory effects of BAB on the whole-cell current through calcium channels, including its N-type component. The physiological significance of these findings is considered in the discussion.

METHODS

Cell culture

Neonatal mice were killed by decapitation, and dorsal root ganglia from all accessible levels of the spinal cord were rapidly collected (approved by the Animal Ethics Committee at the Leiden University Medical Center). Cells were mechanically dissociated from two or three ganglia and cultured on a circular glass cover slip as previously described (Beekwilder et al., 2003). Within 8 h of culture, spherical neurons with a diameter of ~20 µm were selected for patch-clamp measurements. At this stage neurite outgrowth was still negligible.

Electrophysiology

For voltage clamp experiments a cover slip with DRG cell culture was mounted in a chamber on the stage of an inverted microscope. Patch pipettes were pulled from borosilicate glass (Clark GC-150 TF-15) and had resistances of 2.0 to 2.5 MΩ measured in the standard bath solution. Sintered Ag/AgCl electrodes coupled the amplifier input leads to the solutions. To minimize offset caused by low Cl^- pipette solutions, the pipette holder (Buisman et al., 1990) contained a Cl^- rich solution at the Ag/AgCl electrode.

Giga-seals were made in a microbath of ~75 µl, continuously perfused (~300 $\mu l \cdot min^{-1}$) with the standard bath solution (in mM): NaCl 145, KCl 5, $CaCl_2$ 2, $MgCl_2$ 1, HEPES 10, pH 7.4 (NaOH). The pipette solution contained (mM): Cs-methanesulfonate 103, $MgCl_2$ 4, HEPES 9, EGTA 9, (Mg)ATP 4, (tris)GTP 1, (tris)phosphocreatine 14, pH 7.4 (CsOH).

After establishment of the whole-cell configuration the barium current was recorded with voltage-step protocols during extracellular perfusion with (mM): TEA-Cl 160, HEPES 10, EGTA 0.1, $BaCl_2$ 5, pH 7.4 (TEA-OH). A PC running Clampex 7 (Axon Instruments, Foster City, CA) and a List EPC 7 amplifier provided voltage protocols. Up to 80-90% of the series resistance was compensated. The membrane currents were filtered at 3 kHz in general and at 10 kHz for tail current measurements. Control experiments with an equivalent RC-circuit of the whole-cell showed that current transients with time constants of >100 µs can be reliably measured at 10 kHz filter setting (3-pole Bessel) under our conditions. All currents were leak subtracted using the P/4 method. Membrane capacitance of the selected DRG neurons was 14 ± 3 pF (n = 55). Calcium currents during action-potential clamp were measured under constant perfusion with (mM): TEA-Cl 160, HEPES 10, $CaCl_2$ 2, pH 7.4 (TEA-OH). The pipette solution was the same as above in the step voltage-clamp conditions.

Pharmacology

BAB (OPG Farma, Utrecht, The Netherlands) was added to the extracellular solution from a stock of BAB in ethanol (1-500 mM). Final ethanol concentration never exceeded 0.1 %. Because BAB has low water solubility (<700 µM at room temperature, Merck Index 1989) and easily binds to plastic surfaces of the perfusion system, final BAB concentrations up to 500 µM were verified using absorption spectrophotometry (290 nm). ω-Conotoxin-GVIA (CnTx; Peptide Institute Inc., Osaka, Japan) was dissolved in distilled water and added with a final fully blocking concentration of 3.3 or 5 µM (Diochot et al., 1995; Scroggs and Fox, 1992a; Blair and Bean, 2002; Scroggs and Fox, 1992b).

Analysis and statistics

Normalized data were corrected for rundown in the presence of vehicle (0.1 % ethanol) at all potentials measured in control experiments (n = 8). For example, at test pulses of 0 mV an apparent linear barium current decline (rundown) of ~ 6 % in 5 min was observed. The concentration-inhibition data were fitted using the Hill equation: $I/I_o = (1 + ([BAB]/IC_{50})^n)^{-1}$, where the IC_{50} is the concentration at which the current is reduced by 50% and n is the Hill coefficient. Results are presented as mean ± standard deviation (M ± SD) for n cells, unless stated

otherwise, and compared using paired or independent t-tests with the level of significance (p) chosen as 0.05.

RESULTS

BAB blocks whole cell barium currents

In order to assess the effect of BAB on calcium channels in neonatal mouse DRG neurons, barium currents through these channels were elicited by a square test pulse to 0 mV from –80 mV. Application of 200 µM BAB resulted in a decline of the current amplitude, reaching a steady-state value after 2-3 minutes. In Figure 1A the steady-state effect of 200 µM BAB is shown for a representative cell. At this BAB concentration the reduction of the peak whole-cell barium current amounted to 49 ± 7 % (n = 8). During washing out of the drug, the inhibiting effect of BAB proved to be partly reversible, reaching 86 % of the amplitude of

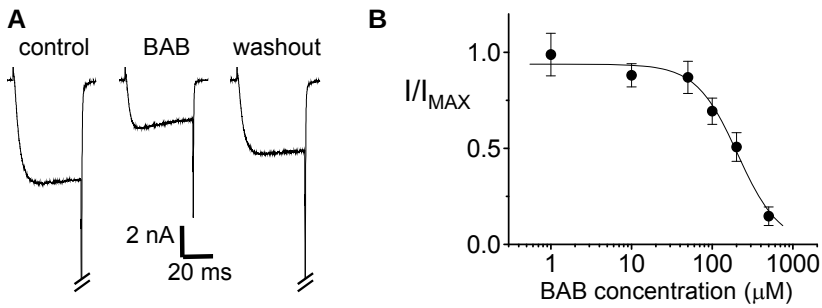

Figure 1: Effect of butamben (BAB) on whole-cell barium currents of a small neonatal mouse DRG-neuron. (A) Currents elicited by a test pulse to 0 mV from a holding potential of –80 mV at 0.1 Hz are shown for the control situation (left), after 3 minutes of 200 µM BAB exposure (middle) and after 3 minutes of washout (right). (B) Relationship between the applied BAB concentration and the relative peak amplitude of whole-cell barium currents (I/I_{MAX}) during test pulses of 0 mV, using an 80 ms prepulse to –120 mV from a holding potential of –80 mV. The solid line represents the fit of the Hill equation to the data. At each concentration n = 5–8 cells, with a total of n = 40. Data was corrected for rundown as described in the text.

the control situation (cf. Van den Berg et al., 1996).

The concentration-dependency of the current reduction by BAB was determined by measuring steady-state barium currents at different BAB concentrations. A prepulse to –120 mV was applied in order to remove possible inactivation at –80 mV (<10%). The peak currents in the presence of BAB were normalized to the corresponding whole-cell peak currents in the absence of BAB and were plotted as a function of concentration in the range from 1 to 500 µM (Figure 1B). A single Hill function could be fitted to the data yielding an IC_{50} of 207 ± 14 µM and a Hill coefficient of 1.7 ± 0.2 (n = 40).

BAB blocks N-type calcium channels

N-type calcium channels have a selective sensitivity to ω-conotoxin-GVIA (CnTx). In order to isolate the N-type current component, we used the procedure shown in Figure 2A,B. Whole-cell barium currents were measured in the absence and presence of 3.3 µM CnTx and the CnTx-insensitive currents were subtracted from the control currents (Figure 2B, left panel). CnTx caused an inhibition in peak current of 58 ± 5% (n=6). To investigate whether N-type currents are affected by the local anesthetic, currents were measured after preincubation with e.g. 200 µM BAB and after the subsequent perfusion with the CnTx solution still containing 200 µM BAB (Figure 2A, right panel). The resulting difference current represents the current through N-type channels in the presence of 200 µM BAB (Figure 2B, right panel). Repeating this procedure at different BAB concentrations and by plotting the normalized current density (pA/pF) as a function of BAB-concentration, the N-type concentration-response curve was obtained shown in Figure 2C (solid curve). Fitting the Hill equation to this relation yielded an IC_{50} of 220 ± 35 µM and a Hill coefficient of 1.4 ± 0.3 (n = 35).

The current decay of the N-type component during maintained depolarization (500 ms) was fitted with a single exponential function. The mean time constant in control solution was 78 ± 12 ms (n = 8), whereas in the presence of 200 µM BAB the N-type current inactivated significantly faster with a time constant of 64 ± 8 ms (n = 7, p=0.024).

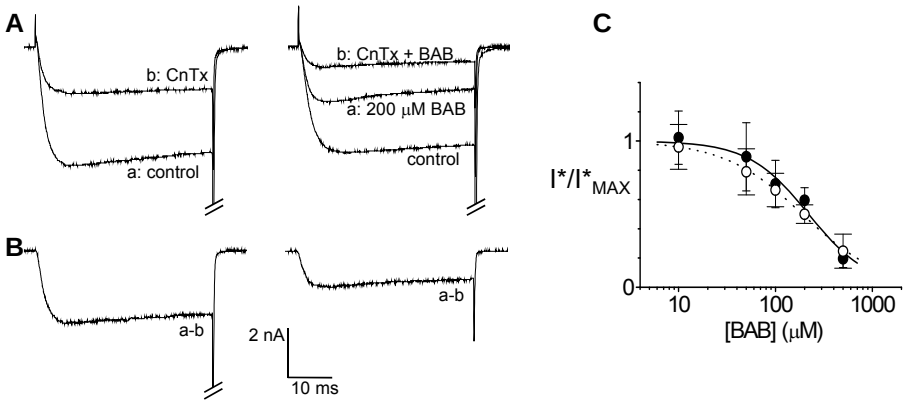

Figure 2: Effects of butamben (BAB) on CnTx-resistant and –sensitive barium current. (A) Control currents elicited by a pulse to 0 mV from a holding of –80 mV at 0.1 Hz with either 0 (left panel, trace a) or 200 μM BAB (right panel: trace a) followed by the application of 3.3 μM CnTx (ω-conotoxin-GVIA, traces b). In (B) the currents 'b' were subtracted from 'a', representing the CnTx-sensitive (N-type) current in the presence of either 0 (left panel) or 200 μM (right panel) BAB. In (C) the normalized current densities (I^*/I^*_{MAX}) of the CnTx-sensitive current (closed circles, solid line) and the CnTx-insensitive current (open circles, dotted line) are plotted against the applied BAB concentration. Current density (pA/pF) was used rather than current in order to minimize variability. At each concentration n = 5-8.

The tail current (cf. Figure 2B), representing the deactivation of the N-type channels, was elicited by stepping back from 0 to –80 mV and could also be fitted by an exponential function (fits not shown), yielding a time constant in control conditions of 167 ± 24 μs (n = 6). In the presence of 200 μM BAB the time constant was 136 ± 20 μs (n = 6), significantly lower (p=0.043) than that obtained under control conditions.

The residual current in the presence of CnTx represents the non-N-type current through calcium channels. It's BAB concentration-response curve is also given in Figure 2C (dotted curve) and is characterized by an IC_{50} of 189 ± 28 μM and a Hill coefficient of 1.1 ± 0.2. Because of its heterogeneity the non-N-type current was not further investigated.

BAB blocks action-potential clamp evoked whole-cell calcium currents

So far, we used voltage-steps to elicit barium currents. However, under physiological conditions calcium ions are the charge carriers and the calcium

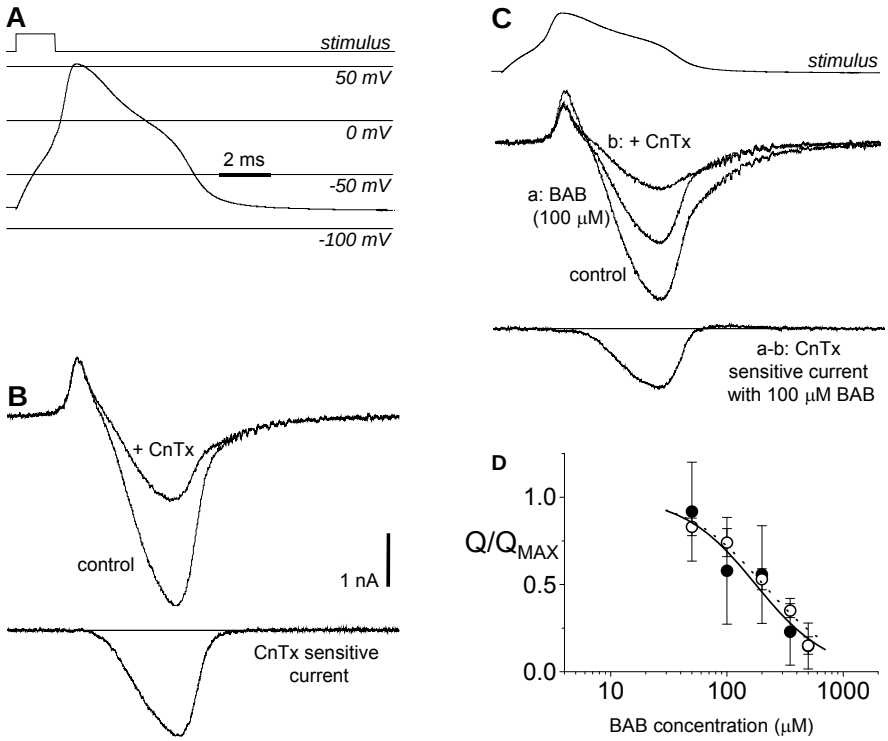

Figure 3: The effect of butamben (BAB) on calcium currents evoked by voltage-clamp stimulation with a 'standard' action potential at 6-s intervals. (A) Action potential recorded in current clamp in a small-size DRG neuron evoked by a 1.5 ms pulse of current injection. The action potential had a peak of +52 mV and a half width of 4.4 ms. Time scale bar applies to all panels. The cell was perfused with (in mM): NaCl 145, KCl 10, $CaCl_2$ 2, $MgCl_2$ 1, HEPES 10, pH 7.4 (NaOH). The pipette solution contained: KCl 140, HEPES 10, EGTA 5, pH 7.4 (KOH). (B) Upper panel: Outward and inward currents under voltage clamp conditions elicited by the action potential from (A) as command voltage in the absence (control) and presence of 3.3μM CnTx (ω-conotoxin-GVIA) in a bath solution with 2mM calcium and 160mM TEA-Cl and with pipettes filled with Cs^+ as the main charge carrier (same pipette solution as in Figs. 1,2). Lower panel: The CnTx-sensitive current obtained by subtraction. Current calibration bar in (B) also applies to (C). (C) Upper panel: stimulus as in (A). Middle panel: Currents elicited by action-potential voltage-clamp stimulation under control conditions, in the presence of 100 μM BAB (record a) and in the additional presence of 3.3 μM CnTx (record b). Lower panel: The CnTx-sensitive current in the presence of 100 μM BAB, obtained by subtracting b from a. (D) The normalized integrated currents of the total calcium (open circles, dotted line) and the CnTx-sensitive current (closed circles, solid line) plotted against the applied BAB concentration. The lines represent fits with a Hill-equation. The n = 47 with at least 4 cells at each concentration.

channels are activated by naturally occurring changes in the transmembrane potential, e.g. during an action potential. Therefore, in the present study we also measured effects of BAB on calcium channels in the presence of a physiological concentration of calcium ions in the extracellular solution and using a previously recorded action potential as command voltage.

Figure 3A shows a representative action potential from a DRG neuron with a resting potential of around -75 mV. Although there is a marked neuron-to-neuron variability in action potential shapes, this action potential was applied as a standard voltage profile to get insight into the participation of the different calcium channels in the generation of the action potential. The 20-ms digitized standard action-potential record was applied from the holding voltage of –80 mV. The resulting control ion current is depicted in Fig. 3B and shows an initial outward current followed by an inward calcium current. This short outward current is resistant to application of 600 µM cadmium (blocking all inward current; n = 5) and does not interfere with the measurement of the subsequent inward calcium current. This current is likely carried by cesium ions flowing through unblocked (fast) sodium and potassium channels (Blair and Bean, 2002). The peak of the inward current coincided with the shoulder in the repolarizing phase of the action potential. The inward current decayed in two phases, an initial fast and subsequent slow one. The slower current decay occurred after nearly complete repolarization of the action potential, i.e. during the afterdepolarization.

BAB caused an overall decrease of the action potential clamp evoked calcium current (Fig. 3C). The initial positive current, the large negative peak and the fast and slow decay components were all affected. Figure 3D gives the concentration-response curve (dotted line) for the effect of BAB on the normalized integral (to reduce variability) of the total inward current. The parameters of the fitted Hill curve were an IC_{50} of 206 ± 8 µM and a Hill coefficient of 1.3 ± 0.1 (n = 47).

BAB blocks action potential clamp evoked N-type calcium currents.

During voltage clamping with the standard action potential, CnTx was perfused over the cell in order to specifically block the N-type current. CnTx did not affect the initial outward current, it neither affected the slower component of the

current decay, whereas the faster decaying current was removed to a great extent (Fig. 3B, upper panel). The difference between the total current and the current in the presence of CnTx is the N-type calcium current (Fig. 3B, lower panel). CnTx blocked 48 ± 10 % (n = 8) of the integrated current corresponding to the total calcium inflow. In order to determine the effect of BAB on the N-type component of the calcium current, action potential clamped currents were measured after preincubation with e.g. 100 µM BAB and after the subsequent perfusion with the CnTx solution still containing 100 µM BAB (Figure 3C, middle panel). The resulting difference current represents the current through N-type channels in the presence of 100 µM BAB (Figure 3C, lower panel). By repeating this procedure at different BAB concentrations, the concentration dependency of the BAB on the CnTx-sensitive current was determined. The relation of BAB and the normalized integral of the CnTx-sensitive current was described with a Hill equation (Figure 3D, solid curve), yielding an IC_{50} of 177 ± 47 µM and a Hill coefficient of 1.4 ± 0.5 (n = 47), similar to the parameters of the total calcium current (see above). For non-N-type calcium currents a similar concentration-response curve is implicated by the very similar curves in Fig. 3D.

DISCUSSION

The present study shows that the local anesthetic butamben (BAB) inhibits voltage clamp evoked barium and calcium currents including their N-type components.

Unlike sodium channels, where effects of 100 µM BAB ranged from a nearly complete block to insensitivity (Van den Berg et al., 1995; Van den Berg et al., 1996), calcium- and potassium channels show similarities in the measured effects of BAB. On both calcium (native) and Kv1.1 channels (native and cloned; Beekwilder et al., 2003) BAB caused an inhibition of the current with an IC_{50} of ~200 µM and a Hill coefficient of 1-2 and an accelerated deactivation. These data allow the possibility of two BAB binding sites per channel and suggest an allosteric mechanism of BAB action, by which the channel is biased towards the

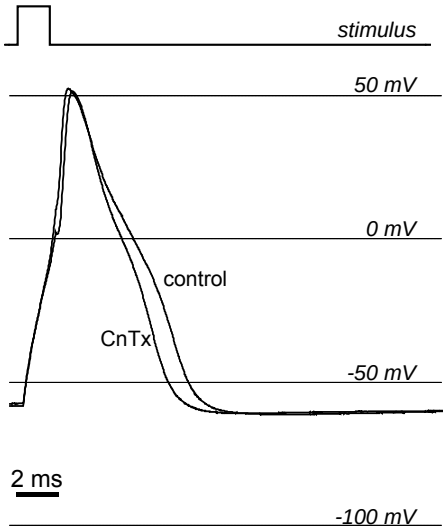

Figure 4: Action potentials evoked by current injections in the absence (control) and presence of 5 µM CnTx (ω-conotoxin-GVIA) , representative for 3 small DRG-neurons. The cell was perfused with (in mM): NaCl 145, KCl 10, $CaCl_2$ 2, $MgCl_2$ 1, HEPES 10, pH 7.4 (NaOH). The pipette solution contained 140 KCl, 10 NaCl, 1 $CaCl_2$, 2 $MgCl_2$ 10 EGTA, 10 HEPES, pH 7.4 (KOH). Stimulus duration and amplitude were chosen to obtain just supramaximal stimulation with minimal interference of the evoked depolarization with the subsequent time course of the action potential. The slight delay in the onset of the action potential as well as the earlier repolarization in the presence of CnTx are illustrative for the role of N-type calcium channels in the excitability of these cells.

closed state. However, more experiments are needed to come to more definite conclusions about the mechanism of current reduction by BAB.

By using the action potential clamp and minimizing sodium and potassium currents total and N-type calcium currents flowing during a ′standard′ action potential could be measured . The shoulder of the action potential coincided with the peaks of the inward currents, as in rat sensory neurons (Scroggs and Fox, 1992a; Blair and Bean, 2002). The finding that CnTx eliminated about half of the total charge displaced through the calcium channels during the applied action potential, suggests a significant role for N-type calcium currents in nociceptive neurons. To illustrate the contribution of the N-type calcium current to the action potential waveform, Figure 4 shows the effect of CnTx on an action potential evoked in current clamp. Upon perfusion with CnTx the ′shoulder′ of

the action potential was partially removed, consistent with the results shown in Fig. 3 and results of others (Scroggs and Fox, 1992a; Blair and Bean, 2002). The importance of the N-type calcium channels in pain signaling is emphasized by findings that nociceptive neurons abundantly express a unique splice variant of the N-type channel (Bell et al., 2004) and that mice lacking the $Ca_v2.2$ gene, encoding for N-type calcium channels, show altered nociceptive responses (Hatakeyama et al., 2001; Kim et al., 2001; Saegusa et al., 2001). The present results indicate that non-N-type calcium currents are also inhibited by BAB. Inhibition of the low voltage-activated T-type calcium channels by BAB was confirmed in separate experiments (IC_{50} =178 ± 21 µM, Hill coefficient 1.5 ± 0.3, n = 40, for barium current peaks measured upon voltage steps from –80 to –40 mV). Thus, inhibition of both N-type and non-N-type calcium channels may contribute to BAB's epidural analgesic action.

The just below-maximal water-solubility BAB concentration of 500 µM (~2.5*IC_{50}) largely inhibited the total calcium current (Fig. 3D). The maximal-solubility concentration is the upper value in the clinical situation where BAB is applied as an aqueous suspension on the spinal dura. In the epidural space BAB diffuses from its depot and will affect the spinal nerves passing that space. Apparently, a local long-lasting BAB-concentration gradient is established as a result of the local balance between release, diffusion and degradation of BAB, including pharmacologically effective concentrations (Grouls et al., 1997).

The interesting question remains why epidural BAB-suspensions selectively affect the small diameter pain transmitting nerve fibres, while the thick motor and sensory fibres are not influenced. For the explanation of this differential blockade three mechanisms should be considered, which all may contribute. The first one explains differential nerve block with the classical observation that thinner axons cease firing with shorter segmental exposure to impulse blocking drugs than thicker axons (Franz and Perry, 1974). Korsten et al. (Korsten et al., 1991) explained in this way the selective action of BAB from differences in critical length of axons traversing the epidural space. Grouls et al. (1997) suggested that selective pain suppression by BAB was the result of a stable establishment of relatively low epidural concentrations due to the low solubility of BAB, which would favour inhibition of the thinner pain fibers. Finally, there are possible differences in BAB-sensitive ion channel expression in axonal

membranes of myelinated and unmyelinated fibers. A rich repertoire of sodium and potassium channels is present in Ranvier nodes, but calcium channels are lacking (Waxman and Ritchie, 1993). For the unmyelinated sensory fibres the spectrum of ion channels is not well studied, but apart from tetrodotoxin-sensitive and –resistant sodium channels, calcium channels belong to their ion channel palette (Elliott, 1990). Calcium spikes have been recorded from human nociceptive C fibers of the sural nerve (Quasthoff et al., 1995) and could be evoked by capsaicin (Mayer et al., 1999). It is thus tempting to speculate that calcium channels play a key role in selective analgesia by BAB by serving as targets for blocking the calcium spikes in pain transmitting fibers. In this respect it is of interest to mention that others have shown that some other, more hydrophilic, local anesthetics (e.g. bupivacaine) also inhibit calcium currents in mammalian sensory neurons (Sugiyama and Muteki, 1994) and dorsal horn neurons (e.g. ropivacaine) (Liu et al., 2001). Ropivacaine, which also has motor sparing properties, seems to act by another mechanism than BAB, since it must have a less localized epidural distribution because of its larger water solubility and insensibility to esterases (cf. Grouls et al., 1997) and because of its property to increase calcium currents at lower concentrations (Liu et al., 2001).

In conclusion, submaximal water-solubility BAB concentrations inhibit the calcium channels of sensory neurons. This inhibition is likely to contribute, in addition to the inhibition of sodium and potassium channels, to the long duration selective analgesia following epidural application of BAB suspensions.

References

Beekwilder JP, O'Leary ME, van den Broek LP, van Kempen GT, Ypey DL, van den Berg RJ (2003) Kv1.1 channels of dorsal root ganglion neurons are inhibited by n-butyl-p-aminobenzoate, a promising anesthetic for the treatment of chronic pain. J Pharmacol Exp Ther 304:531-538.

Bell TJ, Thaler C, Castiglioni AJ, Helton TD, Lipscombe D (2004) Cell-specific alternative splicing increases calcium channel current density in the pain pathway. Neuron 41:127-138.

Blair NT, Bean BP (2002) Roles of tetrodotoxin (TTX)-sensitive Na+ current, TTX-resistant Na+ current, and Ca2+ current in the action potentials of nociceptive sensory neurons. The Journal of Neuroscience : the Official Journal of the Society For Neuroscience 22:10277-10290.

Buisman HP, De Vos A, Ypey DL (1990) A pipette holder for use in patch-clamp measurements. J Neurosci Methods 31:89-91.

Butterworth JFt, Strichartz GR (1990) Molecular mechanisms of local anesthesia: a review. Anesthesiology 72:711-734.

Diochot S, Richard S, Valmier J (1995) Diversity of voltage-gated calcium currents in large diameter embryonic mouse sensory neurons. Neuroscience 69:627-641.

Elliott P (1990) Action of antiepileptic and anaesthetic drugs on Na- and Ca-spikes in mammalian non-myelinated axons. Eur J Pharmacol 175:155-163.

Franz DN, Perry RS (1974) Mechanisms for differential block among single myelinated and non-myelinated axons by procaine. J Physiol 236:193-210.

Grouls RJ, Meert TF, Korsten HH, Hellebrekers LJ, Breimer DD (1997) Epidural and intrathecal n-butyl-p-aminobenzoate solution in the rat. Comparison with bupivacaine. Anesthesiology 86:181-187.

Hatakeyama S, Wakamori M, Ino M, Miyamoto N, Takahashi E, Yoshinaga T, Sawada K, Imoto K, Tanaka I, Yoshizawa T, Nishizawa Y, Mori Y, Niidome T, Shoji S (2001) Differential nociceptive responses in mice lacking the alpha(1B) subunit of N-type Ca(2+) channels. Neuroreport 12:2423-2427.

Kim C, Jun K, Lee T, Kim SS, McEnery MW, Chin H, Kim HL, Park JM, Kim DK, Jung SJ, Kim J, Shin HS (2001) Altered nociceptive response in mice deficient in the alpha(1B) subunit of the voltage-dependent calcium channel. Mol Cell Neurosci 18:235-245.

Korsten HH, Ackerman EW, Grouls RJ, van Zundert AA, Boon WF, Bal F, Crommelin MA, Ribot JG, Hoefsloot F, Slooff JL (1991) Long-lasting epidural sensory blockade by n-butyl-p-aminobenzoate in the terminally ill intractable cancer pain patient. Anesthesiology 75:950-960.

Liu BG, Zhuang XL, Li ST, Xu GH, Brull SJ, Zhang JM (2001) Effects of bupivacaine and ropivacaine on high-voltage-activated calcium currents of the dorsal horn neurons in newborn rats. Anesthesiology 95:139-143.

Mayer C, Quasthoff S, Grafe P (1999) Confocal imaging reveals activity-dependent intracellular Ca2+ transients in nociceptive human C fibres. Pain 81:317-322.

Mintz IM, Adams ME, Bean BP (1992) P-type calcium channels in rat central and peripheral neurons. Neuron 9:85-95.

Quasthoff S, Grosskreutz J, Schroder JM, Schneider U, Grafe P (1995) Calcium potentials and tetrodotoxin-resistant sodium potentials in unmyelinated C fibres of biopsied human sural nerve. Neuroscience 69:955-965.

Saegusa H, Kurihara T, Zong S, Kazuno A, Matsuda Y, Nonaka T, Han W, Toriyama H, Tanabe T (2001) Suppression of inflammatory and neuropathic pain symptoms in mice lacking the N-type Ca2+ channel. Embo J 20:2349-2356.

Scroggs RS, Fox AP (1992a) Multiple Ca2+ currents elicited by action potential waveforms in acutely isolated adult rat dorsal root ganglion neurons. The Journal of Neuroscience : the Official Journal of the Society For Neuroscience 12:1789-1801.

Scroggs RS, Fox AP (1992b) Calcium current variation between acutely isolated adult rat dorsal root ganglion neurons of different size. 445:639-658.

Shulman M (1987) Treatment of cancer pain with epidural butyl-aminobenzoate suspension. Regional Anesth 12:1-4.

Shulman M, Lubenow TR, Nath HA, Blazek W, McCarthy RJ, Ivankovich AD (1998) Nerve blocks with 5% butamben suspension for the treatment of chronic pain syndromes. Reg Anesth Pain Med 23:395-401.

Sugiyama K, Muteki T (1994) Local anesthetics depress the calcium current of rat sensory neurons in culture. Anesthesiology 80:1369-1378.

Van den Berg RJ, Wang Z, Grouls RJ, Korsten HH (1996) The local anesthetic, n-butyl-p-aminobenzoate, reduces rat sensory neuron excitability by differential actions on fast and slow Na+ current components. Eur J Pharmacol 316:87-95.

Van den Berg RJ, Van Soest PF, Wang Z, Grouls RJ, Korsten HH (1995) The local anesthetic n-butyl-p-aminobenzoate selectively affects inactivation of fast sodium currents in cultured rat sensory neurons. Anesthesiology 82:1463-1473.

Waxman SG, Ritchie JM (1993) Molecular dissection of the myelinated axon. Ann Neurol 33:121-136.

CHAPTER 4

THE LOCAL ANESTHETIC BUTAMBEN INHIBITS AND ACCELERATES LOW-VOLTAGE ACTIVATED T-TYPE CURRENTS IN SMALL SENSORY NEURONS.

Jeroen P. Beekwilder, Gertrudis Th.H. van Kempen, Rutgeris J. van den Berg, Dirk L. Ypey.

Anesth Analg (2006) 102:141-5

ABSTRACT

Butamben (BAB) is a local anesthetic, which can be used in epidural suspensions for long-term selective suppression of dorsal root pain signal transmission and in ointments for the treatment of skin pain. Previously, high-voltage activated (HVA) N-type calcium channel inhibition has been implicated in the analgesic effect of BAB. In the present study we show that low-voltage activated (LVA) or T-type calcium channels may also contribute to this effect. Typical transient T-type barium currents, selectively evoked by low-voltage (-40 mV) clamp stimulation of small (~20 µm diameter) dorsal root ganglion neurons from newborn mice, were inhibited by BAB with an IC_{50} value of ~200 µM. Furthermore, 200 µM BAB accelerated T-type current activation, deactivation and inactivation kinetics, comparable to earlier observations for N-type calcium channels. Finally, 200 µM BAB had no effect on the midpoint potential and slope factor of the activation curve, while it caused a ~3 mV hyperpolarizing shift of the inactivation curve, without affecting the slope factor. We conclude that BAB inhibits T-type calcium channels with a mechanism associated with channel kinetics acceleration.

INTRODUCTION

Epidural suspensions of the hydrophobic local anesthetic n-butyl-p-aminobenzoate (BAB), also known as butamben, have been shown to selectively inhibit dorsal root pain signal transmission for periods of months (Korsten et al., 1991), while butamben ointments are used for topical treatment of skin pain and itching. In a previous study of BAB's action mechanism we found that BAB inhibited high-voltage activated (HVA) calcium channels in dorsal root ganglion (DRG) neurons from newborn mice (Beekwilder et al., 2005). We studied both the effects of BAB on the calcium and barium current, which consists mainly of HVA N-type current. In the present study we have extended our investigations of BAB effects on calcium channels to the effects of BAB on low-voltage activated (LVA) or T-type calcium channels of mouse DRG neurons.

Although the T-type calcium currents have already been discovered in sensory neurons in the early eighties of last century and particulary in the small-size pain-sensing neurons (Carbone and Lux, 1984), their exact role has never been made clear. In general, T-type currents are believed to be involved in neuronal pacemaker activity and in promoting calcium entry during short action potentials; for a review see Yunker and McEnery (2003). However, in recent studies T-type calcium currents have been shown to play a role in pain signalling and have also been recognized as therapeutic targets (Bilici et al., 2001; Todorovic et al., 2001; Todorovic et al., 2004; Bourinet et al., 2005). Therefore, it is of interest to investigate whether T-type calcium channels are inhibited by BAB.

The distinct biophysical properties of T-type calcium channels (low voltage activation and its transient nature due to fast inactivation) make it possible to separate effects of BAB on T-type channels from non-T-type calcium channels without the use of ion channel blockers. We were also interested in the question whether an inhibition of T-type channels would be accompanied by an acceleration of channel kinetics, as has been observed in our earlier studies for various channel types, including native and cloned Kv1.1 channels (Beekwilder et al., 2003) and native N-type calcium channels (Beekwilder et al., 2005). The patch-clamp technique in the whole-cell voltage-clamp configuration allowed us

to establish that BAB indeed inhibits T-type currents and, at the same time, accelerates T-type current kinetics in small-size (~20 µm diameter) dorsal root ganglion neurons from neonatal mice. Functional implications of these findings are discussed.

METHODS

Cell culture, electrophysiology and data analysis were as described in detail elsewhere (Beekwilder et al., 2005). In short, small spherical neurons (~20µm in diameter), mainly comprising nociceptive neurons (Todorovic et al., 2001), dissociated from dorsal root ganglia (DRG) of neonatal mice were patch-clamped within 8 h of culture. Patch pipettes of borosilicate glass had resistances of 2.0 to 2.5 MΩ. Giga-seals were made in a microbath of ~75 µl, continuously perfused (~300 µl/min) with standard extracellular solution containing (in mM): NaCl 145, KCl 5, $CaCl_2$ 2, $MgCl_2$ 1, HEPES 10, pH 7.4 (NaOH). The pipette solution contained (in mM): Cs-methanesulfonate 103, $MgCl_2$ 4, HEPES 9, EGTA 9, (Mg)ATP 4, (tris)GTP 1, (tris)phosphocreatine 14, pH 7.4 (CsOH). After establishment of the whole-cell configuration calcium channel currents were measured as barium currents during extracellular perfusion with (in mM): TEA-Cl 160, HEPES 10, EGTA 0.1, $BaCl_2$ 5, pH 7.4 (TEA-OH).

To minimize offset caused by the low Cl^- pipette solution, the pipette holder (Buisman et al., 1990) contained a Cl^- rich solution at the Ag/AgCl electrode. Experiments were carried out at room temperature (~23°C) with a List EPC 7 amplifier (3 kHz filtering) and controlled by pClamp software (Axon Instruments, Foster City, CA). The membrane capacitance of the selected DRG neurons was ~14 pF, the series resistance was largely (80-90%) compensated and the records were leak subtracted.

Butamben (BAB, OPG Farma, Utrecht, The Netherlands) was added to the extracellular solution from a stock of BAB in ethanol (1-500 mM). Normalized data were corrected for rundown in the presence of vehicle (0.1 % alcohol) at all

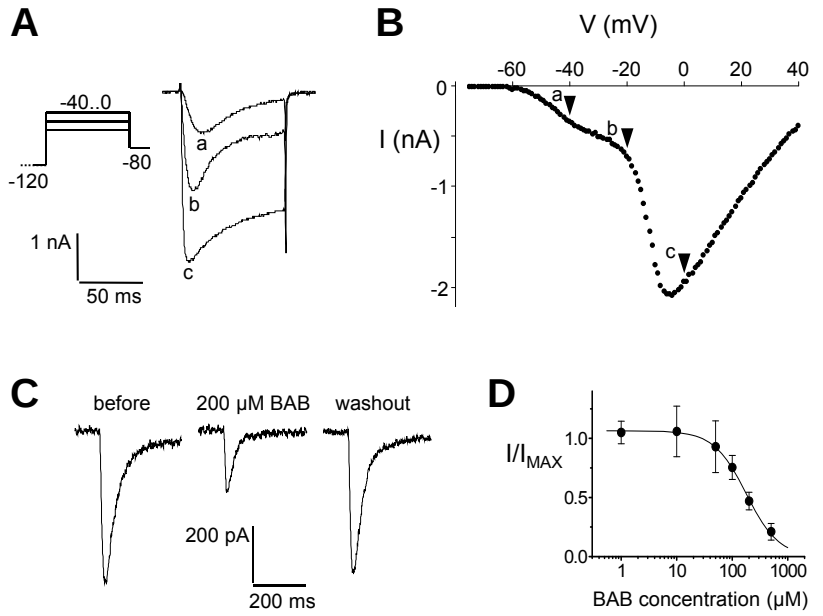

Figure 1: Effects of butamben (BAB) on T-type currents. (A). Current traces with barium as a charge carrier elicited by steps to –40, -20 and 0 mV after an 80 ms prepulse to –120 mV from a holding potential of -80 mV. (B). High-resolution current-voltage relation from a single cell obtained by stepping to various potentials (-75 to +40 mV) with 1 mV intervals after a 80 ms prepulse to –120 mV. Peak values from current traces in 'A' are indicated by arrowheads. Test pulse interval was 10 s. (C). Barium currents elicited by a sustained voltage step to –40 mV from a holding of –80 mV before, during and after application of 200 µM BAB. (D). The effect of BAB concentration on the peak current amplitude after stepping to –40 mV for 40 ms after a 80 ms prepulse to –120 mV from a holding of –80 mV relative to control values. The curve represents a fit with a Hill equation.

potentials measured in control experiments (n=8). At test pulses of -40 mV rundown was < 3 % in 12 min.

The Hill equation, $I/I_o = (1 + ([BAB]/IC_{50})^n)^{-1}$, was fitted to the concentration-inhibition data, where IC_{50} is the concentration at which the current is reduced by 50% and n is the Hill coefficient. The Boltzmann equation, $I/I_o = (1+\exp((V-V_{0.5})/k))^{-1}$, with V the prepulse potential, $V_{0.5}$ the midpoint potential at which the current is half maximal, and k the slope factor, was fitted to the steady-state inactivation data. T-type current kinetics were fitted with a m^2h Hodgkin-Huxley type model: $I(t) = (m^*)^2 \cdot (1-\exp(-t/\tau_m))^2 \cdot (\exp(-t/\tau_h) + h^* \cdot (1-\exp(-t/\tau_h))) \cdot A$, where m* is partial steady-state activation at –40 mV,

obtained from the experiment in Fig. 2C,D, h* is a free parameter representing the partial steady-state inactivation and A is an amplitude factor. The time constants for the m- and h-gate are τ_m and τ_h, respectively.

Results are presented as Means ± Standard Deviations for n cells (unless mentioned otherwise) and compared using paired or independent t-tests with the level of significance P = 0.05.

RESULTS

BAB inhibits T-type calcium channels

DRG neurons express both low-voltage (LVA) and high-voltage activated (HVA) calcium channels. LVA (T-type) channels activate around -55 mV, whereas HVA channels activate at more positive potentials (>-30 mV). Figure 1A shows these properties. Barium currents were evoked by voltage steps to various potentials from a holding potential of –80 mV, whereby the test pulses were preceded by a prepulse of -120 mV. Both the rise and decay of the current were strongly voltage dependent. Plotting the peak values of the currents against the various potentials (-75...+40 mV) with 1 mV intervals results in a high-resolution current-voltage relation of the total current (Fig. 1B). The distinct activation voltage ranges of the LVA and HVA currents can be recognized from the two-component character of the figure. This property allowed us to discriminate effects of BAB on LVA and HVA currents.

The LVA barium current at membrane voltages of –40 mV is carried mainly through T-type calcium channels and is characterized by a relatively fast and nearly-complete inactivation. Other indications confirming that the current we observed was T-type include the crossing of the current traces at successive voltage steps (cf. Fig. 2C) and a relatively slow deactivation compared to currents elicited by stronger depolarizing steps to 0 mV (cf. Fig. 3C) (Randall and Tsien,

1997). The amplitude of the peak barium current, elicited by voltage pulses to -40 mV preceded by a 80 ms prepulse to –120 mV from a holding potential of –80 mV, amounted to 415 ± 357 pA (n = 46) under control conditions. That evoked by 0 mV pulses was 4.7 ± 1.3 nA (n = 37). The T-type barium currents were reversibly reduced by BAB in a concentration dependent way. At the concentration of 200 µM, barium currents at –40 mV were diminished by 52 ± 8

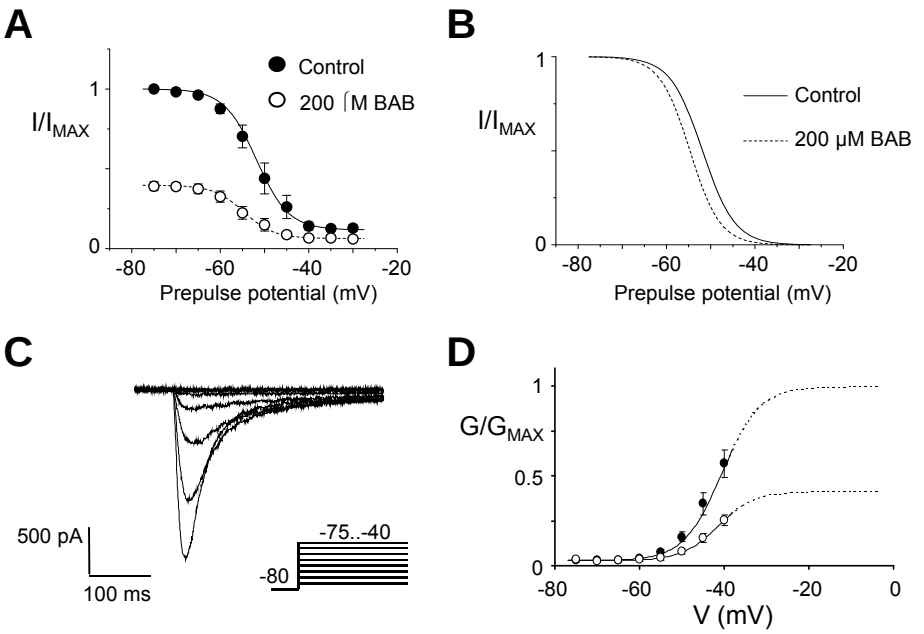

Figure 2: Effect of BAB on the steady state properties of T-type currents. (A). Inactivation curves obtained with a test pulse to –40 mV after a 350 ms prepulse to various potentials from a holding of –80 mV, in the absence (closed symbols) and presence of 200 µM BAB (open symbols). The intervals between the test pulses were 15 s. The currents are normalized to the maximal value of the Boltzmann fit to the control data points (solid line) and are plotted as a function of the prepulse potential. (B). Boltzmann curves from 'A', normalized to their own maximal values. (C). Family of control currents following voltage steps to various potentials with 5 mV intervals from a holding of –80 mV. Test pulse interval was 15 s. (D). Activation curves in the absence (filled circles) and presence (open circles) of 200 µM BAB. Conductance was determined by dividing the peak currents by (V_M-E_{Rev}) with E_{Rev} the reversal potential, which was set at +50 mV, close to the E_{Rev} of the total current-voltage relationship (cf. Fig. 1B). The calculated conductances were rather insensitive to the precise E_{Rev} value, because they were determined for the lower half of the voltages of the activation curve, far from E_{Rev}. The curves are Boltzmann fits to the data points. The dashed right parts of the curves indicate the extrapolated parts of the curves. Error bars indicate Standard Errors of the Means (SEM , n=9).

% (n=6) (Fig. 1C). After washout the currents completely recovered to 96 ± 10 % of the control amplitude. In Figure 1D, the concentration-response relation is shown for the peak of the T-type barium current. This relation was described using the Hill equation, resulting in an IC_{50} of 178 ± 21 µM and a Hill coefficient of 1.5 ± 0.3 (n=40). This IC_{50} is similar to that found for the N-type barium current evoked at 0 mV (~220 µM (Beekwilder et al., 2005)).

Effect of BAB on the T-type steady-state properties

A hyperpolarizing shift in the inactivation curve has been shown to be a possible current reducing mechanism of action of BAB for sodium channels (Van den Berg et al., 1995; Van den Berg et al., 1996). The typical inactivating time course of the T-type current makes this current an excellent model to look at the effects of BAB on inactivation of calcium channels. For that reason, we measured the steady-state inactivation of the T-type barium current by using a test pulse to –40 mV after applying a 350 ms prepulse to varying potentials from the holding potential -80 mV. The interval between the test pulses was 15 s. This was performed both in the absence and presence of 200 µM BAB. Plotting the relative current as a function of prepulse voltage resulted in the inactivation curves shown in Fig. 2A. A Boltzmann equation fitted to the data of individual cells yielded midpoint potentials of the inactivation curves under control conditions with a mean value of -52 ± 4 mV (n=5). Application of 200 µM BAB reduced the currents to less than 50% and induced a small but significant shift of the midpoint to –55 ± 4 mV (P=0.001), which could be reversed by washout towards –53 ± 3 mV (P=0.002). The normalized voltage-dependent inactivation curves are shown in Fig. 2B. BAB induced a shift of the midpoint of -2.8 ± 0.8 mV, which was not accompanied by a significant change in slope factor, with values of 3.6 ± 0.3, 3.4 ± 0.4 and 3.5 ± 0.2 mV for control, BAB and washout, respectively. It is clear from Fig. 2A,B that the small BAB-induced hyperpolarizing shift of the steady-state inactivation curve of T-type calcium channels is not responsible for the current reduction observed at the test pulse of –40 mV.

The T-type activation curve can only be obtained in a limited range of voltages due to the overlap with the activation curves of the HVA calcium channels at the more depolarized potentials. In Fig. 2C currents are shown elicited by depolarizing steps to various potentials ranging from –75 mV to –40 mV from a holding potential of –80 mV. This voltage range was limited to these values to

only activate the T-type currents. The resulting peak values were converted to conductance assuming a linear relation between current and driving force with a reversal potential of +50 mV. Subsequently, the conductance-voltage relations for the individual cells were fitted with a Boltzmann equation, which also described the activation curve for the higher range of potentials by extrapolation. The resulting values were averaged to obtain the mean activation curve, which showed no significant shift of the midpoint potential with –41 ± 5 mV for control and –41 ± 3 mV in the presence of 200 µM BAB (n = 9). Nor was there a difference in slope factor with 4.5 ± 0.9 mV and 4.3 ± 0.8 mV for control and BAB, respectively.
In conclusion, BAB caused and overall inhibition of T-type currents, but the steady-state properties of the currents were not or hardly affected. Only the midpoint potential of the inactivation curve was slightly shifted in the hyperpolarizing direction.

Effects of BAB on T-type current kinetics

The current during a maintained depolarizing step to –40 mV from a holding potential of –80 mV for control and with BAB is shown in Fig. 3A. Scaling of the currents to the control peak value showed an accelerating effect of 200 µM BAB on the currents (Fig. 3B). This acceleration could well be quantified by describing the T-type current traces with a m^2h Hodgkin-Huxley model (Tarasenko et al., 1998), (see methods). The time constant of the activation gate (τ_m) reduced significantly in the presence of BAB from 11.3 ± 2.5 ms to 8.7 ± 3.0 ms ($P < 0.001$, n = 9). The inactivation gate (τ_h) accellerated as well with time constants for control and BAB of 91 ± 52 ms and 40 ± 14 ms, respectively ($P = 0.007$, n = 9).

Upon repolarization to –80 mV, after a 15 ms pulse to –40 mV, the tail current was measured, representing the deactivation of T-type channels (Fig. 3C,D). In control solution the tail currents decayed with a time constant of 1.70 ± 0.23 ms (n=5). Application of 200 µM BAB significantly reduced this to a time constant of 1.17 ± 0.23 ms ($P < 0.001$). This effect was completely reversible with a time constant of 1.84 ± 0.36 ms ($P < 0.001$) following washout.

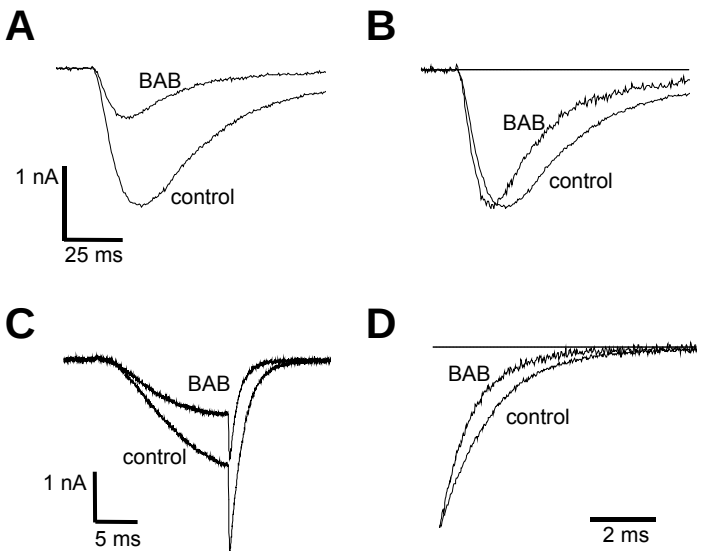

Figure 3. Effects of BAB on T-type current kinetics. (A). Activation and inactivation time course of T-type current records upon a step to –40 mV from a holding potential of –80 mV. Recordings for control and 200 µM BAB are superimposed. (B). Currents from 'A' normalized to the control peak value. (C). Barium currents elicited by a 15 ms voltage step to –40 mV from a holding of –80 mV. Recordings for control and 200 µM BAB are superimposed. (D). Tail currents from 'C' normalized to their own maximal values.

In conclusion, besides inhibiting T-type currents, BAB also accelerates activation, inactivation and deactivation kinetics of this current.

DISCUSSION

In the present study we specifically determined and analysed the effect of the local anesthetic butamben (BAB) on native low-voltage activated (T-type) calcium channels in the smaller mouse sensory neurons including the nociceptive neurons. BAB reduced the peak currents of the T-type barium current with an IC_{50} of ~200 µM and accelerated the kinetics of activation, deactivation and inactivation of this current. These effects of BAB on T-type current are very similar to those on high-voltage activated N-type current (Beekwilder et al., 2005).

Possible mechanism of T-type current inhibition by BAB

In the Hodgkin-Huxley model describing ion channel behavior, altered kinetics are typically reflected in a change of the midpoint potential and slope factor of the steady-state activation and inactivation curves. However, the BAB-induced accelerating effects on T-type current kinetics were not or only weakly accompanied by changes in these parameters. This would imply that the voltage dependent rates of gate opening and closing are roughly proportionally increased. In this interpretation the current inhibition by BAB cannot be fully explained by the observed kinetic changes, because the maximal currents are reduced. Therefore, we consider other than purely kinetic Hodgkin-Huxley mechanisms. The faster deactivation with BAB argues against a classical open-channel block, since that type of block is rather accompanied by slowed deactivation (see Snyders et al., 1992). The described effects on T-type currents are also similar to what was found for Kv1.1 potassium channels (Beekwilder et al., 2003). BAB accelerated both activation and deactivation kinetics without shifting the midpoint potential of activation for Kv1.1 current. In addition there was also an accelerated current decay or inactivation of these currents. These results were explained by an allosteric mechanism with BAB biasing the channels towards nonconducting channel states. Vedantham and Cannon (1999) hypothesized a preferential binding to intermediate closed states, causing increased inactivation in those states and a hyperpolarizing shift of the inactivation curve. Though they studied lidocaine effects, others have found confirming results for benzocaine, which is structurally very similar to BAB (Wang et al., 2004). However, in order to come to definitive conclusions on the underlying mechanisms more experiments would be needed.

The role of T-type currents in pain suppression.

The T-type calcium current seems to be a common neuronal process for mediating excitability. However its biophysical properties determine that it can have complex and paradoxical roles. The activation of the current in the low voltage range has a depolarizing effect, leading to a faster recruitment of sodium channels and therefore to the firing of an action potential. Raman and Bean (1999) showed in Purkinje neurons that blocking the T-type current using mibefadril resulted in a 30 % slowing of the firing rate, which indicated that the

presence of T-type current enhances excitability. McCallum et al. (2003) however, showed an increased excitability in sensory neurons as a result of a T-type current blockade, which means that the T-type presence would be responsible for less excitability. Here the authors suggested that the relatively slow deactivation of the T-type current results in prolonged calcium entry at the end of the action potential. Taking this calcium influx away would lead to higher excitability. The apparent discrepancy between these studies can be explained by the different actions of the T-type current on an action potential depending on the timing of the peak T-type current during this action potential and on the presence of other types of ion channels. The depolarizing action of the T-type current is enhancing the firing rate if it coincides with the uprise of the action potential, yet it inhibits the firing rate if it does so during the repolarizing phase, for example by activating hyperpolarizing calcium activated K channels.

It should also be considered that the T-type current may be carried by three different α-subunits, each with a specific expression pattern in the body. These three pore-forming subunit isotypes contribute differently to neuronal excitability through their different biophysical properties (Chemin et al., 2002). It is this variety of actions that makes it difficult to predict the role of inhibiting T-type calcium currents by BAB in its pain suppressing actions. This is also illustrated by several other studies. Modifying the T-type currents in vivo has shown that T-type currents are involved in pain signalling. Agents that selectively enhance T-type currents result in exaggerated thermal and mechanical nociception, whereas T-type current reducing agents do the opposite (Todorovic et al., 2001). Moreover, suppressing $Ca_V3.2$ (α_{1H}) T-type current, which are expressed in DRG neurons, using the mRNA antisense technique results in antinociceptive, anti-hyperalgesic and anti-allodynic effects (Bourinet et al., 2005). These studies suggest an enhancing nociceptive role for T-type currents. Apparent contradictory results have been found in mice lacking the $Ca_V3.1$ (α_{1G}) gene (Kim et al., 2003), with the absence of T-type currents in the thalamic neurons resulting in hyperalgesia, suggesting an anti-nociceptive role for central T-type currents. This might indicate that T-type currents have different roles depending on where they are located along the pain pathway. The ultralong duration of the pain suppression seems due to a slow steady release of butamben from the suspension in the confined epidural space (grouls?). Hence, the calcium channels present in this space will be subjected to butamben

continuously. Although it is unlikely that inhibiting the T-type calcium current in sensory neurons can alone explain the described pain suppressing effects of epidural BAB, either directly or via the interplay with other BAB affected channels (K_V, and Na_V), BAB effects on T-type calcium channels are likely to play a role, if T-type channels are expressed by dorsal root fibers. However, in the light of the above discussion of the role of T-type channels in pain signal generation in the peripheral nerve endings, the present results do implicate inhibition of T-type channels in BAB containing topical skin applications.

References

Beekwilder JP, Winkelman DLB, van Kempen GTH, van den Berg RJ, Ypey DL (2005) The block of total and N-type calcium conductance in mouse sensory neurons by the local anesthetic n-butyl-p-aminobenzoate. Anesth Analg in press.

Beekwilder JP, O'Leary ME, van den Broek LP, van Kempen GT, Ypey DL, van den Berg RJ (2003) Kv1.1 channels of dorsal root ganglion neurons are inhibited by n-butyl-p-aminobenzoate, a promising anesthetic for the treatment of chronic pain. J Pharmacol Exp Ther 304:531-538.

Bilici D, Akpinar E, Gursan N, Dengiz GO, Bilici S, Altas S (2001) Protective effect of T-type calcium channel blocker in histamine-induced paw inflammation in rat. Pharmacol Res 44:527-531.

Bourinet E, Alloui A, Monteil A, Barrere C, Couette B, Poirot O, Pages A, McRory J, Snutch TP, Eschalier A, Nargeot J (2005) Silencing of the Cav3.2 T-type calcium channel gene in sensory neurons demonstrates its major role in nociception. Embo J 24:315-324.

Buisman HP, De Vos A, Ypey DL (1990) A pipette holder for use in patch-clamp measurements. J Neurosci Methods 31:89-91.

Carbone E, Lux HD (1984) A low voltage-activated, fully inactivating Ca channel in vertebrate sensory neurones. Nature 310:501-502.

Chemin J, Monteil A, Perez-Reyes E, Bourinet E, Nargeot J, Lory P (2002) Specific contribution of human T-type calcium channel isotypes (alpha(1G), alpha(1H) and alpha(1I)) to neuronal excitability. J Physiol 540:3-14.

Kim D, Park D, Choi S, Lee S, Sun M, Kim C, Shin HS (2003) Thalamic control of visceral nociception mediated by T-type Ca2+ channels. Science 302:117-119.

Korsten HH, Ackerman EW, Grouls RJ, van Zundert AA, Boon WF, Bal F, Crommelin MA, Ribot JG, Hoefsloot F, Slooff JL (1991) Long-lasting epidural sensory blockade by n-butyl-p-aminobenzoate in the terminally ill intractable cancer pain patient. Anesthesiology 75:950-960.

McCallum JB, Kwok WM, Mynlieff M, Bosnjak ZJ, Hogan QH (2003) Loss of T-type calcium current in sensory neurons of rats with neuropathic pain. Anesthesiology 98:209-216.

Raman IM, Bean BP (1999) Ionic currents underlying spontaneous action potentials in isolated cerebellar Purkinje neurons. J Neurosci 19:1663-1674.

Randall AD, Tsien RW (1997) Contrasting biophysical and pharmacological properties of T-type and R-type calcium channels. Neuropharmacology 36:879-893.

Snyders J, Knoth KM, Roberds SL, Tamkun MM (1992) Time-, voltage-, and state-dependent block by quinidine of a cloned human cardiac potassium channel. Mol Pharmacol 41:322-330.

Tarasenko AN, Isaev DS, Eremin AV, Kostyuk PG (1998) Developmental changes in the expression of low-voltage-activated Ca2+ channels in rat visual cortical neurones. J Physiol 509 (Pt 2):385-394.

Todorovic SM, Jevtovic-Todorovic V, Meyenburg A, Mennerick S, Perez-Reyes E, Romano C, Olney JW, Zorumski CF (2001) Redox modulation of T-type calcium channels in rat peripheral nociceptors. Neuron 31:75-85.

Todorovic SM, Pathirathna S, Brimelow BC, Jagodic MM, Ko SH, Jiang X, Nilsson KR, Zorumski CF, Covey DF, Jevtovic-Todorovic V (2004) 5beta-reduced neuroactive steroids are novel voltage-dependent blockers of T-type Ca2+ channels in rat sensory neurons in vitro and potent peripheral analgesics in vivo. Mol Pharmacol 66:1223-1235.

Van den Berg RJ, Wang Z, Grouls RJ, Korsten HH (1996) The local anesthetic, n-butyl-p-aminobenzoate, reduces rat sensory neuron excitability by differential actions on fast and slow Na+ current components. Eur J Pharmacol 316:87-95.

Van den Berg RJ, Van Soest PF, Wang Z, Grouls RJ, Korsten HH (1995) The local anesthetic n-butyl-p-aminobenzoate selectively affects inactivation of fast sodium currents in cultured rat sensory neurons. Anesthesiology 82:1463-1473.

Vedantham V, Cannon SC (1999) The position of the fast-inactivation gate during lidocaine block of voltage-gated Na+ channels. J Gen Physiol 113:7-16.

Wang SY, Mitchell J, Moczydlowski E, Wang GK (2004) Block of inactivation-deficient Na+ channels by local anesthetics in stably transfected mammalian cells: evidence for drug binding along the activation pathway. J Gen Physiol 124:691-701.

Yunker AM, McEnery MW (2003) Low-voltage-activated ("T-Type") calcium channels in review. J Bioenerg Biomembr 35:533-575.

CHAPTER 5

THE LOCAL ANESTHETIC BUTAMBEN INHIBITS TOTAL AND L-TYPE BARIUM CURRENTS IN PC12 CELLS.

Laurentius J.A. Rampaart, Jeroen P. Beekwilder, Gertrudis Th. H. van Kempen, Rutgeris J. van den Berg, Dirk L. Ypey.

Anesth Analg in press

ABSTRACT

Background: Butamben or *n*-Butyl-*p*-Aminobenzoate is a long acting experimental local anesthetic for the treatment of chronic pain when given as an epidural suspension. We have investigated whether Cav1.2/L-type calcium channels may be a target of this butamben action.

Methods: The effect of butamben on these channels was studied in undifferentiated rat PC12-cells with the whole-cell patch-clamp technique in voltage-clamp. Ba^{2+} ions were used as the charge carriers in the calcium channel currents, while K^+ currents were removed by using K^+ free solutions.

Results: Butamben 500 μM reversibly suppressed the total whole-cell barium current by 90 ± 3% (n=15), while 10 μM nifedipine suppressed this barium current by 75 ± 7% (n=6). Pre-exposure to butamben followed by wash-out lowered the inhibition by nifidepine to 47 ± 5 % (n=10). These suppressive effects were not due to the measurement procedure and the drug vehicles in the solutions (<0.1% ethanol; n=6). Conclusions: Butamben inhibits the total barium current through expressed calcium channel types in PC12 cells, including Cav1.2/L-type channels. Because Cav1.2 channels may also occur in human nociceptive C fibers, this result allows the possibility that these L-type channels are involved in the analgesic action of butamben.

INTRODUCTION

Terminal cancer patients often suffer from severe pain due to tissue damage caused by either the primary tumor or metastasis. Palliation can be achieved by opioids or, if this does not adequately alleviate the pain, sometimes by ablating sensory nerves. These treatments may cause severe side effects, among which motor dysfunction is the most prominent one. A current experimental approach to chronic pain treatment is the epidural administration of an aqueous suspension of the local anesthetic *n*-butyl-*p*-aminobenzoate, also known as butamben (Shulman, 1987; Korsten et al., 1991). The suspension of butamben applied to the spinal dura results in a long lasting (median 29 days) relief from pain, without impairing motor function or other sensory functions. How butamben produces this extraordinary effect is still largely unresolved.

The butamben molecule is an aminobenzoate ester-linked to a butyl group. Its structure is similar to that of other ester-linked local anesthetics such as benzocaine and procaine, which block sodium channels involved in impulse generation and transmission in neurons (Butterworth and Strichartz, 1990; Hille, 2001). The effects of butamben on sodium currents have previously been studied in small DRG neurons (Van den Berg et al., 1995), which are believed to include the cell bodies of nociceptive fibers (Van den Berg et al., 1996). Butamben (100 μM) had a diverse effect on the various types of sodium channels, ranging from nearly completely blocking fast sodium currents to having no effect on slow sodium currents. The inhibition of DRG fast sodium currents resulted in reduced excitability of DRG neurons, which is likely to contribute to the butamben anesthesia. However, the blocking effect of butamben on the fast sodium currents does not seem to be the only mechanism of butamben analgesia (Butterworth and Strichartz, 1990).

Inward current through calcium channels also plays an important role in action potential generation in sensory neurons (Scroggs and Fox, 1992) and possibly also in human impulse transmission in C-type nocifibers (Quasthoff et al., 1995). Recently, two types of calcium channels that are expressed in neonatal mouse dorsal root ganglion (DRG) neurons, N-type and T-type, were shown to be suppressed by butamben (Beekwilder et al., 2005; Beekwilder et al., 2006) with

a 50% inhibiting concentration of ~200 μM, similar to that for inhibition by butamben of the total calcium or barium current through all the calcium channels . These mouse DRG neurons also express L-type calcium channels (subtype Cav1.2), but in a proportion too small (7 ± 6 %, n=7; unpublished observations) to study with our whole-cell current recording technique. In small adult rat DRG neurons, however, voltage gated L-type calcium channels seem to constitute a significant portion of calcium currents (Scroggs and Fox, 1992). Hence, it is interesting to explore the effect of butamben on L-type calcium currents.

Therefore, we addressed the question whether butamben inhibits the Cav1.2/L-type current component of whole-cell barium currents through calcium channels. To this end, the patch-clamp technique in whole-cell voltage-clamp configuration was applied to undifferentiated PC12 (pheochromocytoma) cells. These are rat adrenal medullar chromaffin tumor cells that express various types of calcium channels, with a relatively strong expression of the cardiac L-type (α1C; Avidor et al., 1994; Liu et al., 1996), denoted as Cav1.2 in modern terminology (Hille, 2001). By making use of nifedipine, a specific L-type calcium channel blocker (Hille, 2001), we show that butamben, besides blocking the total barium current through calcium channels, at least partly blocks the L-type barium current component in PC12 cells. In the discussion, we consider the implications of the present results for the analgesic action of butamben.

METHODS

PC12 cell culture

PC12 cells from the Hubrecht Laboratory (Utrecht, The Netherlands) were maintained in RPMI 1640 medium (Gibco, Grand Island, NY, USA) supplemented with 10% heat-inactivated horse serum, 5% fetal calf serum (both sera from Invitrogen, Breda, the Netherlands), 100 IU/mLpenicillin, and 100 μg/mL streptomycin (both from Sigma-Aldrich, Zwijndrecht, the Netherlands). After

cells were grown in a poly-L-lysine (MW 70,000-150,000 D, Sigma-Aldrich) coated culture flask for 7 days and had formed a nearly confluent monolayer, they were dissociated with Versene (Invitrogen) and plated on poly-L-lysine coated cover slips, after which they were grown in a culture dish in a humidified 5% CO_2 incubator at 37˚C to obtain undifferentiated PC12 cells (Avidor et al., 1994). Experiments were conducted 4-7 days after plating.

Whole-cell recording

The patch-clamp experiments were carried out at room temperature (~23 ^{o}C). A glass coverslip was mounted in a chamber on the stage of an inverted microscope (Zeiss Axiovert 35). Patch pipettes were fabricated from borosilicate glass (Harvard Apparatus, Edenbridge, Kent, UK) and were giga-sealed to the cells in a microbath (75 µL) continuously perfused with a standard extracellular solution (ECS), containing (in mM) 125 NaCl, 5.5 KCl, 0.8 MgCl2, 2 CaCl2, 10 HEPES/NaOH (pH 7.3), 21.8 glucose and 36.5 sucrose, which is similar to the solution used by (Westerink et al., 2000) for PC12-cells. The pipette was filled with a CsCl containing intracellular solution (CsICS), consisting of 130 CsCl, 1 CaCl2, 10 HEPES/CsOH (pH 7.2), 10 EGTA, 5 MgATP and 0.5 TrisGTP. Pipette resistance measured in ECS was 4.2 ± 0.1 MΩ (mean ± SEM, n = 23). Flattened adhered polygonal cells were preferred over phase-bright spherical cells, because they exhibited larger calcium channel currents (Janigro et al., 1989). Seal resistances were 1.8 ± 0.2 GΩ (n=18). After establishment of the whole-cell configuration, the microbath was perfused with a solution containing barium (BaECS), consisting of 140 NaCl, 5 CsCl, 2 MgCl2, 10 BaCl2 and 10 HEPES/NaOH (pH 7.3). The combined use of BaECS and CsICS enhanced the current through calcium channels and fully removed potassium currents (cf. Fig. 1). Occasional (in <5% of the cells) inward sodium-like currents (Garber et al., 1989) were small and so fast (~3-ms duration) that they did not interfere with our measurements of the slower barium currents. Butamben (OPG Farma, Utrecht, The Netherlands) was added to the BaECS in a concentration of 500 µM, from a stock of 500 mM butamben in ethanol. Nifedipine (Sigma-Aldrich) was used to identify currents through L-type channels. It was added to the BaECS in a concentration of 10 µM, from a stock of 10 mM nifedipine in ethanol. This concentration is close to that for maximal and specific inhibition of Ca1.2/L-type channels under our measurement conditions, i.e. at a holding potential of -80 mV (Hille, 2001).

Both for the butamben and nifedipine solution the concentration of ethanol never exceeded 0.1%.

A PC running Clampex 8 (Axon Instruments, Foster City, CA) and a List EPC 7 amplifier provided voltage protocols. The membrane currents were filtered at 3 kHz. The PC12 cell currents were leak subtracted using the P/4 method. The single exponential capacitive transients revealed the absence of electrical coupling between cells, even when they were visibly in contact. The membrane capacitance of the cells derived from these transients was 24.4 $\pm$ 3.1 pF (n=27). The series resistance was 7.2 $\pm$ 0.6 MΩ (n=9) and was not compensated because of the small size of the recorded currents. Data are presented as mean ± SEM for n cells. Means are compared using paired or independent t-tests with the level of significance (p) chosen as 0.05.

RESULTS

Upon depolarization, the selected PC12 cells exhibited a small inward calcium current in ECS, consisting of currents through various types of calcium channels (Garber et al., 1989; Janigro et al., 1989; Liu et al., 1996). To enhance the current flowing through the calcium channels, barium ions were used as charge carriers (instead of calcium ions) by applying a barium solution (BaECS) to the cells. The cell membrane was held at a voltage of –80 mV and was then step-depolarized to +10 mV for 60 ms at regular intervals of 15 s until the inward barium current reached its maximal increase (within 4 min, including the arrival-delay of Ba-ECS through the perfusion tubing). Figure 1A shows the inward calcium current of a PC12 cell at 10 mV, as well as the gradual increase in the current at that test potential upon infusion of the barium containing solution into the bath. The calcium current records in ECS showed a variable composition of a faster and slower inactivating current (see example in Fig. 1A). A current-voltage (I-V) relationship of the barium current was created by applying test potentials between –60 and +40 mV to the PC12 cells at 15 s intervals and by measuring

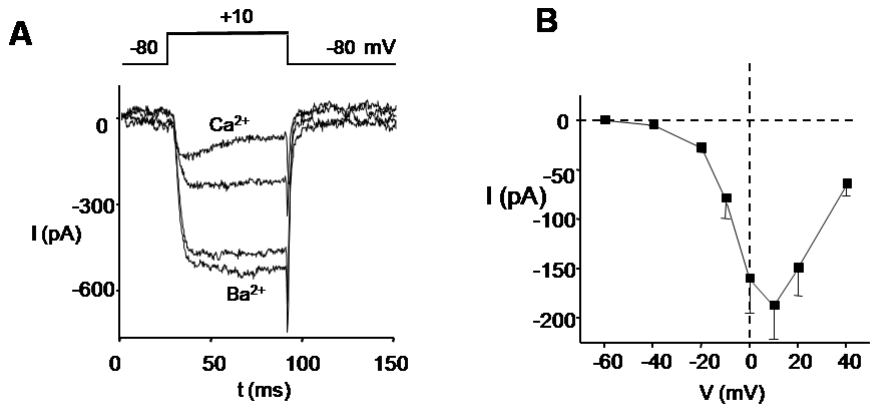

Figure 1. (*A*) Progress in calcium channel current increase upon exchanging the calcium containing bath solution (ECS) for a barium containing solution. Current records were evoked by voltage steps from –80 to +10 mV with 15-s intervals, of which here every 4th response is shown. The upper record is taken in the calcium containing ECS, just before infusing the barium solution. The lowest record is an early steady-state record in the barium containing solution. Note also the absence of the fast inactivation time course in the increased barium current. (*B*) Mean I-V relationship gained by applying depolarizing voltages from a holding potential of –80 mV, after which the barium current's maximum was measured which was then plotted against the voltage at which it was elicited (mean ± SEM, n=8).

the maximal barium current at each test potential (Fig. 1B). From about –40 mV upwards the barium current increased in amplitude until it reached its maximum at +10 mV (~-200pA), after which it declined and reversed at potentials extrapolated to >40 mV. To establish whether butamben inhibited the barium current, 500 µM butamben was applied to the cells. This concentration of butamben blocked 90 ± 3% of the control barium current ($P < 0.05$, n=15) (Figure *2A*), which level was reached within 4 min, including the butamben arrival delay. This inhibitory effect was largely reversible to 76 ± 6 % (n=8) after ~ 5 minutes wash-out. Now that the blocking effect of butamben on the total barium current through calcium channels expressed in PC12 cells was established, 10 µM nifedipine was applied to the cells to prove that at least part of the calcium channels in the PC12 cell membranes was of the L-type. 10 µM nifedipine blocked 75 ± 7% of the control barium current ($P < 0.05$, n=6) (Fig. 2B) within about 3 min. This effect was partly reversible to 47 ± 7 % (n=6) of the initial

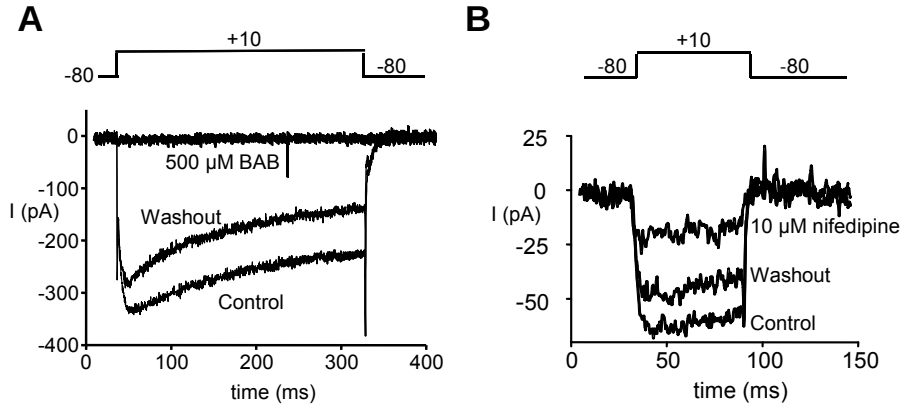

Figure 2. (A) Addition of 500 µM butamben (BAB) resulted in an almost complete inhibition of the barium current. Note also the increased inactivation rate in the washout record. (*B*) Addition of 10 µM nifedipine resulted in an inhibition of a large part of the barium current. Note the difference in time scales in A and B and Fig. 1, indicating variability in calcium channel expression between cells.

control current, after ~5 min (Fig. 2B). Assuming that the nifedipine only affected the L-type current (Hille, 2001), we conclude that at least three quarters of the barium currents generated by the PC12 of the L-type and that since 500 µM butamben blocked 90% of that current, L-type calcium channels are at least partly blocked by butamben.

To gain further support for this conclusion, an experiment was done in which the effects of butamben and nifidepine were determined on the same cell. After an initial barium current control period, a PC12 cell was first exposed to 500 µM butamben for 4 min, after which buamben was washed out for 5.5 min and 10 µM nifedipine was added for 4 min. Finally, nifedipine was washed out for 3.5 min to check for reversibility of the nifedipine effect. During the application and washing out of the drugs, the cells were step-depolarized from a holding potential of –80 mV to 10 mV with 15-s intervals to elicit the barium current and explore the effect of the drugs on the current. Figure 3A shows example records, while the mean results of 10 of these experiments are shown in Figure 3B. Butamben 500 µM caused a 93 ± 2% inhibition of the inward barium current ($P < 0.05$, n=10), reproducing the above results. When butamben was washed out, 74 ± 5% of the original current was regained ($P < 0.05$, n=10), also corresponding

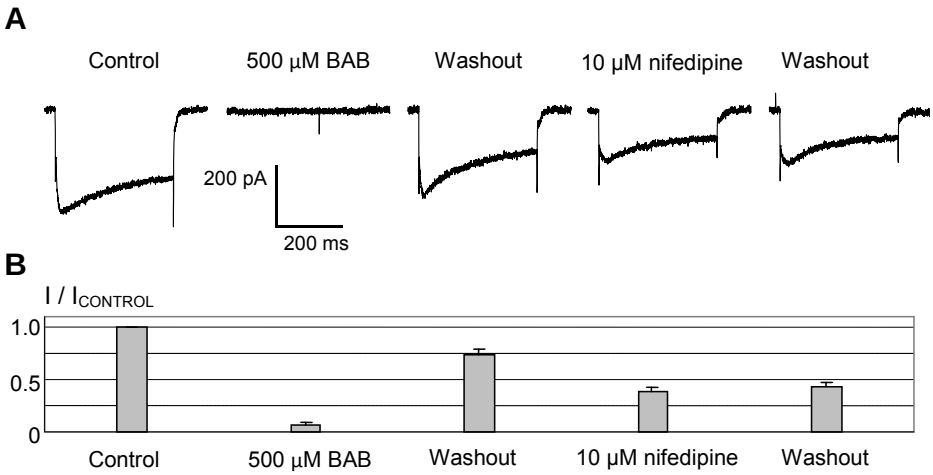

Figure 3. (*A*) The effect of butamben (BAB) and nifedipine on barium currents elicited in one and the same cell by a voltage step to +10 mV from a holding potential of –80 mV. Barium currents are given for the control condition, after addition of 500 µM butamben, after washout of butamben, after addition of 10 µM nifedipine and after washout of nifedipine, respectively. (*B*) Results of 10 experiments in which the cells were exposed to 500 µM butamben as well as to 10 µM nifedipine, according to the protocol in A. Normalized mean peak barium currents ± SEM are given for each condition.

to the above results. When 10 µM nifedipine was then applied to the cells, we found an inhibition of 47 ± 5 % (n=10) of the preceding butamben wash-out current peak, corresponding to a remaining 38 ± 4% of the original current ($P < 0.05$, n=10). This inhibition is smaller than the fresh exposure inhibition of 75% described above. The final barium current amplitude after washout of nifedipine was 43 ± 4% of the original current amplitude ($P > 0.05$ washout versus nifedipine, n=7), which corresponds to a recovery of ~57% of the preceding butamben wash-out peak current.

Since the inward barium current did not completely recover after washout of butamben and nifedipine, the possibility remained that part of the inhibition of the barium current seen during and after the administration of butamben and nifedipine was caused by rundown of the barium current. Therefore, we carried out a vehicle/rundown control experiment, in which the same drug application protocol was used as in the experiment described above. After an initial Ba

wash-in period of ~4 min, we exposed the cells, instead to butamben and nifedipine, to 0.1% vehicle (ethanol), which also allowed us to check whether the inhibiting effects of butamben and nifedipine were not due to ethanol. Figure 4 shows only a slight decline of the normalized peak barium-current amplitude during the course of the experiment. At the end of the experiment (after ~18 min), 85 ± 3% (n=6) of the original barium current remained. The conclusions that can be drawn from this experiment are that the inhibiting effects seen during the administrations of butamben and nifedipine were not caused by the vehicle (0.1% ethanol) and that the rundown of the barium current may only explain a small percentage (≤15%) of the incomplete recovery after butamben and nifedipine exposure.

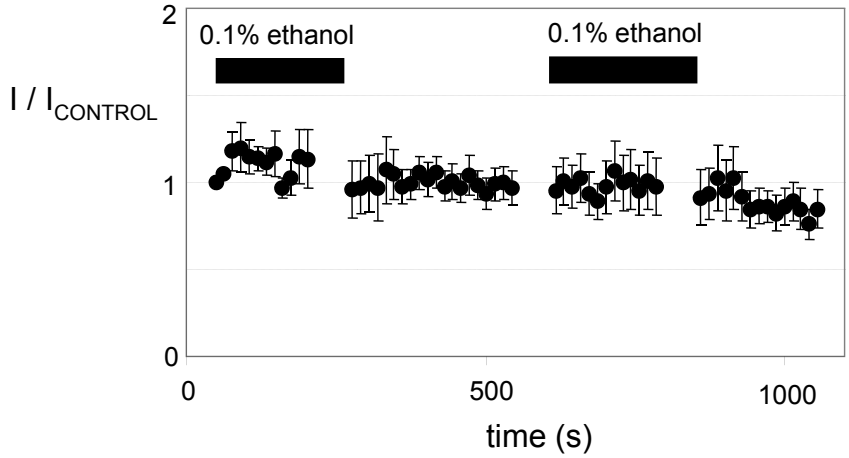

Figure 4. The rundown/vehicle control experiment. Peak barium currents were measured upon depolarizing steps to +10 mV from a holding potential of –80 mV, applied with 15-s intervals. Black horizontal bars indicate the addition of vehicle (0.1% ethanol) according to the protocol in Fig. 3. Peak currents were normalized by dividing these currents by the peak current at t = 0 s. All experiments were preceded by a 4-min in-wash period of BaECS (not shown). Mean normalized peak currents ± SEM are plotted for 6 cells. Empty spaces in the plot are interruptions for voltage-clamp protocols to determine I-V curves.

DISCUSSION

In the present study we examined the inhibiting effect of butamben on calcium channels, including Cav1.2/L-type channels, in PC12 cells. These channels are expressed in small rat DRG neurons and therefore may contribute to pain signal transmission (Scroggs and Fox, 1992). We rather used undifferentiated PC-12 cells than DRG-neurons, because L-type calcium channels constitute in these cells a significant part of the expressed calcium channels (Janigro et al., 1989; Avidor et al., 1994), providing about 75 % of the peak barium current in our study. We found that the clinically relevant concentration of 500 μM butamben (close to the maximum solubility concentration of ~700 μM in butamben suspensions, see chemical 1504 in The Merck Index , 1989) blocked ~90 % of the total peak barium current that was mediated by the various types of calcium channels (besides L- probably also N- and T-type) expressed in PC12 cells (Garber et al., 1989; Janigro et al., 1989; Avidor et al., 1994). This result is consistent with our earlier studies (Beekwilder et al., 2005; Beekwilder et al., 2006) on sensory neurons, which showed that butamben inhibits the total barium or calcium current of the smaller neonatal mouse dorsal-root ganglion neurons and specifically the barium currents through N- and T-type channels by 80-90%. Total Kv and isolated Kv1.1 currents were also inhibited for ~80% by 500 μM butamben (Beekwilder et al., 2003). The concentration response curves in all these cases had an IC50 around 200μM (range 177-238) and a Hill coefficient of ~1.5 (range 1.1-1.8). We expect therefore that Cav1.2 currents have a similar concentration response curve for butamben.

In our preparations of sensory neurons the L-type currents were too small to be of use for the study of the effect of butamben. We proved here that at least part of the L-type calcium channels in PC12 cells was inhibited by butamben, because the inhibition of the total barium current (~90%) was clearly larger than the percentage of L-type current, which was 75 or 47%, depending on the used inhibition protocol. Our results also show that the inhibiting effect of butamben on calcium channels is not cell type or species dependent.

It is noteworthy that in the longer protocol, where first butamben was applied to the cells and washed out, and then nifedipine was administered, nifedipine

seemed to inhibit a smaller portion of the barium current (47%) than in the protocol in which nifedipine was the first-exposure drug (75%). One reason may be that the different calcium channel subtype components have differences in run-down and/or run-up time courses, changing the proportions of these components of the total barium current at the observed run-down of ~15% over 18 min. Another possibility is that washout of the butamben effect was not complete, and that remaining butamben molecules interfere with nifedipine binding. Nevertheless, it was proven that butamben inhibits L-type calcium channels. Through which mechanism butamben reaches this effect is still unknown. One mechanism might be that butamben causes a relative acceleration of deactivation and inactivation kinetics, which would make it more difficult for the channel to open and stay open in the presence of butamben. This would be consistent with a BAB induced increase in deactivation and inactivation rate of other calcium channels (N- and T-type) and of Kv1.1 channels as observed by Beekwilder et al. (2003; 2005; 2006). In this respect it is worth mentioning that incompletely recovered barium currents after butamben wash-out often showed an increased inactivation rate (Figs. 2A and 3A). Further studies directed at butamben's effect on the gating kinetics of the L-type calcium channel could help clarify butamben's mechanism of action.

The mechanism of butamben analgesia depends on butamben's ability to suppress the generation and/or transmission of action potentials in the neurons that transmit pain signals to the brain. Since L-type calcium channels are possibly present in human nociceptive C fibers (Quasthoff et al., 1995), Butamben's blocking effect on this type of calcium channels might contribute to analgesia when administered epidurally. The present results and those of Beekwilder et al. (2005; 2006) add butamben to the list of local anesthetics inhibiting calcium channels (Sugiyama and Muteki, 1994). They also implicate anesthetic actions of butamben on the peripheral autonomous nervous system. Future studies should be directed at the question how the integrated effects of butamben on the various types of ion channels in DRG neurons, result in analgesia.

ACKNOWLEDMENTS

We thank Prof. Dr. A. van der Laarse (Cardiology, LUMC, Leiden) for the use of his laboratory facilities.

References

Avidor B, Avidor T, Schwartz L, De Jongh KS, Atlas D (1994) Cardiac L-type Ca2+ channel triggers transmitter release in PC12 cells. FEBS Lett 342:209-213.

Beekwilder JP, van Kempen GT, van den Berg RJ, Ypey DL (2006) The local anesthetic butamben inhibits and accelerates low-voltage activated T-type currents in small sensory neurons. Anesth Analg 102:141-145.

Beekwilder JP, Winkelman DL, van Kempen GT, van den Berg RJ, Ypey DL (2005) The block of total and N-type calcium conductance in mouse sensory neurons by the local anesthetic n-butyl-p-aminobenzoate. Anesth Analg 100:1674-1679.

Beekwilder JP, O'Leary ME, van den Broek LP, van Kempen GT, Ypey DL, van den Berg RJ (2003) Kv1.1 channels of dorsal root ganglion neurons are inhibited by n-butyl-p-aminobenzoate, a promising anesthetic for the treatment of chronic pain. J Pharmacol Exp Ther 304:531-538.

Butterworth JFt, Strichartz GR (1990) Molecular mechanisms of local anesthesia: a review. Anesthesiology 72:711-734.

Garber SS, Hoshi T, Aldrich RW (1989) Regulation of ionic currents in pheochromocytoma cells by nerve growth factor and dexamethasone. J Neurosci 9:3976-3987.

Hille B (2001) Ionic Channels of Excitable Membranes. Sunderland MA: Sinauer Associates.

Janigro D, Maccaferri G, Meldolesi J (1989) Calcium channels in undifferentiated PC12 rat pheochromocytoma cells. FEBS Lett 255:398-400.

Korsten HH, Ackerman EW, Grouls RJ, van Zundert AA, Boon WF, Bal F, Crommelin MA, Ribot JG, Hoefsloot F, Slooff JL (1991) Long-lasting epidural sensory blockade by n-butyl-p-aminobenzoate in the terminally ill intractable cancer pain patient. Anesthesiology 75:950-960.

Liu H, Felix R, Gurnett CA, De Waard M, Witcher DR, Campbell KP (1996) Expression and subunit interaction of voltage-dependent Ca2+ channels in PC12 cells. J Neurosci 16:7557-7565.

Quasthoff S, Grosskreutz J, Schröder JM, Schneider U, Grafe P (1995) Calcium potentials and tetrodotoxin-resistant sodium potentials in unmyelinated C fibres of biopsied human sural nerve. Neuroscience 69:955-965.

Scroggs RS, Fox AP (1992) Multiple Ca2+ currents elicited by action potential waveforms in acutely isolated adult rat dorsal root ganglion neurons. Journal Of Neuroscience 12:1789-1801.

Shulman M (1987) Treatment of cancer pain with epidural butyl-amino-benzoate suspension. Regional Anesth 12:1-4.

Sugiyama K, Muteki T (1994) Local anesthetics depress the calcium current of rat sensory neurons in culture. Anesthesiology 80:1369-1378.

Van den Berg RJ, Wang Z, Grouls RJ, Korsten HH (1996) The local anesthetic, n-butyl-p-aminobenzoate, reduces rat sensory neuron excitability by differential actions on fast and slow Na+ current components. Eur J Pharmacol 316:87-95.

Van den Berg RJ, Van Soest PF, Wang Z, Grouls RJ, Korsten HH (1995) The local anesthetic n-butyl-p-aminobenzoate selectively affects inactivation of fast sodium currents in cultured rat sensory neurons. Anesthesiology 82:1463-1473.

Westerink RH, de Groot A, Vijverberg HP (2000) Heterogeneity of catecholamine-containing vesicles in PC12 cells. Biochem Biophys Res Commun 270:625-630.

CHAPTER 6

BUTAMBEN INHIBITS HERG CHANNELS EXPRESSED IN HEK/TSA CELLS WHILE ACCELERATING BOTH ACTIVATION AND INACTIVATION KINETICS

Jeroen P. Beekwilder, Laurentius J. A. Rampaart, Wilbert van Meerwijk, B. van Duijn, M. Vennik, Rutgeris J. van den Berg, Dirk L. Ypey

ABSTRACT

Butamben (BAB) is a hydrophobic local anesthetic, which has been used in epidural suspensions for long-term selective suppression of pain signal transmission in dorsal root nerve fibers. Our previous studies have shown that BAB has atypical inhibiting effects on various cation (Kv, Nav and Cav) channels. In order to analyse the mechanism of BAB's inhibitory action on voltage-activated channels, we expressed hERG channels heterologously in HEK/tsA cells and studied the effects of BAB on the amplitude and kinetics of these currents using the voltage-clamp method. Our results show that hERG currents are inhibited by BAB with an IC_{50} of ~112 µM and that this inhibition is accompanied by an acceleration of all kinetic processes of activation and inactivation. Small shifts (~8 mV) of the activation and inactivation curves were observed, but could not explain the current inhibition, because they rather caused current increase. Mathematical modelling was used to explore mechanisms of the inhibiting BAB effects, based on the accelerated kinetics. We show that a Hodgkin-Huxley type model cannot explain the BAB-induced current inhibition from the kinetic changes of the current. However, a multi-state model allows such an explanation, when it is assumed that BAB biases hERG channels towards an intermediate closed state, which is in rapid equilibrium with an inactivated state.

Butamben or n-butyl-p-aminobenzoate (BAB) is an ester-linked local anesthetic that has long been considered of little use because of its hydrophobicity (solubility <1 gr in 7 l water at room temperature). However, epidural injections of aqueous butamben suspensions have shown to be a promising alternative for the treatment of intractable chronic pain (Shulman, 1987; Korsten et al., 1991), because it results in an ultralong relief of pain (median 29 days) without impairment of motor function.

It is not yet clear how butamben selectively blocks the pain signals for prolonged periods of time. Previously, the effect of butamben has been studied on sodium and calcium channels of neurons from rat and mouse dorsal root ganglion (DRG) (van den Berg et al., 1996; Beekwilder et al., 2005; Beekwilder et al., 2006) of which the small-size neurons are for pain detection and transmission (Harper and Lawson, 1985). Of the various potassium channels Kv1.1 and Kv4.2 have been studied in more detail (Beekwilder et al., 2003; Winkelman et al., 2005). All these studies showed that butamben has atypical effects on the different ion channels, i.e. current inhibition associated with kinetics acceleration, which might be part of the reason for the specific actions of butamben as an analgesic.

In the present study we looked at the effects of butamben on the human ERG channel (hERG or Kv11.1). ERG stands for Ether-a-go-go Related Gene and was first found in the hippocampus (Warmke and Ganetzky, 1994), but has been shown to be present in DRG neurons as well (Polvani et al., 2003). It is best known for its function in the repolarization of the action potential in the heart (Sanguinetti et al., 1995). The ERG potassium current is rather extraordinary, because it displays very slow activation kinetics in combination with fast inactivation kinetics (cf. Zhou et al., 1998). During depolarization of the cell membrane, this results in a steady-state inactivation of the channels when activation has barely begun. The ERG current was found to modulate the firing frequency of cerebellar Purkinje neurons (Sacco et al., 2003). Although its role in DRG neurons has not been determined, it is likely to be involved in pain signal generation or transmission. Therefore, pharmacological effects on the ERG current could affect both pain signal generation and transmission. Furthermore,

the slow activation kinetics of ERG channels allows studying the effect of BAB on this kinetics, which could lead to a better insight into BAB's interaction with ion channels in general.

In the present work we found an inhibition of the hERG current by butamben accompanied with accelerated activation, deactivation and inactivation kinetics as well as a faster recovery from inactivation (de-inactivation). In order to elucidate butamben's mechanism of action, these findings were compared with mathematical models. The BAB effects on hERG currents could be mimicked in a simple multi-state model by changing the transition rates towards an intermediate closed state, in rapid equilibrium with an inactivated state. A Hodgkin-Huxley type model failed to explain BAB-induced hERG current inhibition from kinetic changes alone. The possible functional implications for the analgesic effect of BAB will be considered in the discussion.

METHODS

hERG transfected HEK/tsA culture

The HEK293/tsA201 cells (a gift from professor Spaink, Clusius Laboratory, Leiden University) were grown in a 25 cm^2 culture flask in Dulbecco's Modified Eagle's Medium (DMEM, Sigma-Aldrich, Zwijndrecht, The Netherlands) complemented with 10% Fetal Calf Serum and penicillin/streptomycin (enriched DMEM). When the culture was 70-80% confluent, it was dissociated using Versene (Gibco, Breda, The Netherlands) and diluted by 50% using enriched DMEM. After the cells were left to attach to the bottom of the culture flask for ~2.5 hours, a suspension of 15 µl lipofectamine 2000 (Invitrogen, Breda, The Netherlands), 3.6 µg plasmid coding for hERG and Green Fluorescent Protein and 2 ml DMEM was added. After an incubation period of 5 hours, the transfection suspension was removed from the flask and enriched DMEM was added. Approximately 20 hours after transfection, the medium was removed from the cell culture, transfection efficiency was checked using a fluorescence microscope

and the culture was dissociated with Versene and plated on glass coverslips. Experiments were performed 2-4 days after transfection.

Whole-cell recording

For the patch-clamp experiments, a glass coverslip culture was mounted on the stage of an inverted fluorescence microscope (Zeiss Axiovert 35). The HEK/tsA cells were continually perfused in a microbath (35 µl) with extracellular solution which consisted of (in mM): NaCl 137, KCl 4, $CaCl_2$ 1.8, $MgCl_2$ 1, HEPES 10, Glucose 10, pH 7.4 (NaOH). Transfected cells lit up green (507 nm) upon illumination with blue light (488 nm) and could thus be selected for hERG-current measurements.
Patch pipettes were fabricated from borosilicate glass (Harvard Apparatus, Edenbridge, Kent, UK) and were filled with (in mM): KCl 115, $MgCl_2$ 1, HEPES 10, EGTA 5, Na_2ATP 10, pH 7.4 (KOH). Cells were brought in the giga-sealed whole-cell configuration and up to 70-90% of the series resistance was compensated resulting in series resistance values < 1 MΩ. Capacitive currents were largely cancelled.
For BAB-experiments on hERG-transfected HEK-tsA cells, various concentrations of BAB were added to the extracellular solution, with a final ethanol concentration of 0.1%. Vehicle experiments in which the transfected cells were exposed to 0.1% ethanol showed that ethanol caused neither reduction of the hERG current nor changes in hERG gating kinetics (n=6). All experiments occurred at room temperature.

Analysis and statistics

The Hill equation: $I/I_{MAX} = (1 + ([BAB]/IC_{50})^{n})^{-1}$, was fitted to the concentration-inhibition data of the hERG-currents, where IC_{50} is the concentration of half maximal inhibition and n is the Hill coefficient. The activation and inactivation data of the hERG currents were fitted to a Boltzmann equation: $I/I_{MAX} = (1+\exp-((V-V_{0.5})/k))^{-1}$, where V is the prepulse potential, $V_{0.5}$ the voltage at which the current is activated or inactivated half-maximally, and k is the slope factor.
The data described in this report are represented as Mean ± Standard Error of the Mean (M ± SEM) for a given number (n) of cells, unless stated otherwise, and Mean values are compared using paired or independent t-tests with the level of significance (p) chosen as 0.05.

Modelling

Mathemathical modelling to explore mechanisms of action of BAB was carried out with the use of the software package Mathematica 5.2 (Wolfram Research Inc, Champaign, IL). In one approach we constructed a classical Hodgkin-Huxley type of model from our data, assuming $I_{hERG}=a*i*G_{hERGmax}*(V-V_K)$. The activation gating variable 'a' stands for the slow, depolarization induced opening of hERG channels. The inactivation gating variable 'i' stands for the fast, depolarization induced closing process. The voltage dependency of a and i represented by x is described by $dx/dt = (x_\infty(V)-x)/\tau_x(V)$, whereby the steady state $x_\infty(V)$ and $\tau_x(V)$ are determined from the data by fitting procedures. $G_{hERGmax}$ is the maximal conductance, V the membrane potential and V_K the Nernst equilibrium potential for the K^+ gradient across the cell membrane. The two gating variables were taken to be independent. Since activation and deactivation clearly showed a double exponential behavior, we decided to use an empirical description for the activation process with two exponential components in the form of $a(t) = a_1[0]e^{-t/\tau1} + a_2[0]e^{-t/\tau2} + a[\infty]$, where a is the amplitude. Time constants (τ) represent the kinetics of these processes and were taken from the experimental data of

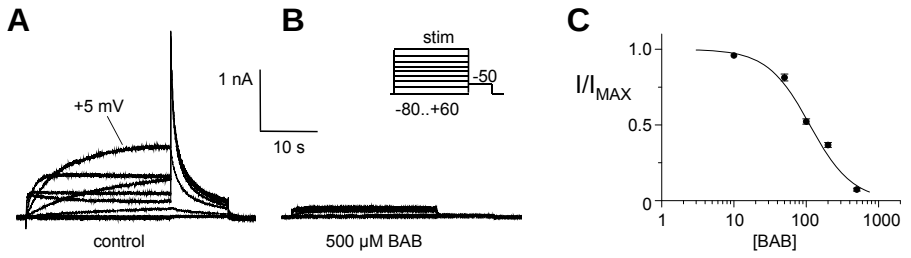

Figure 1. The effect of butamben (BAB) on hERG currents expressed in HEK/tsA cells. (A) Control current records evoked by the protocol in the inset of frame B. The protocol consisted of a 25-s voltage step to various potentials (-80, -60, -40, -25,-10, +5, +20, +40 and +60 mV) with a subsequent test pulse to –50 mV fo 10 s before returning to the holding potential of –80 mV. The resting interval between episodes was 10 s. Note the increased rate of activation with higher depolarization steps and the decline in the steady-state currents at voltages > +5 mV. Note also the characteristic hooked tail current records upon the backstep to –50 mV due to fast de-inactivation followed by slower deactivation. (B) Current records evoked by the same protocol in the presence of 500 µM BAB. (C). Concentration-response curve of butamben. The normalized tail current peaks were evoked by a backstep to –50 mV from a 5-s prepulse of +40

Figures 4 and 5. The steady-state values were obtained from the Boltzmann fits in Figures 2 and 3. The HH model was also used to estimate step duration times for the design of an efficient voltage-clamp 'staircase' protocol (see inset Fig. 2A).
In an alternative approach we made use of the multi-state model of Kiehn et al. (1999), which we simplified as depicted in Figure 6B and which we tried to fit to our hERG-data. The channel distribution as a function of time was calculated using the transition rates listed in Table 1 and the relative conductance was determined as the percentage of channels in the open state.

EXPERIMENTAL RESULTS

BAB inhibits hERG currents

Figure 1A shows a family of currents from a HEK/tsA cell with the heterologously expressed hERG channels. Currents were activated with a 25-s step to various depolarizing potentials from –80 mV with a subsequent repolarizing 10-s step to –50 mV eliciting a large (hooked) tail current. Sham-transfected cells contained small endogenous slowly inactivating K_V currents at positive potentials (peak values at +20 mV of 117 ± 27 pA, n=7) with fast activation upon depolarization and fast deactivation upon repolarization to –50 mV (not shown; cf. Zhou et al., 1998). Therefore, the endogenous currents do not or hardly interfere with expressed hERG currents.

Adding a concentration of 500 µM BAB results in an almost complete reduction of the current (Fig. 1B), which shows that hERG currents are sensitive to BAB. In order to determine the concentration dependency of the BAB effect a 10-s step to +40 mV was applied to the cell with a subsequent step to the test pulse at –50 mV and the large reproducible peak of the evoked tail current was measured at different BAB concentrations. The resulting concentration response curve is shown in Figure 1C. Fitting a Hill equation to the data showed an IC_{50} of 112 ± 4 µM and a Hill coefficient of 1.5 ± 0.1 (n = 39).

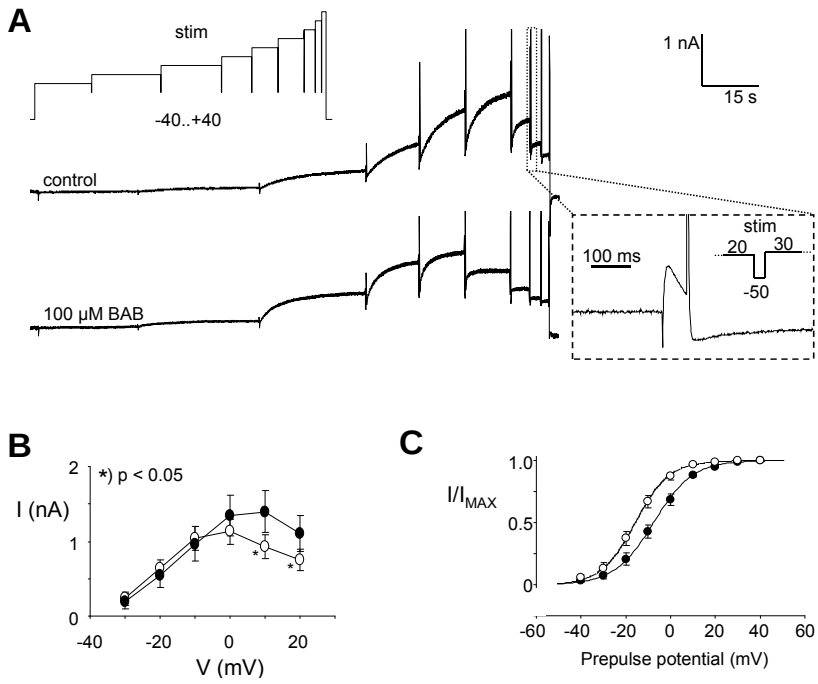

Figure 2. The effect of BAB on the steady-state activation of hERG currents. (A) Stair-case protocol with variable long-duration steps to various increasing potentials, with 10 mV interval, preceded by short interrupting 60-ms steps to –50 mV (see upper left inset). The lower right inset shows the current during one step to –50 mV in more detail. Records are shown for both control conditions (top) and in the presence of 100 µM BAB (bottom). (B) Steady-state currents plotted against potential for both control (closed symbols) and in the presence of BAB (open symbols). Plotted values were derived from fits with a double exponential function. (C) The steady-state activation curve as obtained by plotting the normalized tail peak current upon a –50 mV step as a function of the prepulse potential in the absence (closed symbols) and presence (open symbols) of 100 µM BAB. The recorded values at -50 mV were multiplied by the fitted steady-state amplitudes of the prepulse divided by the recorded amplitudes at the end of the prepulse.

BAB shifts hERG steady-state activation

To study the effect of BAB on steady-state activation, a special time saving "stair-case" voltage protocol was constructed to measure the activation curve in one run. It consisted of subsequent depolarizing steps to various potentials with varying durations, only separated by 60-ms test pulses to –50 mV (Fig. 2A). The long duration of the subsequent voltage steps was based on estimated time

constants for activation during pilot experiments. Fig. 2A shows the current records evoked by this protocol in the absence (control) and presence of 100 µM BAB (~IC_{50} in the tail-current concentration response curve in Fig. 1C). The records show increased activation rates at higher depolarizations and in the presence of BAB, but to our surprise, we could only see a BAB-induced reduction of the extrapolated steady-state or 'window' currents at potentials > -10 mV (Fig. 2B).

The steady-state activation curves were obtained by plotting the peaks of the tail responses to the steps to –50 mV as a function of prepulse potential (Fig. 2C). In

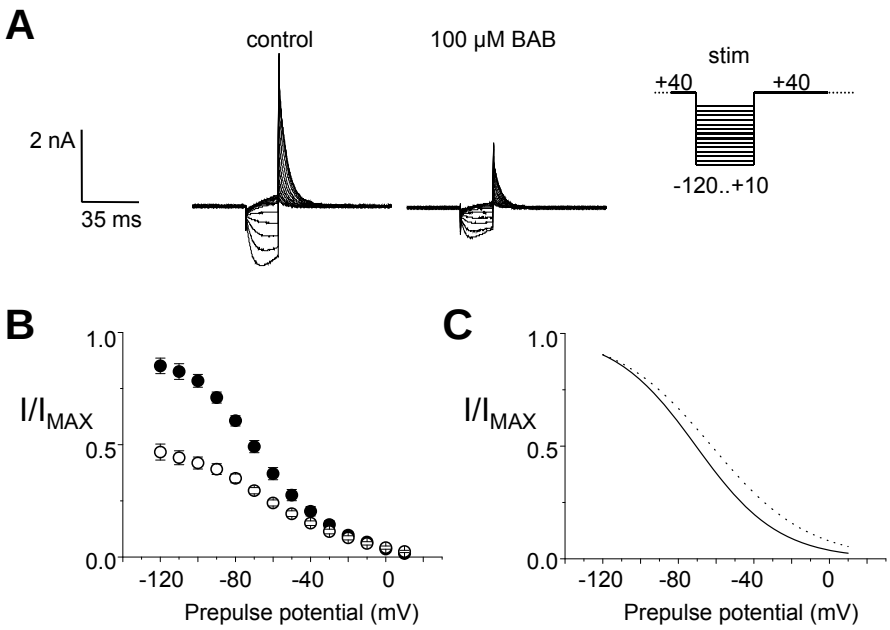

Figure 3. The effect of BAB on steady-state inactivation of hERG channels. (A) Currents evoked by 20 ms voltage steps to various potentials (-120 to +10 mV, see inset) following a 1200 ms prepulse to +40 mV and a subsequent step back to +40 mV. Records are shown for both the control condition (left) and 100 µM BAB (right). (B) Voltage dependence of channel availability, determined by curve fitting of the records with a single exponential for both control (closed symbols) and in the presence of BAB (open symbols). The deactivation was compensated by a factor representing the current deactivation occurring during the 20 ms pre-potential. The values were normalized to the maximal value of the Boltzmann curve fitted to the control data. Current values larger than 5 nA were omitted to exclude unreliable voltage-clamp data. (C) Boltzmann fits of the data in (B) with the BAB-curve (dotted) also normalized to its

the control situation a Boltzmann equation fitted to the data resulted in a midpoint potential of -8 ± 2 mV and a slope factor of 8.7 ± 0.8 mV (n = 6). In the presence of 100 µM BAB these values significantly changed to respectively –16 ± 2 mV ($p = 2.2e^{-4}$) and 7.6 ± 0.6 mV (p = 0.02). These changes revealed both a hyperpolarizing shift of 8 mV and a slightly steeper slope of the activation curve in the presence of BAB. These values completely recovered upon washout to –10 ± 3 mV and 8.8 ± 0.6 mV, respectively. A hyperpolarizing shift of the activation curve counteracts inhibition in the voltage range of activation, which includes membrane potentials between -40 and +20 mV. This shift can obviously not be responsible for the reduced currents at higher potentials found in the presence of 100 µM BAB (Fig. 2A,B).

BAB affects channel availability.

The inactivation curve of hERG currents has a shallow slope and includes most of the physiological membrane potentials (Berecki et al., 2005). This means that a shift of this curve will have effects on currents over almost the whole range of physiological potentials. Therefore, the study of drug effects on hERG currents should always include steady-state inactivation properties. Because of the rapid nature of the inactivation of the hERG currents compared to hERG activation, a 3-step voltage protocol was needed to obtain the steady-state inactivation curve. Currents were first fully inactivated at maximal activation with a step to +40 mV for 1200 ms before stepping down to various test potentials for 20 ms in order to allow inactivation to reach a new steady-state at maximal activation (Fig. 3A). The instant current at the subsequent step to +40 mV was a measure for the channel availability after correction for the current deactivation at the most negative prepulse potentials (legend Fig. 3B). To determine the effect of BAB on steady-state inactivation, this protocol was repeated in the presence of 100 µM BAB. In Figure 3B the inactivation curve for the control situation as well as with 100 µM BAB is shown. In the presence of 100 µM BAB the currents were reduced at all prepulse potentials <-10 mV. Fitting with a Boltzmann equation showed a significant shift of the midpoint potential of 8.0 ± 1.5 mV in the depolarizing direction from –71 ± 2 mV in control to –63 ± 3 mV in the presence of BAB (p = 0.006; n=5). The slope of the curve did not change significantly with 22 ± 2 mV and 25 ± 1 mV in the absence and presence of BAB, respectively. This shift alone would increase the currents over the whole voltage range and

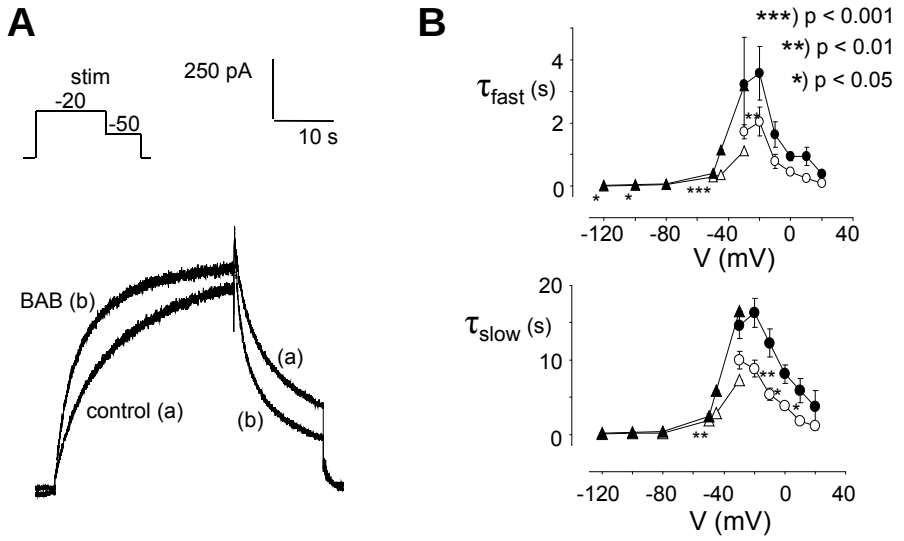

Figure 4. The effect of BAB on hERG channel activation kinetics. (A) Two example records, one control and one in the presence of 100 µM BAB, evoked by the voltage step protocol in the inset. (B) Time constants for activation and deactivation for the slow (top panel) and fast component (lower panel). Values were obtained from deactivation (▲) or activation kinetics (●) for both control (filled) and 100 µM BAB (open symbols). For -120, -100, -80, -50, -45, -30, -20, -10, 0, 10, 20 mV the values are based on 5, 5, 4, 9, 1, 4, 10, 3, 4, 4, 5 cells, respectively. Significant differences are indicated by stars.

therefore it cannot be directly responsible for the large reduction of the currents observed.

Effects of BAB on hERG activation kinetics

Having shown that BAB does not cause its current reducing action through a shift of the activation and inactivation curve along the x-axis, we subsequently looked at the effects of BAB on hERG activation kinetics. Figure 2 already illustrates, besides the inhibitory effect on the current amplitude, the overall accelerating effect of 100 µM BAB on activation kinetics. Figure 4A shows, besides an effect on activation kinetics, accelerated deactivation kinetics in the presence of BAB. Time constants were obtained by fitting a double exponential function to the current traces obtained at different step voltages. The resulting fast and slow time constants were plotted against potential in Figure 4B. The plot shows that

application of 100 µM BAB resulted in the voltage range more than -40 mV in acceleration for both the fast and the slow time constants of respectively, 46 ± 4% and 42 ± 5% (n=51).

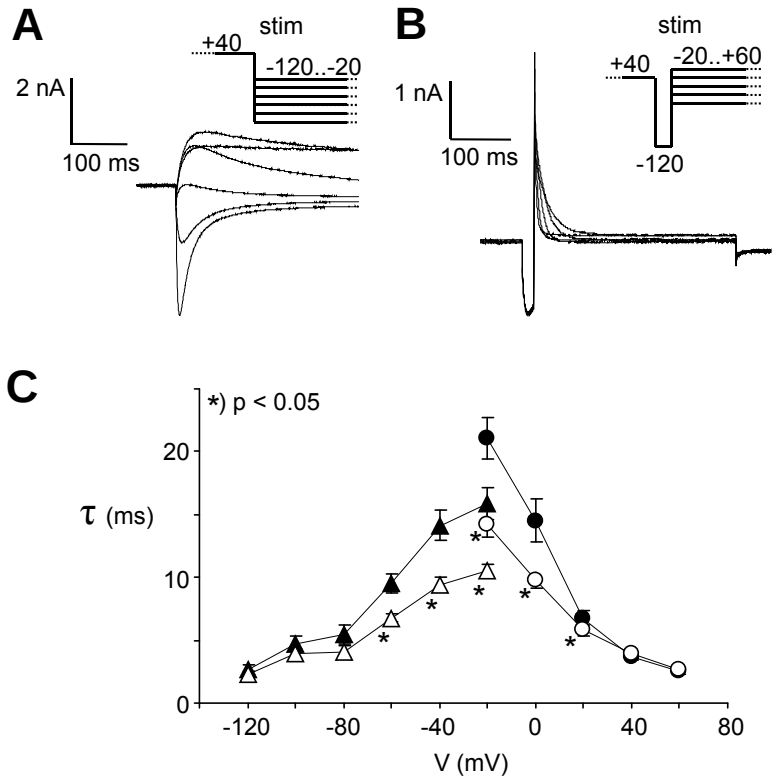

Figure 5. The effect of BAB on hERG channel inactivation kinetics. (A) From a potential of +40 mV with fully activated and inactivated currents a voltage step to various more negative potentials was made to allow for recovery from inactivation. Currents traces were fitted to a double exponential function of which the slower component reflected deactivation and the faster one recovery from inactivation. The latter one was plotted against voltage in C. (B) From a potential of +40 mV with fully activated and inactivated currents a 20 ms step to –120 mV was made to remove inactivation. Subsequently steps to various potentials ranging from –20 mV to +60 mV were made to allow for current inactivation. Inactivation kinetics were fitted with a single exponential for the construction of the plot in C. (C) Voltage dependence of the inactivation gate time constant. For all data points n=5. Significant differences are indicated by

BAB effects on hERG inactivation kinetics

For studying the effect of BAB on the recovery from inactivation a 2-s pulse to +40 mV was applied to fully inactivate the hERG current at maximal activation. This was followed by a down-step to various potentials in order to allow the channels to recover from their fully inactivated state and exhibit their activation (Fig. 5A). Fitting with a double exponential function allowed the recovery from inactivation (de-inactivation) to be separated from deactivation. The application of 100 µM BAB resulted in a significant acceleration of the de-inactivation at the potentials –60 to -20 mV.

To determine the effect of 100 µM BAB on the fast hERG inactivation kinetics a 3-step protocol was used in which the hERG currents were fully inactivated at maximal activation by applying a 2-s step to +40 mV and fitting a double exponential function to the current traces obtained at different step voltages. Subsequently, a 20-ms step to –120 mV was applied in order to allow full recovery from inactivation, before stepping to various test potentials (Fig. 5B). The large difference in time constants for deactivation and inactivation allow a direct measurement of the latter (not shown). At the tested potentials –20 to +20 mV inactivation accelerated significantly in the presence of BAB, whereas higher potentials did not show a significant acceleration. The time constants from both the inactivation and its recovery are shown in Figure 5C. The estimated inactivation time constants at –20 mV were usually larger than the de-inactivation time constants at that potential. Nevertheless, BAB accelerated the kinetics of the inactivation gate both in the closing and opening rate.

MODEL EVALUATION OF BAB EFFECTS

Modelling BAB effects with a Hodgkin-Huxley type mode.

There are three distinct effects of BAB on the hERG currents. First, the left shift of the activation curve and the right shift of the inactivation curve. Second, the

speeding up of the activation and inactivation processes and third, a reduction of the steady-state current in a voltage dependent manner. In a Hodgkin-Huxley (HH) type description of the currents, the first two effects can never explain the third one (current reduction) without assuming channel conductance changes. To illustrate this we made a HH model of the hERG current. Figure 6A shows a simulation of the hERG current (cf. experimental records in Fig. 1A and Fig. 6C left panel) with stationary activation/inactivation properties and kinetic rates obtained from our experiments (Figs. 2-5). The effects of the BAB induced changes of these rates are shown. Clearly there is an overall increase in current amplitude, which is contrary to our observations (cf. experimental records in Fig. 6C, right panel). This means that the Hodgkin-Huxley description of the hERG currents is inappropriate to explain the current inhibition from the kinetic effects of BAB and the shifting effects on the activation and inactivation curve. Thus, an additional effect of BAB must be presumed for a Hodgkin-Huxley type model. This additional effect could either be a complete block of part of the channel population or a reduced single channel conductance.

BAB effects are inconsistent with open channel block as the sole mechanism.

As a second possibility we studied the hypothesis that BAB specifically binds one particular state in a multi-state channel gating model, whether it is of the Hodgkin-Huxley type or not. BAB would then introduce an additional state into the model representing a non-conducting BAB bound state, which is

Figure 6 (*next page*). Modelling BAB effects on hERG currents. (A) Simulation of hERG currents with a Hodgkin-Huxley type model. Parameters were obtained from experimental data in this study. In the left panel parameters were used from the experimental control data. The right panel shows the inadequate simulation of BAB affected hERG currents in the same model with kinetic parameters taken from BAB experiments in this study. (B) Kinetic multi-state ion channel model used to describe hERG currents. C2 and C1 are closed states, O is the open (conducting) state and I is the inactivated state. (C) Current records obtained with a voltage protocol as shown in the inset for control (left panel) and in the presence of 100 µM BAB (right panel). (D) Simulation of hERG currents with the model from B using the voltage protocol from C. Parameter values are listed in Table 1, where bold values indicate parameters different for the BAB simulations. The resting or starting channel distributions over the states for both control and BAB were taken 0.001 in states O, C1 and I, and the remaining 0.997 in C2.

connected to a binding (receiving) state. A classical example of this type of block is open channel block in which a drug solely binds to the open channel thus making it non-conducting. For the channel to return to the closed state the drug

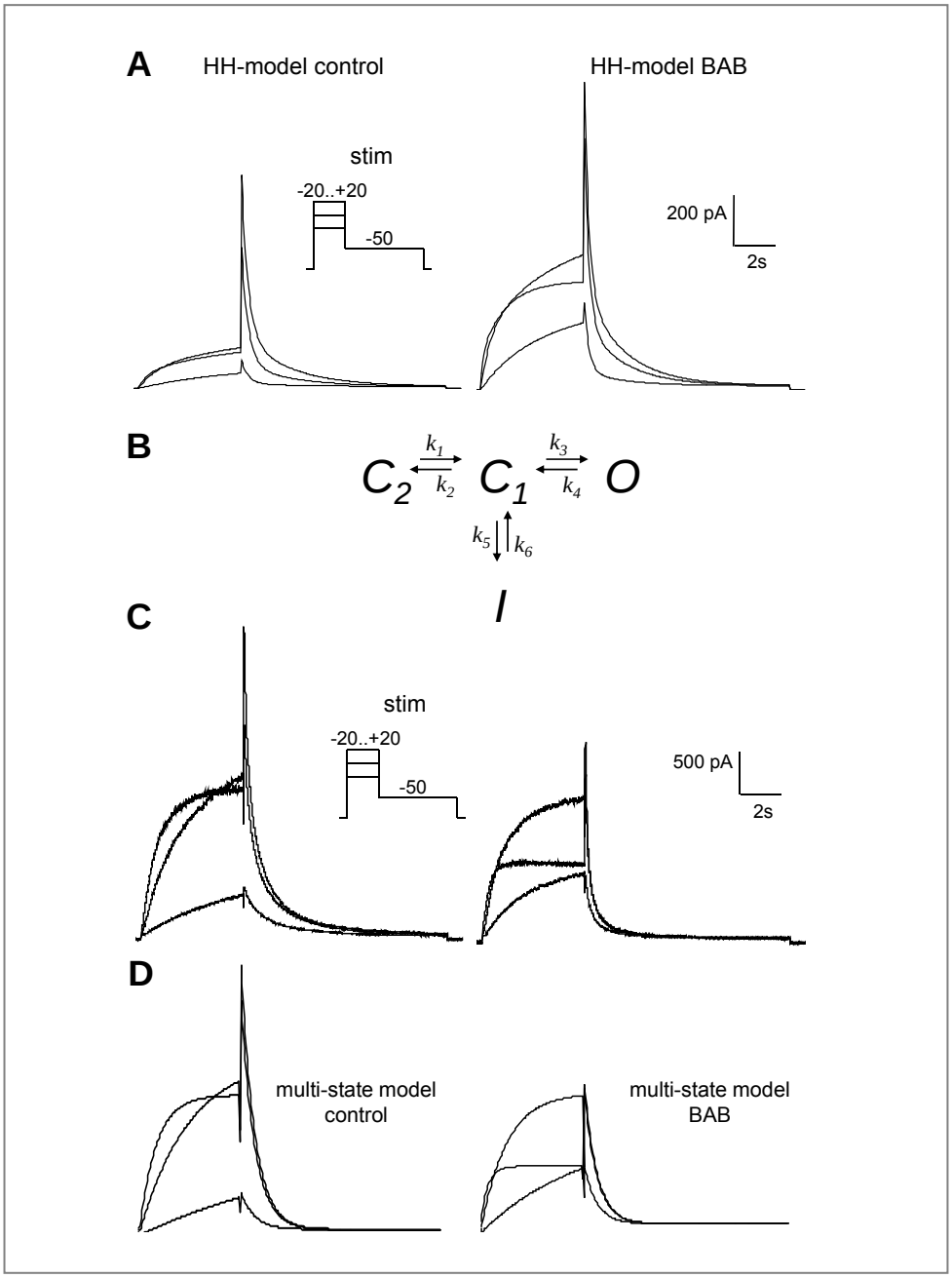

has to unbind first.

The introduction of a new, non-conducting drug-bound state which only connects to one conducting open state can never lead to increased current amplitude, as is the case in our experiments for steps to –20 mV (Fig 4A). Furthermore, unbinding of BAB from the open state during deactivation can never cause an increased rate of deactivation as observed for BAB (Fig. 4). Therefore, we conclude that open channel block cannot be the sole mechanism of hERG-current inhibition by BAB, whether it is dependent or independent on membrane voltage.

	-50 mV	*-20 mV*	*0 mV*	*+20 mV*
k_1	0.035 **0.1**	0.04 **0.13**	0.4 **0.8**	1.19 **3**
k_2	2.1	0.8	0.3	0.4
k_3	2600	1500	650	300
k_4	15000 **30000**	2400 **4200**	300 **400**	250 **300**
k_5	80	1500	3000	4000
k_6	300	140	40	60
A	30000	60000	80000	100000

Table 1: Parameters of the simulations in Figures 6D of the model as shown in Figure 6B. Added bold numbers indicate values different for the BAB simulation.

Modelling BAB-effects with a multi-state model

Various multi-state models have been used by others to describe hERG currents. A property they have in common is the presence of multiple closed states. One of the most simple models is the one described by Kiehn et al. (1999), which we adapted for our case. Their model consists of three consecutive closed states and one open state (C-C-C-O), while one inactivated state was connected to the

last closed state before opening. That model sufficed to simulate their recorded hERG currents. However, their simulations showed that the third closed state most distant from the open state was of little importance in the model behavior. To test this we simulated currents using the original model with three closed states with the parameters from the Kiehn et al (1999) paper. We added a realistic amount of white noise and subsequently fitted the simulated currents with the simpler model with only two closed states (Fig. 6B). This also resulted in a good fit (not shown). Therefore, and in order to limit the number of free parameters in our model, we investigated whether this simplified model (Fig 6B) could be used to describe our experimental hERG currents and the BAB effects on it. Thus, our model has two closed states, one open state and a single inactivated state connected to the intermediate closed state. As can be seen in Figure 6D, the model mimics the measured currents rather well, when single records (as in Fig. 6C) were fitted. Simulating the BAB affected hERG currents turned out to be possible over the whole voltage range with only the parameters k_1 and k_4 affected by BAB. These are the transition rates towards the intermediate closed state. Thus, by only increasing the values of k_1 and k_4 the simulated currents behaved qualitatively similar to the hERG recordings in the presence of 100 µM BAB. Fitting a Boltzmann curve (not shown) through the three peak currents at –50 mV from the simulations, results in a midpoint potential for the simulated control currents of –11 mV, while this midpoint was shifted to –19 mV by the 'presence of BAB'. This indicates that the simple model used is in principle capable of explaining the BAB effects on hERG currents by only modifying a subset of the transition rates between the different states without touching the number of channels or the single channel conductance.

So far, it was impossible to fit the model to a complex sequence of records as in Figure 2A instead of to separate records, as in Figure 6C. Besides the possibility that this is due to interference by the intrinsic K_V current, this illustrates the limitations of using a simplified model as we did. The imperfection of the model is also displayed by the slower tail currents as compared to the recorded ones in Figure 6C. In order to substantiate the conclusions the model might need adjustments. However, the present model does show that the effects of BAB on hERG current (acceleration and inhibition) do not necessarily contradict each other, but rather may originate from a single mechanism.

DISCUSSION

In the present study we investigated the effects of the local anesthetic butamben (BAB) on human ERG currents expressed in HEK/tsA cells. We found inhibitory effects associated with changes of both steady-state properties and kinetics.

The effects of other local anesthetics like ropivacaine, bupivacaine, levobupivacaine and cocaine have been studied on hERG before by others (O'Leary, 2001; Gonzalez et al., 2002). Consistent with these studies we found an overall inhibition of the current and an acceleration of the inactivation kinetics by BAB. However, in contrast to those other local anesthetics, which cause a slower deactivation, we found also an acceleration of deactivation kinetics. Furthermore, the depolarizing shift of the inactivation curve in the presence of 100 µM BAB is in the opposite direction as was found for bupivacaine, ropivacaine and levobupivacaine (Gonzalez et al., 2002). Therefore, it is not possible to establish a general biophysical mechanism of ERG current reduction by local anesthetics. Hence, the mechanisms of action of different local anesthetics must be studied individually.

Modelling aspects

Simulation of the described kinetic effects in terms of Hodgkin-Huxley type models revealed that the kinetic effects are counteracting the steady-state current reduction. Therefore, an additional current reducing effect of BAB must be presumed for such a model. This may be a reduced single channel conductance, which can be determined experimentally. On the other hand, in Kiehn's (1999) simplified multi-state model the inhibitory BAB effects could be explained by just kinetic effects. Thus, although the 4-state model we used to describe the hERG currents is likely to be an oversimplified reflection of the real gating processes in the ion channel, it does adequately describe the main kinetic and steady-state properties of the hERG currents. The BAB effects as we observed could in this simple model be mimicked by increased transition rates from the open and the second closed state to the intermediate closed state. Interestingly, Vedantham and Cannon hypothesized a preferential binding of the

local anesthetic lidocaine to intermediate closed states of sodium channels (Vedantham and Cannon, 1999). Others have found confirming results for benzocaine, which is structurally very similar to BAB (Wang et al., 2004).

The effects of BAB on the hERG currents show similarities with effects of BAB on other ion channels described previously. Heterologously expressed Kv1.1 channels showed in the presence of BAB faster kinetics as well a reduced steady state current (Beekwilder et al., 2003). Native N- and T-type calcium channels of DRG neurons displayed accelerated kinetics as well as a reduced current in the presence of BAB (Beekwilder et al., 2005; Beekwilder et al., 2006). These similarities suggest a common mechanism of BAB affecting the different ion channels.

Molecular mechanisms

If the multi-state model is right, one has to explain how the molecular structure of the hERG channel (Sanguinetti and Tristani-Firouzi, 2006) would allow rapid preferential inactivation from the intermediate closed state and increased residency in this intermediate closed state in the presence of BAB.

The establishment of the molecular mechanism of the inhibitory action of BAB on hERG currents may require a mutational analysis of the BAB effects as in Winkelman et al. (2005), where evidence was presented for the presence and location of a high-affinity binding site for a partial blocking effect of BAB on A-type K_V channels. However, the majority of the inhibitory BAB effects seem to occur at larger concentrations (low affinity binding with an IC_{50}~100μM) and the observed kinetic accelerations do not necessarily implicate the presence of a specific binding site for these concentrations. In the light of a recent publication of the MacKinnon group (Schmidt et al., 2006), the lipophilic BAB molecules could affect the lipid environment of the voltage sensors in such a way that they cause an acceleration of the gating kinetics towards the intermediate closed state, thus favoring increased inactivation. A third possibility is of course a combination of a binding-site model and a non-binding-site model, but new experiments are required to further explore molecular mechanisms.

Functional implications

Due to the distinct properties of the ERG channels, it is complicated to translate the found BAB effects to functional implications. More so since, unlike in the heart, the role of ERG currents in the peripheral nervous system is not yet well understood. In the current study we did our measurements at room temperature as opposed to body temperature (~37ºC), which affects the currents (Berecki et al., 2005). Furthermore, the kinetic effects of BAB show increased as well as decreased current amplitudes depending on the time scale. The prolonged steady depolarizations mostly used in the voltage protocols for ERG currents are not physiological. Pain signals are coded as action potential trains. Under these dynamic voltage conditions the ERG currents are likely to increase in the presence of BAB, due to the faster activation and recovery of inactivation. A decreased ERG component results in a higher firing frequency as was shown in cerebellar Purkinje neurons (Sacco et al., 2003). Consequently, an increased ERG component would result in a decreased firing frequency. This way, the effects of BAB on ERG currents could play a role in the analgesic effects of BAB, be it in epidural suspensions or in topical skin applications. However, for a definite conclusion on BAB's analgesic mechanisms, the concerted actions of BAB on all affected voltage-activated cation channels should be considered. Mathematical modelling of these actions could be very helpful in this respect.

Conclusion

BAB shows atypical effects on hERG currents compared to cocaine, bupivacaine and ropivacaine, indicating that there is no general mechanism of action for local anesthetics. For the mechanism of BAB action on hERG channels we showed in a simple (non-Hodgkin/Huxley) multi-state model that all BAB effects can be explained by an increase in the rates of certain state transitions by the presence of BAB. The data suggest that BAB biases channels towards an intermediate closed state, which is in rapid equilibrium with an inactivated state. Whatever the mechanism of BAB action, we conclude that BAB effects on channel kinetics must be considered in explaining the anesthetic/analgesic effects of BAB.

ACKNOWLEDGEMENTS.

We thank Prof. H. Spaink, Dr. E. Snaar and Mrs. Rueb of the Cell Biology Department (IMP, Leiden University) and Mrs. G.Th.H. Van Kempen of the Department of Molecular Cell Biology (Div. Neurophysiology, LUMC) for their help in the culture and transfection procedures.

References

Beekwilder JP, van Kempen GT, van den Berg RJ, Ypey DL (2006) The local anesthetic butamben inhibits and accelerates low-voltage activated T-type currents in small sensory neurons. Anesth Analg 102:141-145.

Beekwilder JP, Winkelman DL, van Kempen GT, van den Berg RJ, Ypey DL (2005) The block of total and N-type calcium conductance in mouse sensory neurons by the local anesthetic n-butyl-p-aminobenzoate. Anesth Analg 100:1674-1679.

Beekwilder JP, O'Leary ME, van den Broek LP, van Kempen GT, Ypey DL, van den Berg RJ (2003) Kv1.1 channels of dorsal root ganglion neurons are inhibited by n-butyl- p-aminobenzoate, a promising anesthetic for the treatment of chronic pain. JPharmacolExpTher 304:531-538.

Berecki G, Zegers JG, Verkerk AO, Bhuiyan ZA, de Jonge B, Veldkamp MW, Wilders R, van Ginneken AC (2005) HERG channel (dys)function revealed by dynamic action potential clamp technique. Biophys J 88:566-578.

Gonzalez T, Arias C, Caballero R, Moreno I, Delpon E, Tamargo J, Valenzuela C (2002) Effects of levobupivacaine, ropivacaine and bupivacaine on HERG channels: stereoselective bupivacaine block. Br J Pharmacol 137:1269-1279.

Harper AA, Lawson SN (1985) Conduction velocity is related to morphological cell type in rat dorsal root ganglion neurones. J Physiol Lond 359:31-46.

Kiehn J, Lacerda AE, Brown AM (1999) Pathways of HERG inactivation. Am J Physiol 277:H199-210.

Korsten HH, Ackerman EW, Grouls RJ, van Zundert AA, Boon WF, Bal F, Crommelin MA, Ribot JG, Hoefsloot F, Slooff JL (1991) Long-lasting epidural sensory blockade by n-butyl-p-aminobenzoate in the terminally ill intractable cancer pain patient. Anesthesiology 75:950-960.

O'Leary ME (2001) Inhibition of human ether-a-go-go potassium channels by cocaine. Mol Pharmacol 59:269-277.

Polvani S, Masi A, Pillozzi S, Gragnani L, Crociani O, Olivotto M, Becchetti A, Wanke E, Arcangeli A (2003) Developmentally regulated expression of the mouse homologues of the potassium channel encoding genes m-erg1, m-erg2 and m-erg3. Gene Expr Patterns 3:767-776.

Sacco T, Bruno A, Wanke E, Tempia F (2003) Functional roles of an ERG current isolated in cerebellar Purkinje neurons. J Neurophysiol 90:1817-1828.

Sanguinetti MC, Tristani-Firouzi M (2006) hERG potassium channels and cardiac arrhythmia. Nature 440:463-469.

Sanguinetti MC, Jiang C, Curran ME, Keating MT (1995) A mechanistic link between an inherited and an acquired cardiac arrhythmia: HERG encodes the IKr potassium channel. Cell 81:299-307.

Schmidt D, Jiang QX, MacKinnon R (2006) Phospholipids and the origin of cationic gating charges in voltage sensors. Nature 444:775-779.

Shulman M (1987) Treatment of cancer pain with epidural butyl-amino-benzoate suspension. Regional Anesth 12:1-4.

van den Berg RJ, Wang Z, Grouls RJE, Korsten HHM (1996) The local anesthetic, n-butyl-p-aminobenzoate, reduces rat sensory neuron excitability by differential actions on fast and slow Na+ current components. Eur J Pharmacol 316:87-95.

Vedantham V, Cannon SC (1999) The position of the fast-inactivation gate during lidocaine block of voltage-gated Na+ channels. J Gen Physiol 113:7-16.

Wang SY, Mitchell J, Moczydlowski E, Wang GK (2004) Block of inactivation-deficient Na+ channels by local anesthetics in stably transfected mammalian cells: evidence for drug binding along the activation pathway. J Gen Physiol 124:691-701.

Warmke JW, Ganetzky B (1994) A family of potassium channel genes related to eag in Drosophila and mammals. Proc Natl Acad Sci U S A 91:3438-3442.

Winkelman DL, Beck CL, Ypey DL, O'Leary ME (2005) Inhibition of the A-type K+ channels of dorsal root ganglion neurons by the long-duration anesthetic butamben. J Pharmacol Exp Ther 314:1177-1186.

Zhou Z, Gong Q, Ye B, Fan Z, Makielski JC, Robertson GA, January CT (1998) Properties of HERG channels stably expressed in HEK 293 cells studied at physiological temperature. Biophys J 74:230-241.

CHAPTER 7

GENERAL DISCUSSION

Butamben (n-butyl-p-aminobenzoate, BAB) has been successfully applied in patients with chronic intractable pain, resulting in a relief from this pain as can be deducted from lowering the dosage or even a complete stop of the intake of morphine by the patients themselves (Shulman, 1987). Epidural administration of BAB results in ultra-long lasting, selective sensory effects. In the method refined by Korsten et al. (1991), the BAB is applied in the form of a suspension. It contains, besides normal saline and BAB, the surfactant polysorbate 80. In addition, polyethylene glycol 3350 has been used as well. The aqueous suspension is injected in patients over a period of several days. The large amount of the BAB suspension necessary for long-term pain relief excludes the possibility of a single injection. The selective block of nociception develops gradually during this period and lasts for several months with a low incidence of side effects, which are mostly associated with the actual injection. After injection, the suspension can be localized along the spinal nerve roots in paste-like aggregates, which serve as a depot releasing the BAB slowly to its local environment over a period of months.

These *in vivo* effects of BAB-supensions were simulated in a preliminary *in vitro* experiment (personal communication of D.L.B. Winkelman and L.J.A. Rampaart), in which DRG-neurons reversibly lost their inward Na^+ and outward K^+ currents upon exposure to saturated BAB solutions (~700 µM at a 5 mM nominal concentration with visible undissolved BAB particles). This simple experiment demonstrates that saturated BAB concentrations of BAB suspensions are strongly inhibiting sensory neuron excitability and that this action involves besides Na^+ channels also K^+ channels

Currently, BAB is still in clinical trial awaiting FDA approval. However, given the strong inhibitory effect of saturated BAB-concentrations, it is still unclear by what mechanism BAB displays its useful and selective analgesic properties. In order to elucidate more of this mechanism we studied the effects of BAB on different ion channels and review these results here in this General Discussion.

In the present thesis we investigated the effects of BAB on voltage-gated calcium (Ca_V) and potassium channels (K_V). N-, T- and L-type currents served as specific examples of currents through Ca_V channels, while K_V1.1 and erg-1 (K_V11.1 or hERG) potassium channels were chosen as relevant representatives of K_V channels. In order to come to a complete understanding of the analgesic action of BAB it is important to consider all known effects of BAB on ion channels at different concentrations.

Voltage gated sodium channels

Previously, BAB effects have already been studied on sodium channels (Van den Berg et al., 1995; Van den Berg et al., 1996). In dorsal root ganglion neurons five types of sodium current components were found, which could be divided into three fast and two slow sodium currents. These components were differentially affected by a concentration of 100 µM BAB. The midpoint potentials of the inactivation of the three fast components were shifted in a hyperpolarizing direction. Only one component however, showed reduced maximal amplitude. No shift of the midpoint was observed in the slow components. One of the two slow components had a reduced amplitude, whereas the other was insensitive to the application of 100 µM BAB. Especially, the slow insensitive sodium channel is a candidate to be part of the selective nerve fiber actions.

Voltage gated calcium channels

In Chapters 3, 4 and 5 the effects of BAB on different Ca_V channel types were described (Beekwilder et al., 2005; Beekwilder et al., 2006). Both N-type and T-type calcium currents (Chapters 3 and 4), which constitute together most of the total calcium current in mouse DRG neurons, displayed accelerated kinetics and a reduced current amplitude (IC_{50}~200µM). Because the L-type current does not have a significant component in neonatal mouse DRG neurons, we checked the effect of BAB on L-type currents in undifferentiated PC12-cells, where they constitute the larger part of the total calcium conductance. These L-type currents were also inhibited by BAB with a tendency towards inactivation acceleration (Chapter 5). The latter result was also found in a preliminary study

of the effect of BAB on cloned L-type calcium channels (α1C-eGFP/α2δ/β2a), expressed in HEK-tsA cells (personal communication of D.L. Ypey).

Voltage gated potassium channels

Chapter 2 and 6 of the thesis report about the effects of BAB on Kv1.1 and hERG channels (Beekwilder et al., 2003). Approximately a third of the total potassium current in mouse DRG-neurons is dendrotoxin-K-sensitive, which is Kv1.1 specific. When expressed in tsA cells, Kv1.1 channel opening and closing was accelerated by BAB, but the midpoint of steady state activation was not altered. BAB appears to inhibit Kv1.1 by stabilizing closed conformations of the channel.

hERG channels have distinct features. The characteristic slow activation gate makes that the kinetics of this gate and the effects on it by BAB can be studied in more detail. BAB reduced the overall current amplitude and accelerated all kinetic processes of hERG channels expressed in HEK-tsA cells. These BAB effects could be explained by an effect on a single process component if the currents were described by a multistate model for channel gating. Only two kinetic parameters towards an intermediate closed state were increased, resulting in a bias towards this state. Since so many currents from the K_V- and the Ca_V-type are affected similarly by BAB, the question became important whether such a kinetic effect could be applied to other current types.

However, there has been one other study about BAB and a specific potassium channel. Winkelman et al (2005) looked at what BAB does to the Kv4.2 potassium channel, conducting an A-type potassium current. This channel is also present in DRG neurons. Interestingly, they found a high affinity binding site for BAB, located near the narrow cytoplasmic entrance of the channel, with an IC_{50} of 59 nM (!) without altering the kinetics or the voltage sensitivity of the current. The maximum inhibition reached was ~35% and a low affinity inhibition comparable to that in other potassium channels was absent. These drastically different results show that BAB effects on K_V channels in general cannot be generalized and indicate that further studies of relevant individual potassium channel types should be done.

BOX 1

BAB blocks Gap Junctional Channels in Fibroblastic Normal Rat Kidney (NRK) Cells*).
NRK cells in culture are coupled to each other with gap junctional channels (mainly Cx43). The single-electrode whole-cell patch-clamp technique was used to stimulate cells of growing subconfluent NRK-cultures (clone 49F) with depolarizing voltage clamp steps of 20 mV from a holding potential of -80 mV to evoke capacitive current transients for the analysis of electrical coupling to neighbour cells. Cells connected to neighbour cells in cell clusters of 5-30 cells (n = 4) or in monolayer islands of hundreds of cells (n = 8) showed responses typical for electrically coupled cells, i.e. with a multi-exponential transient towards a steady-state current reflecting an input resistance considerably smaller (25-300 MΩ) than the membrane resistance Rm of an isolated single cell (~2 GΩ). Addition of 500 µM BAB, ~2 IC_{50} for K_V and Ca_V channel block, uncoupled the cells from the surrounding cells, since the recorded capacitive current transient of the stimulated cell was typical for single cells: a single-exponential decay (τ < 1ms) towards a steady-state current reflecting a 1-3 GΩ membrane resistance (Figure 1). Uncoupling was usually largely reversible, was not due to the effect of the vehicle (~0.1 % ethanol; n = 3) and was similar to that occurring upon the addition of 300 µM octanol (n = 3), a well known gap junctional uncoupler. The data indicate uncoupling of the cells and therefore an inhibiting effect of BAB on gap junctions.

*)Adapted from Rampaart et al. (2004) Biophys J 86 Suppl:584a, 3029-Pos.

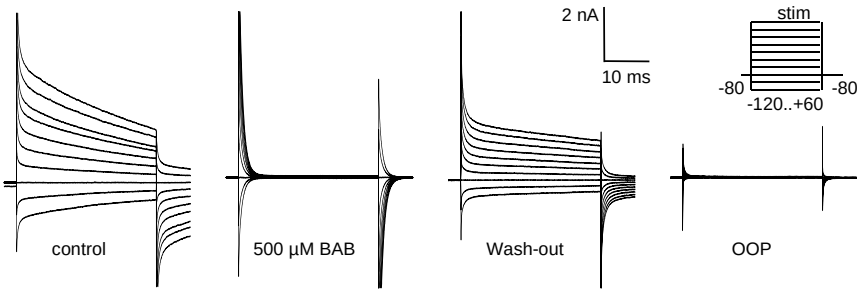

Figure 1. *The effect of 500 µM BAB on electrical coupling between cells in a 30-cell cluster. Holding potential –80 mV, voltage step increments 20 mV from –120 mV, step intervals 4 s. Pipette resistance Rpip ~3 MΩ, initial seal resistance Rseal > 1 GOhm, steady-state input resistance Rinss = 200 MΩ before BAB addition (control), Rinss = 2 GΩ in the presence of BAB and Rinss = 250 MΩ in the control records after BAB removal (wash-out). Recovery from BAB was not yet complete in the control-after records. Rinss was determined in longer-duration records. Series resistance Rser = 14 MΩ and membrane capacity Cm = 46 pF after uncoupling. The outside-out-patch (OOP) configuration pulled at the end of the experiment (bottom right records) indicates that the large control currents did not flow through a decreased seal resistance (Rseal>Roop ~4.5 GΩ).*

Gap Junctional channels

Gap junctions are formed by the concatenation of two connexons, or hemichannels, in the plasma membrane of adjacent cells (Hille, 2001). In this way, the connexons form an intercellular aselective channel and groups of such channels form small-resistance gap junctions between cells. This results in electrical coupling of the two cells. Each connexon consists of six connexins. To date, more than twenty different connexins are known, each with slightly different properties concerning permeability and regulation. Besides forming gap junctions, connexons have also been shown to be functional as well in single-cell plasma membranes (for a review see Goodenough and Paul, 2003).

Pilot studies (Rampaart et al., 2004) have shown an inhibitory effect of BAB on electrical coupling of NRK cells (see Box 1). The possible role of gap junctional block by BAB is not self-evident, since gap junctions have not been shown to be expressed in DRG neurons. However, the satellite cells surrounding the DRG neuron do express functional gap junctions (Pannese et al., 2003). These gap junctions are mainly formed between the satellite cells surrounding the same DRG neuron. And even, though limited, some electrical coupling has also been shown between the satellite cells encapsulating different nerve cells. The functional role of these glial cells has long been ignored, but has recently been recognized (Watkins and Maier, 2002). Among others glially derived neurotrophic factor (GDNF) is released by the satellite cells (Hammarberg et al., 1996). GDNF is known to have several effects, like the regulation of the pain associated $Na_V1.9$ channel and the Vanilloid receptor (VR1) (Ogun-Muyiwa et al., 1999; Cummins et al., 2000). Peripheral nerve injury has been shown to stimulate activated satellite cells to release proinflammatory cytokines (Copray et al., 2001). And recently, the gap junctional coupling between the satellite cells has been shown to increase following inflammatory pain (Dublin and Hanani, 2007). This shows that DRG neurons and their satellite cells should be seen together as a functional unit. Although, it is not clear what the effect of gap junctional block of the satellite cells is on the function of the DRG neurons, it should be considered as a possible and likely target for BAB's analgesic action.

Something similar can be said of gap junctions present in Schwann cells around the nerve fibers. The myelin sheaths wrapped around the axon express gap

junctional channels which mediate a radial pathway of diffusion between the different layers (Schmidt-Lanterman incisures; (Balice-Gordon et al., 1998). It has been hypothesized that the gap junctions facilitate diffusion of K^+, taken up by the Schwann cell in the paranodal region in order to avoid accumulation of K^+ in the periaxonal space (Arroyo and Scherer, 2000). Impairment of Cx32, expressed by Schwann cells, is one of the causes of X-linked Charcot-Marie-Tooth disease, an inherited demyelinating peripheral neuropathy (Bergoffen et al., 1993). This illustrates the important function of these gap junctions and therefore, the possible implications of their inhibition by BAB.

HOW DOES BAB AFFECT ION CHANNELS?

In sodium channels a local anesthetic binding site has been found. Mutations in specific amino acids in the S6 transmembrane segment of domains I, III and especially IV lead to a reduction of the local anesthetic affinity (Ragsdale et al., 1994; Wang et al., 2000). Current opinion is that the S6 segments of the four domains line the internal vestibule of the pore. Charged local anesthetics can reach this binding site only from the intracellular side. Whereas the uncharged, unprotonated form is necessary to cross the membrane, the sodium channels are more susceptible to the charged form (Ritchie and Greengard, 1966; Narahashi and Frazier, 1971). At least this is the case for the charged amine-type anesthetics. It is still unclear whether the ester-linked BAB and benzocaine bind to the same binding site. Localizing the BAB and benzocaine molecules inside a lipid bilayer has revealed that both these molecules reside in the lipid headgroup region (Kuroda et al., 2000). From this position they cannot directly reach the presumed local anesthetic receptor on the S6 segment, as this is located near the center of the bilayer, which leaves the existence and nature of the BAB-binding site unclear.

The low-affinity IC_{50}'s of BAB on the different ion channels that have been studied are quite comparable (~200µM). Therefore, distinct binding sites on all channels affected by BAB with the same affinity would be required. Moreover,

local anesthetics do not only block the typical voltage gated ion channels (K_V, Na_V, Ca_V). A binding site would have to be present at the before-mentioned gap junctiontional channels as well. Other ion transport proteins like Na-K-ATPase are inhibited by local anesthetics as well (Kutchai et al., 2000). Here, local anesthetics decrease its affinity for sodium and potassium. Furthermore, G-protein-coupled receptor mediated pathways are inhibited. A local anesthetic target site on the Gαq protein has been proposed (Hollmann et al., 2001). With these effects only being a selection, many more membrane-associated proteins and processes have been found to be affected by local anesthetics. The wide variety of cellular structures and processes affected by BAB makes it tempting to speculate about the effect of BAB and other local anesthetics on a common feature they share. An obvious candidate for this would be the cellular membrane. The membrane of mammalian cells contains over 2000 species of lipid molecules. Furthermore, the composition of the membrane is not evenly distributed in space nor time. An example of this are the lipid rafts. For K_V channels it has been shown that the subcellular localization of these channels is correlated to these lipid rafts (O'Connell and Tamkun, 2005). This colocalization of proteins may help the cell to modulate protein function in well defined membrane microdomains. Depletion of raft lipid has been shown to alter functional properties of ion channels (Martens et al., 2001). Schmidt et al. (2006) have recently shown that the membrane surrounding an ion channel directly takes part in the functionality of the voltage sensor. In that light the membrane should be seen as part of the functional ion channel. Effects of cholesterol in the membrane on the position of BAB in the bilayer have been shown (Kuroda et al., 2000). It is possible however, that this interaction is bilateral and that BAB on its turn has an influence on the lipid composition surrounding the membrane proteins involved in action potential transmission (Schmidt et al. 2006). Effects of BAB on the ion currents could be explained in terms of an interaction of the membrane with the ion channel. As was illustrated in Chapter 6, transition rates between different ion channel states can be influenced without the need for the anesthetic to actually bind to or block the ion channel in question.

In conclusion, it can be said that the assumption of a specific local anesthetic receptor for such a nonspecific drug as BAB is premature and alternatives deserve further investigation.

The epidural administration of BAB in a suspension results in an ultra-long selective analgesia. This raises the question what the determining factor in this specific action is. The pharmacological effect of epidural administration of solutions with BAB has a life span of minutes as opposed to months in the case of the suspension (Grouls et al., 1997b). On the other hand, a suspension of lidocaine, which is a more hydrophilic local anesthetic, results in a nonselective nerve block with a duration of hours rather than months (Grouls, 1997). As a conclusion it can be said that neither just BAB nor the administration method alone is responsible for the ultra-long lasting effect of the analgesia.

The properties that seem to set BAB apart from the other local anesthetics in the clinical situation is the combination of the low dura-arachnoid barrier permeability and the low octanol/water partition coefficient (Grouls et al., 1997a; Grouls et al., 2000). BAB is released slowly, because of its low water solubility and is spatially confined at active concentrations in the epidural space, since it is restricted by the dura mater and the arachnoid membrane. Lidocaine on the other hand, dissolves much faster and is less restricted by the dura-arachnoid. For that reason the lidocaine concentrations are much higher, but the lidocaine diffuses easily away and it is cleared much faster. The low dura-arachnoid membrane permeability of BAB prevents the occurrence of higher BAB concentrations in the blood. The BAB that does diffuse through these layers is broken down fast enough by cholinesterase to prevent a build-up of high enough concentrations to cause side effects elsewhere in the body.

Epidural injections of BAB solutions result, besides in analgesic block, in complete sensory and motor block due to the high availability of the BAB. This shows that the motor nerve cells are not insensitive to BAB, but they just have a sensitivity that is lower than the pain sensing neurons. This property of local anesthetics has long been recognized, but considered of little use, because of the small concentration window with a selective block (Rang et al., 2003). Bupivacaine was the first local anesthetic with a prolonged - and therefore useful - differential blockade. It might just be that the BAB suspension results in an ultralong-lasting concentration gradient that is high enough to suppress the pain

signals, but not high enough to cause a complete sensory block and motor impairment.

The lower sensitivity to local anesthetics of motor neurons may have several reasons. Traditionally, nerve diameter and degree of myelinization have been thought to be the reason for differential blockade. However, it has been shown that neither is the determining factor alone (Jaffe and Rowe, 1996).

A possible explanation for lower sensitivity of motor neurons to BAB is the different action potential shape of the motor action potential and the pain action potential. As is shown in this thesis, the inhibition or even enhancement of the ionic currents is time-dependent. As a result of that the same ionic current can be affected differently in slow action potentials compared to fast action potentials. Another explanation is related to the differences in action potential shape and refers to the differences in ion channel composition for the different types of neurons. A lower overall sensitivity for BAB of the ion channels expressed in motor neurons compared to the ones in pain transmitting neurons could result in a differential blockade. An example could be the effects of BAB on the calcium channels as described in Chapters 3 to 5. The Ranvier nodes of motor neurons contain a wide spectrum of ion channels, but calcium channels have not been found (Waxman and Ritchie, 1993). Unmyelinated C-fibers however, do contain calcium channels (Quasthoff et al., 1995; Quasthoff et al., 1996; Mayer et al., 1999). Therefore, blockade of the calcium channels would not affect action potential transmission of the motor neurons, but it would affect the slow action potential of the C-fibers. Evidence is growing that the calcium channels do play a prominent role in pain physiology. This is illustrated by the use of ziconotide (SNX-111). Ziconotide is a synthetic conotoxin and a specific blocker of the N-type calcium channels. Intrathecal administration results in a relief of severe pain and has been proposed and approved as another alternative to traditional methods for chronic pain treatment (Cox, 2000). Furthermore, several studies with mice lacking the N-type calcium channel have shown an altered nociception (Hatakeyama et al., 2001; Kim et al., 2001; Saegusa et al., 2001). Although, the explanation for these changes is sought in the neurotransmitter release function of these channels, the axonal N-type channels are likely to be involved too. This is even more clear for the T-type calcium currents which are not associated with the neurotransmitter release of DRG

neurons. A recent study shows that mice lacking $Ca_V3.2$ T-type channels have attenuated pain responses (Choi et al., 2007).

A similar but more complex evaluation could be given of the effect of BAB on the potassium channels as was described in Chapters 2 and 6. At clinically relevant concentrations BAB inhibits Kv1.1 currents. This dendrotoxin-like effect by itself would rather increase than decrease the excitability of the nerves (Glazebrook et al., 2002). However, in combination with effects of BAB on other channels it could lead to a reduction of excitability. For instance, BAB shifts the steady-state inactivation of the fast sodium channels towards more negative potentials (Van den Berg et al., 1995). By reducing the afterhyperpolarization, which in C-type neurons is carried in part by dendrotoxin-sensitive currents (Glazebrook et al., 2002), the sodium channel availability could be decreased even more. So, blocking the dendrotoxin-sensitive channels could indirectly lead to a reduced excitability.

For the erg channels the question would be first whether BAB reduces or enhances this current. Since BAB affects the kinetics of the current in such a way that steady-state currents are reduced, while a faster onset leads to a bigger current on a short time scale. Since the *in vivo* behavior of the erg currents outside the heart is poorly understood, it is not possible to predict what the effect will be. However, assuming a dynamic membrane potential it is likely that the erg currents will be enhanced in the presence of BAB. This in itself would result in a lowering of the firing frequency, which are usually considered as less painful stimuli.

CONCLUSION

In conclusion, the physicochemical properties of the BAB suspension make the analgesic BAB effect long-lasting. For the differential effects of BAB on pain and motor fibers there are several explanations. The first is due to the bad solubility of BAB, which limits BAB concentrations around the BAB-suspension particles to

values smaller than complete inhibition of most channel types. The second is differential ion channel expression between sensory nerve and motor nerve fibers and between fibers of different diameters and degrees of myelinization. The third is differential BAB sensitivity of the different ion channel classes, as seen for example between potassium channels and sodium channels. The fourth is the lower safety factor of impulse transmission in the small unmyelinated nerve fibers for local inhibition of excitability by BAB in the epidural space. How these factors contribute to selective analgesia can probably best be evaluated by computer modeling of the complete nerve tissue in the epidural space. Such a model would require more knowledge of the spectrum of ion channels present in pain fibers and of the effect of BAB on these channels. Nevertheless, it is likely that all mentioned explanations contribute to BAB's unique selective analgesic effects.

References

Arroyo EJ, Scherer SS (2000) On the molecular architecture of myelinated fibers. Histochem Cell Biol 113:1-18.

Balice-Gordon RJ, Bone LJ, Scherer SS (1998) Functional gap junctions in the schwann cell myelin sheath. J Cell Biol 142:1095-1104.

Beekwilder JP, van Kempen GT, van den Berg RJ, Ypey DL (2006) The local anesthetic butamben inhibits and accelerates low-voltage activated T-type currents in small sensory neurons. Anesth Analg 102:141-145.

Beekwilder JP, Winkelman DL, van Kempen GT, van den Berg RJ, Ypey DL (2005) The block of total and N-type calcium conductance in mouse sensory neurons by the local anesthetic n-butyl-p-aminobenzoate. Anesth Analg 100:1674-1679.

Beekwilder JP, O'Leary ME, van den Broek LP, van Kempen GT, Ypey DL, van den Berg RJ (2003) Kv1.1 channels of dorsal root ganglion neurons are inhibited by n-butyl-p-aminobenzoate, a promising anesthetic for the treatment of chronic pain. J Pharmacol Exp Ther 304:531-538.

Bergoffen J, Scherer SS, Wang S, Scott MO, Bone LJ, Paul DL, Chen K, Lensch MW, Chance PF, Fischbeck KH (1993) Connexin mutations in X-linked Charcot-Marie-Tooth disease. Science 262:2039-2042.

Choi S, Na HS, Kim J, Lee J, Lee S, Kim D, Park J, Chen CC, Campbell KP, Shin HS (2007) Attenuated pain responses in mice lacking CaV3.2 T-type channels. Genes Brain Behav 6:425-431.

Copray JC, Mantingh I, Brouwer N, Biber K, Kust BM, Liem RS, Huitinga I, Tilders FJ, Van Dam AM, Boddeke HW (2001) Expression of interleukin-1 beta in rat dorsal root ganglia. J Neuroimmunol 118:203-211.

Cox B (2000) Calcium channel blockers and pain therapy. Curr Rev Pain 4:488-498.

Cummins TR, Black JA, Dib-Hajj SD, Waxman SG (2000) Glial-derived neurotrophic factor upregulates expression of functional SNS and NaN sodium channels and their currents in axotomized dorsal root ganglion neurons. J Neurosci 20:8754-8761.

Dublin P, Hanani M (2007) Satellite glial cells in sensory ganglia: their possible contribution to inflammatory pain. Brain Behav Immun 21:592-598.

Glazebrook PA, Ramirez AN, Schild JH, Shieh CC, Doan T, Wible BA, Kunze DL (2002) Potassium channels Kv1.1, Kv1.2 and Kv1.6 influence excitability of rat visceral sensory neurons. JPhysiol 541:467-482.

Goodenough DA, Paul DL (2003) Beyond the gap: functions of unpaired connexon channels. Nat Rev Mol Cell Biol 4:285-294.

Grouls R, Korsten E, Ackerman E, Hellebrekers L, van Zundert A, Breimer D (2000) Diffusion of n-butyl-p-aminobenzoate (BAB), lidocaine and bupivacaine through the human dura-arachnoid mater in vitro. EurJPharmSci 12:125-131.

Grouls RJ, Ackerman EW, Korsten HH, Hellebrekers LJ, Breimer DD (1997a) Partition coefficients (n-octanol/water) of N-butyl-p-aminobenzoate and other local anesthetics measured by reversed-phase high-performance liquid chromatography. J Chromatogr B Biomed Sci Appl 694:421-425.

Grouls RJ, Meert TF, Korsten HH, Hellebrekers LJ, Breimer DD (1997b) Epidural and intrathecal n-butyl-p-aminobenzoate solution in the rat. Comparison with bupivacaine. Anesthesiology 86:181-187.

Grouls RJE (1997) Thesis, University of Eindhoven, Chapter 6.

Hammarberg H, Piehl F, Cullheim S, Fjell J, Hokfelt T, Fried K (1996) GDNF mRNA in Schwann cells and DRG satellite cells after chronic sciatic nerve injury. Neuroreport 7:857-860.

Hatakeyama S, Wakamori M, Ino M, Miyamoto N, Takahashi E, Yoshinaga T, Sawada K, Imoto K, Tanaka I, Yoshizawa T, Nishizawa Y, Mori Y, Niidome T, Shoji S (2001) Differential nociceptive responses in mice lacking the alpha(1B) subunit of N-type Ca(2+) channels. Neuroreport 12:2423-2427.

Hille B (2001) Ionic Channels of Excitable Membranes. Sunderland MA: Sinauer Associates.

Hollmann MW, Durieux ME, Graf BM (2001) Novel local anaesthetics and novel indications for local anaesthetics. Curr Opin Anaesthesiol 14:741-749.

Jaffe RA, Rowe MA (1996) Differential nerve block. Direct measurements on individual myelinated and unmyelinated dorsal root axons. Anesthesiology 84:1455-1464.

Kim C, Jun K, Lee T, Kim SS, McEnery MW, Chin H, Kim HL, Park JM, Kim DK, Jung SJ, Kim J, Shin HS (2001) Altered nociceptive response in mice deficient in the alpha(1B) subunit of the voltage-dependent calcium channel. Mol Cell Neurosci 18:235-245.

Korsten HH, Ackerman EW, Grouls RJ, van Zundert AA, Boon WF, Bal F, Crommelin MA, Ribot JG, Hoefsloot F, Slooff JL (1991) Long-lasting epidural sensory blockade by n-butyl-p-aminobenzoate in the terminally ill intractable cancer pain patient. Anesthesiology 75:950-960.

Kuroda Y, Nasu H, Fujiwara Y, Nakagawa T (2000) Orientations and locations of local anesthetics benzocaine and butamben in phospholipid membranes as studied by 2H NMR spectroscopy. JMembrBiol 177:117-128.

Kutchai H, Geddis LM, Farley RA (2000) Effects of local anaesthetics on the activity of the Na,K-ATPase of canine renal medulla. PharmacolRes 41:1-7.

Martens JR, Sakamoto N, Sullivan SA, Grobaski TD, Tamkun MM (2001) Isoform-specific localization of voltage-gated K+ channels to distinct lipid raft populations. Targeting of Kv1.5 to caveolae. JBiolChem 276:8409-8414.

Mayer C, Quasthoff S, Grafe P (1999) Confocal imaging reveals activity-dependent intracellular Ca2+ transients in nociceptive human C fibres. Pain 81:317-322.

Narahashi T, Frazier DT (1971) Site of action and active form of local anesthetics. NeurosciRes(NY) 4:65-99.

O'Connell KM, Tamkun MM (2005) Targeting of voltage-gated potassium channel isoforms to distinct cell surface microdomains. J Cell Sci 118:2155-2166.

Ogun-Muyiwa P, Helliwell R, McIntyre P, Winter J (1999) Glial cell line derived neurotrophic factor (GDNF) regulates VR1 and substance P in cultured sensory neurons. Neuroreport 10:2107-2111.

Pannese E, Ledda M, Cherkas PS, Huang TY, Hanani M (2003) Satellite cell reactions to axon injury of sensory ganglion neurons: increase in number of gap junctions and formation of bridges connecting previously separate perineuronal sheaths. Anat Embryol (Berl) 206:337-347.

Quasthoff S, Grosskreutz J, Schroder JM, Schneider U, Grafe P (1995) Calcium potentials and tetrodotoxin-resistant sodium potentials in unmyelinated C fibres of biopsied human sural nerve. Neuroscience 69:955-965.

Quasthoff S, Adelsberger H, Grosskreutz J, Arzberger T, Schroder JM (1996) Immunohistochemical and electrophysiological evidence for omega- conotoxin-sensitive calcium channels in unmyelinated C-fibres of biopsied human sural nerve. Brain Res 723:29-36.

Ragsdale DS, McPhee JC, Scheuer T, Catterall WA (1994) Molecular determinants of state-dependent block of Na+ channels by local anesthetics. Science 265:1724-1728.

Rampaart LJA, Camina JP, Beekwilder JP, Harks EGA, Dernisosn MM, Peters PHP, van Meerwijk WPM, Theuvenet APR, Ypey DL (2004) The local anesthetic n-butyl-p-aminobenzoate (BAB) blocks gap junctional channels in fibroblastic normal rat kidney (NRK) cells. Biophys J 86 Suppl:584a, 3029-Pos.

Rang HP, Dale MM, Ritter YM, Moore PK (2003) Pharmacology, 5th Edition. Edinburgh: Churchill Livingstone.

Ritchie JM, Greengard P (1966) On the mode of action of local anesthetics. AnnuRevPharmacol 6:405-430.

Saegusa H, Kurihara T, Zong S, Kazuno A, Matsuda Y, Nonaka T, Han W, Toriyama H, Tanabe T (2001) Suppression of inflammatory and neuropathic pain symptoms in mice lacking the N-type Ca2+ channel. Embo J 20:2349-2356.

Schmidt D, Jiang QX, MacKinnon R (2006) Phospholipids and the origin of cationic gating charges in voltage sensors. Nature 444:775-779.

Shulman M (1987) Treatment of cancer pain with epidural butyl-amino-benzoate suspension. Regional Anesth 12:1-4.

Van den Berg RJ, Wang Z, Grouls RJ, Korsten HH (1996) The local anesthetic, n-butyl-p-aminobenzoate, reduces rat sensory neuron excitability by differential actions on fast and slow Na+ current components. Eur J Pharmacol 316:87-95.

Van den Berg RJ, Van Soest PF, Wang Z, Grouls RJ, Korsten HH (1995) The local anesthetic n-butyl-p-aminobenzoate selectively affects inactivation of fast sodium currents in cultured rat sensory neurons. Anesthesiology 82:1463-1473.

Wang SY, Nau C, Wang GK (2000) Residues in Na(+) channel D3-S6 segment modulate both batrachotoxin and local anesthetic affinities. BiophysJ 79:1379-1387.

Watkins LR, Maier SF (2002) Beyond neurons: evidence that immune and glial cells contribute to pathological pain states. Physiol Rev 82:981-1011.

Waxman SG, Ritchie JM (1993) Molecular dissection of the myelinated axon. Annals Of Neurology 33:121-136.

Winkelman DL, Beck CL, Ypey DL, O'Leary ME (2005) Inhibition of the A-type K+ channels of dorsal root ganglion neurons by the long-duration anesthetic butamben. J Pharmacol Exp Ther 314:1177-1186.

Nederlandse Samenvatting

Pijn is een nuttige functie van het lichaam ter waarschuwing voor schade en gevaar. Echter, als de waarschuwing is overgekomen, maar de oorzaak van de pijn niet kan worden weggenomen is er sprake van een chronisch ongemak of lijden dat direct de kwaliteit van leven beïnvloedt.

Een van de methoden in ontwikkeling om chronische pijn te bestrijden is de epidurale toediening van een butambensuspensie. Butamben is een lokaal anestheticum dat slecht oplost in water. Deze epidurale suspensie heeft in enkele studies laten zien dat het pijn selectief kan onderdrukken voor een lange periode zonder de motoriek uit te schakelen. Het mechanisme hiervan was echter niet duidelijk.

Om meer inzicht hierin te krijgen is in dit proefschrift onderzoek gedaan met behulp van cellulaire elektrofysiologie naar het effect van butamben op verschillende ionenkanalen. Deze kanalen zijn verantwoordelijk voor het vuurgedrag van de neuronen die de pijninformatie doorgeven naar het brein.

In **hoofdstuk 2** is gekeken naar het effect van butamben op spanningsafhankelijke kaliumkanalen van het type $K_V1.1$ dat voorkomt in de sensorische neuronen in het dorsale wortel ganglion (DRG). Het grootste deel van de kaliumstroom in DRG neuronen aktiveert snel en inaktiveert langzaam tijdens depolarisaties. Butamben remde deze kaliumstroom met een 50% inhiberende concentratie (IC_{50}) van 228 µM. Met behulp van het slangengif dendrotoxine-K, een specifieke remmer van $K_V1.1$ kanalen, werd gedemonstreerd dat $K_V1.1$ een groot aandeel heeft in de kaliumstromen van de DRG neuronen. Vervolgens werden $K_V1.1$ kaliumkanalen tot expressie gebracht in gemakkelijk te kweken tsA201 cellen om de stromen door deze kanalen in isolatie te kunnen bestuderen. Butamben remde de $K_V1.1$-stroom met een vergelijkbare concentratie als de totale kaliumstroom in DRG-neuronen. Butamben versnelde het openen en sluiten van de $K_V1.1$-kanalen zonder de 'steady-state'-aktivatie curve op de spanningsas te verschuiven. Butamben leek de gesloten toestand van het $K_V1.1$-kanaal te stabiliseren. Co-expressie van kv1.1 kanaal met de $K_V\beta1$-subunit resulteerde in snelle inaktivatie van de $K_V1.1$-stroom en verlaagde de gevoeligheid voor butamben. Vergelijking van de $K_V1.1$-stromen

in de tsA201-cellen en de DRG-neuronen suggereren dat in DRG-neuronen de $K_V\beta1$-subunit nauwelijks een rol speelt in de eigenschappen van deze stromen.

Het effect van butamben op spanningsafhankelijke calciumkanalen in DRG-neuronen, en daarvan het N-type in het bijzonder, is beschreven in **hoofdstuk 3**. Butamben remde de stroom door de calciumkanalen met een IC_{50} van 207 µM. Door de dominante N-type stroom te isoleren met behulp van gif van een zeeslak, ω-conotoxin-IVA, werd duidelijk dat de N-type stroom met een vergelijkbare concentratie werd geremd. De tijdconstanten van inaktivatie en deaktivatie van de kanalen werden kleiner in de aanwezigheid van butamben, wat er op duidt dat er kinetische processen betrokken zijn bij de remming van de stromen. Ook als de stromen werden opgewekt met een fysiologisch spanningsprotocol in de vorm van een aktiepotentiaal waren dezelfde effecten van butamben zichtbaar.

Hoofdstuk 4 behandelt de effecten van butamben op reeds bij lagere membraanspanning geaktiveerde T-type calciumkanalen. T-type calcium-stromen, die in de literatuur reeds geassocieerd werden met pijnsensatie, werden ook geremd door butamben met een IC_{50} van ongeveer 200 µM. De T-type stromen met hun typische transiënte karakter, hadden onder invloed van butamben een versnelde aktivatie, inaktivatie, en deaktivatiekinetiek. Dit is geheel vergelijkbaar met het efect van butamben op de N-type stromen uit hoofdstuk 3. Butamben had geen effect op de ligging en vorm van de aktivatiecurve. Daarentegen was er wel een hyperpolariserende verschuiving van de inaktivatiecurve.

In **Hoofdstuk 5** werd het effect van butamben op L-type calciumkanalen onderzocht. Hoewel deze kanalen bij humane DRG neuronen voor kunnen komen, konden deze door hun geringe aantal in DRG-neuronen van neonatale muizen niet daarin bestudeerd worden. Derhalve werd gekozen voor ongedifferentieerde rat PC12 cellen, waarin L-type kanalen in voldoende mate voorkomen. Butamben (500 µM) haalde het overgrote deel van de calciumkanaal-stromen weg op reversibele wijze. Nifedipine, een specifieke L-type stroomremmer, inhibeerde ook de meerderheid van de calciumkanaal-stromen, erop duidend dat het merendeel van die stromen de L-type calcium-kanalen betrof.

Hoofdstuk 6 beschrijft de effecten van butamben op kaliumkanalen van het hERG-type. Deze kanalen zijn spanningsafhankelijk, maar hebben atypische eigenschappen die zorgen voor een langzame aktivatie en een veel snellere inaktivatie. Butamben remde de hERG stromen met een IC_{50} van 112 µM, maar versnelde tevens alle kinetische processen van aktivatie en inaktivatie. Ook werden kleine verschuivingen gevonden van de aktivatie- en inaktivatiecurves. Deze konden echter niet de inhibitie verklaren, omdat zij van dien aard waren dat de stromen eerder zouden moeten vergroten. Met mathematische modellen is gekeken of iets kon worden gezegd over het mechanisme, gebaseerd op de gevonden kinetische veranderingen als gevolg van butamben. De resultaten lieten zien dat de kinetische veranderingen in een Hodgkin-Huxley model de inhibitie niet konden verklaren. Een 'veel-toestanden'-model echter, liet wel zo'n verklaring toe. Het duidde op een mechanisme waarbij butamben de verdeling van de hERG kanalen over de verschillende toestanden verschuift in de richting van een intermediair gesloten 'state', welke in een snel evenwicht is met een geinaktiveerde 'state'.

Tot slot worden in **hoofdstuk 7** de resultaten op een rijtje gezet. Butamben blijkt een aspecifieke modulator van ionenkanalen. Over het mechanisme waarmee butamben een effect heeft op ionenkanalen wordt gespeculeerd. De veronderstelling dat er een speciale receptor voor butamben zou zijn op de verschillende ionenkanalen is prematuur en onwaarschijnlijk. Over het mechanisme van de selectieve analgesie kan nog geen definitieve uitspraak worden gedaan. Maar voor de specifiek analgetische werking van butamben in epidurale suspensies spelen waarschijnlijk in meer of minder mate een rol de verschillen tussen motorische en sensorische vezels met betrekking tot formaat, ionenkanaalsamenstelling en myelinisatie. De stabiele concentratie van butamben rondom de suspensie bevindt zich waarschijnlijk juist boven de pijn-sensorische gevoeligheid voor butamben en onder de motorische gevoeligheid voor butamben.

Publicaties

Rampaart, L.J.A., Beekwilder, J.P., van Kempen, G.Th.H., van den Berg, R.J. and Ypey, D.L. The Local anesthetic butamben inhibits native total and L-type currents through Calcium Channels in PC12 cells. Anesth Analg *In press*

Westerink, R. H., Rook, M. B., Beekwilder, J. P., and Wadman, W. J. (2006). Dual role of Calbindin-D in vesicular catecholamine release from mouse chromaffin cells. J Neurochem 99, 628-640.

Beekwilder, J. P., van Kempen, G. T., van den Berg, R. J., and Ypey, D. L. (2006). The local anesthetic butamben inhibits and accelerates low-voltage activated T-type currents in small sensory neurons. Anesth Analg 102, 141-145.

Beekwilder, J. P., Winkelman, D. L., van Kempen, G. T., van den Berg, R. J., and Ypey, D. L. (2005). The block of total and N-type calcium conductance in mouse sensory neurons by the local anesthetic n-butyl-p-aminobenzoate. Anesth Analg 100, 1674-1679.

Beekwilder, J. P., O'Leary, M. E., van den Broek, L. P., van Kempen, G. T., Ypey, D. L., and van den Berg, R. J. (2003). Kv1.1 channels of dorsal root ganglion neurons are inhibited by n-butyl-p-aminobenzoate, a promising anesthetic for the treatment of chronic pain. J Pharmacol Exp Ther 304, 531-538.

Dijkhuizen, R. M., Beekwilder, J. P., van der Worp, H. B., Berkelbach van der Sprenkel, J. W., Tulleken, K. A., and Nicolay, K. (1999). Correlation between tissue depolarizations and damage in focal ischemic rat brain. Brain Res 840(1-2):194-205

Curriculum vitae

Jeroen Beekwilder werd op 26 juli 1973 geboren te Helmond. In Asten behaalde hij op het College Asten Someren (CAS) zijn VWO diploma in 1991. Vervolgens begon hij met zijn studie biologie aan de Universiteit Utrecht. Tijdens de specialisatiefase werden twee stages gelopen. Eerst werd bij de afdeling *In vivo* NMR spectroscopie van het Bijvoetcentrum voor Biomoleculair Onderzoek onder leiding van Dr. R.M. Dijkhuizen en Prof. Dr. K. Nicolay een NMR-compatibele elektrofysiologische studie verricht naar ischemische depolarisaties tijdens de acute fase van cerebrale ischemie. De tweede stage werd gelopen bij de afdeling Neurotoxicologie van het Research Instituut Toxicologie onder leiding van Dr. H.P.M. Vijverberg. In deze studie werd gekeken naar membraancapaciteit-verandering als maat voor vesiculaire neurotransmitterafgifte. Het doctoraal examen werd behaald in november 1996.

Vanaf januari 1997 werd onderzoek verricht aan de Universiteit Leiden bij het laboratorium voor Fysiologie en Fysiologische Fysica onder leiding van Dr. PC Molenaar en Prof. Dr. D.L. Ypey. Hier werd gekeken naar de rol van calcium kanalen in het Lambert-Eaton Myastheen Syndroom.

In januari 2000 is Jeroen begonnen aan zijn promotieonderzoek waarvan de resultaten in dit proefschrift beschreven staan.

Van april 2002 tot en met augustus 2004 heeft hij een postdoctorale studie gedaan bij de afdeling Neurobiologie van het Swammerdam Institute for Life Sciences van de UvA, alwaar hij onder leiding van Prof Dr. W.J. Wadman onderzoek deed naar de rol van calbindine in de calciumhuishouding van hippocampus neuronen. Van maart 2005 tot en februari 2007 heeft Jeroen aan de Universiteit Twente in de groep van Prof. Dr. P.H. Veltink meegewerkt aan het ontwerp van een chip waarop neuronale netwerken gekweekt en bemeten kunnen worden.

Sinds juli 2007 is Jeroen werkzaam als wetenschappelijk medewerker van het Twin - Instituut voor Neuromodulatie. In die hoedanigheid is hij tevens verbonden aan de Universiteit Twente en het UMC St Radboud in Nijmegen.

Nawoord

Achter een proefschrift zit meer dan een verzameling studies uitgevoerd door de auteur. Het is een bijproduct van de wetenschappelijke volwassenwording. Een dergelijk proces vindt niet alleen plaats binnen de muren van het laboratorium, maar is iets dat je ondergaat 24 uur per dag, 7 dagen per week. Daarom zou het niet misstaan om een groep mensen hier te danken die in de voorafgaande pagina's niet zijn terug te vinden, maar in de afgelopen jaren toch een positieve rol hebben gespeeld. Bij dezen wil ik allen danken die als familie, vrienden, buren studenten en collega's er mede voor hebben gezorgd dat ik positief op deze periode kan terugkijken en deze promotie succesvol heb kunnen afronden. Toch wil ik in het bijzonder nog de naam noemen van Tu-Anh, mijn levenspartner. Ook wil ik uiteraard noemen mijn kinderen Thomas, Philip en Henry. Zij samen maakten van mijn huis mijn thuis en zij vormen mijn output met de hoogste impact factor.